Diss. ETH No. 16302

Modal Pollutant Emissions Model of Diesel and Gasoline Engines

A dissertation submitted to the

SWISS FEDERAL INSTITUTE OF TECHNOLOGY ZURICH

for the degree of

Doctor of Technical Sciences

presented by

Delia Elisabeta Ajtay
M.Sc. Mathematics
Born 11^{th} August 1975
Nationality Romanian

accepted on the recommendation of

Prof. Dr. Lino Guzella, examiner
Prof. Dr. Stefan Hausberger, co-examiner
Dr. Martin Weilenmann , co-examiner

2005

Abstract

Road traffic accounts for an important part of air pollution. For roughly 30 years, emission limits have been enforced by legislation in Europe and elsewhere. The success of the stringent regulations has been monitored by the environmental agencies. Although in the early days the interest was in the fulfillment of the legislation limits, real-world emissions represent today's main focus.

Emissions models are used to derive international, national and regional emission inventories using measurements performed in emissions laboratories and to predict the impact of different traffic related measures. These emission models connect driving behaviour and fleet data to the emission measurements from the test bench investigations.

The availability of vehicle emission models has improved significantly in the recent years. There are basically two types of emissions and fuel consumption models: one based on bag measurements and the other based on instantaneous measurements. Emission models based on bag values give results for the traffic situations similar to the one used to fill the bag. If the driving behaviour changes, new measurements with comparable driving patterns have to be performed. To account for the additional effects as load, slope or gearshift strategies, bag based models include correction functions. However, these correction functions are based on a small number of measurements with few vehicles which may not be representative for the emissions behaviour. Moreover, the combination of these correction factors (i.e. when a vehicle drives uphill with a full load) can be extremely misleading.

Instantaneous emissions modelling maps the emissions at a given time to their generating "engine state", like vehicle speed, engine speed, torque, etc. This makes it possible to integrate new, unmeasured driving patterns over the model and calculate their emission factors without further measurements. Thus, emission factors for a large number of driving situations can be determined from a small number of measurements.

The goal of this thesis is to develop an instantaneous emissions and fuel consumption model. Such a model should be capable to predict emission factors for any unmeasured speed diagram using a limited number of measurements. Beside that, contributory aspects like load, road gradient, gearshift strategies should be also included. Such a model shall be, thus, significantly more flexible than the existing approaches and would be especially useful for the assessment of local studies (i.e. the impact of traffic management schemes, change of driving behaviour, etc).

Due to the fact that the instantaneous emission model relates at each moment of time the emission signals to their generating engine variables, the accuracy of the measurements is one of the key issues for a successful result. But, the original emission signals measured in a test are delayed to their time of formation, since the exhaust gas is transported from the engine to the analysers, and the emission peaks are flattened by convolution.

If these dynamic aspects of the exhaust transport are neglected, the emission events are correlated to the wrong second, resulting in incorrect engine status in emissions modelling. For instantaneous emissions modelling, emission values can be correlated to the correct engine state of the car only if they are at their right location on the time scale. Therefore, these delays and mixing dynamics must be compensated, i.e. the behaviour of the gas transport systems must be modelled and inverted. The modelling of the different gas transport systems is performed using linear time-varying approaches, such that emissions at their location of formation (engine-out or catalyst-out) are reconstructed from the signals recorded at the analyser.

Using the reconstructed emissions data, an instantaneous emissions model is developed for different classes of pollutants and for various categories of vehicles. The model performs reliably, emission factors from several real-world driving situations being accurately forecasted.

For the modern gasoline cars equipped with a three-way catalyst, the approach has to be extended by modelling separately the engine-out emissions and, afterwards, the catalyst-out emissions. In order to take into account the transient generation of exhaust gases, the engine-out emissions are modelled using a 4D emissions model. With the engine-out emissions as input data, a simple catalyst submodel is developed, based on the oxygen storage mechanism. The validity of the model and the parameters estimation procedure is checked by applying them to real world case studies. It is demonstrated that the model is capable of predicting the operating behaviour of the catalyst under realistic conditions and is, thus, suited for use within emissions modelling.

Zusammenfassung

Der Strassenverkehr ist eine der Hauptquellen der Luftverschmutzung. Die Emissionsgrenzen von Motorfahrzeugen wurden seit etwa 30 Jahren durch die Gesetzgebung in Europa stufenweise verschärft. Der Erfolg dieser Regulierungschritte wurde seither durch Umweltbehörden kontrolliert. Während das Interesse früher mehr der Erfüllung der gesetzlichen Vorschriften galt, stehen heute die Ermittlung der realen Emissionen im Mittelpunkt.

Emissionsmodelle, welche auf Messungen an Rollenprüfständen basieren, werden benötigt um internationale, nationale und regionale Emissionsbestandsaufnahmen abzuleiten. Ausserdem werden diese Modelle genutzt, um den Einfluss unterschiedlicher Verkehrsparameter (z.B. Geschwindigkeitslimiten) auf die Emissionen vorhersagen zu können. In diesen Emissionsmodellen werden Daten zu Fahrverhalten und Fahrzeugbeständen mit den Emissionsmessungen von Rollenprüfstandsuntersuchungen gefaltet.

Seit den letzten Jahren stehen mehr und mehr Fahrzeugemissionsmodelle zur Verfügung. Es gibt grundsätzlich zwei Arten von Emissions- und Kraftstoffverbrauchsmodellen: der eine Typ basiert auf Sackmessungen und der andere auf "online" Messungen. Emissionsmodelle, die auf Sackwerten basieren, erzeugen nur Ergebnisse für jene Verkehrssituationen, die zum Füllen der Abgassäcke genutzt wurden. Wenn sich das Fahrverhalten ändert, müssten neue Messungen mit entsprechenden Fahrmustern durchgeführt werden. Modelle, welche auf Sackmessungen beruhen, beinhalten teilweise Korrekturfunktionen, mit denen man zusätzliche Effekte wie Zuladung, Steigung und Schaltstrategie zu berücksichtigen versucht. Allerdings basieren diese Korrekturen meist auf einer geringen Anzahl Messungen mit wenigen Fahrzeugen, welche nicht repräsentativ für das Emissionsverhalten der Flotte sein könnten. Ausserdem kann die Kombination solcher einzeln ermittelter Korrekturen extrem irreführend sein. Wie soll z.B. eine Bergfahrt mit Zuladung berechnet weden, wenn Steigungsfahrten und Fahrten mit Zuladung separat gemessen wurden?

Die "online" Emissionsmodellierung bezieht die Emissionen zu einem bestimm-

ten Zeitpunkt auf den aktuellen Motorzustand: Fahrzeuggeschwindigkeit, Motordrehzahl, Drehmoment, etc. Dies ermöglicht es, neue, nicht gemessene Fahrmuster in das Modell zu integrieren und deren Emissionsfaktoren ohne weitere Messungen zu berechnen. Dadurch können für eine grosse Anzahl von Fahrsituationen Emissionsfaktoren aus einer kleinen Anzahl von Messungen bestimmt werden.

Das Ziel dieser Doktorarbeit ist es, ein "online" Emissions- und Kraftstoffverbrauchsmodell zu entwickeln. Ein solches Modell sollte geeignet sein für Einzelfahrzeuge und Fahrzeugklassen Emissionsfaktoren für jeden beliebigen, ungemessenen Geschwindigkeitsverlauf vorherzusagen. Zudem sollten Aspekte wie Ladung, Strassengefälle und Schaltsstrategien korrekt mit einbezogen werden. Ein solches Modell wird dadurch flexibler als vorhandene Ansätze und ist besonders nützlich für die Bestimmung von lokalen Studien (d.h. Einfluss von Verkehrslenkungsmassnahmen, änderungen in Fahrverhalten, etc.).

Aufgrund der Tatsache, dass die Emissionssignale in den "online" Modellen für jeden Zeitpunkt dem Zustand des Motors zugeordnet werden müssen, ist die zeitliche Exaktheit der Messung einer der wichtigsten Aspekte für erfolgreiche Ergebnisse. Die direkten gemessenen Emissionssignale treffen jedoch auf Grund des Transports durch das Auspuffsystem und die Messleitung verspätet im Analysator ein. Zudem werden die Emissionsereignisse durch den turbulenten Transport "verschmiert".

Wenn diese dynamischen Aspekte des Abgastransportes vernachlässigt werden, werden die Emissionsereignisse mit zeitlich verschobenen Motorzuständen korreliert. Für "online" Emissionsmodelle können Emissionswerte nur zum richtigen Motorenzustand korreliert werden, wenn sie sich auf den richtigen Zeitpunkt beziehen. Daher müssen diese Verschiebungen kompensiert werden, d. h. das Verhalten des Gastransportsystems muss modelliert und invertiert werden. Die Modellierung der unterschiedlichen Gastransportsysteme wird mit einem linearen zeit-variabeln Ansatz durchgeführt, so dass die Emissionen am Ort der Entstehung (Austritt aus dem Motor oder Austritt aus dem Katalysator) aus dem vom Analysator aufgezeichneten Signal rekonstruiert werden können.

In der Folge wird aus den zeitlich korrigierten Emissionsignalen ein Emissionsmodell für verschiedene Schadstoffklassen und Fahrzeugkategorien entwickelt. Es basiert auf der Korrelation der Emissionswerte mit Drehzahl und Drehmoment des Motors. Das Modell funktioniert für gewisse Fahrzeugklassen zuverlässig: die Emissionsfaktoren werden für ann"hrend alle realen Fahrsituationen genau vorhergesagt.

Dieser Ansatz musste jedoch für moderne Benzinfahrzeuge, ausgestattet mit einem Drei-Wege-Katalysator, ausgeweitet werden. Die Emissionen aus dem Motor und das Verhaltnis des Katalysators werden separat modelliert. Die Emissionen aus dem Motor mussten mit einem vier-dimensionalen Kennfeld modelliert werden, um die transiente Abgasproduktion zu berücksichtigen. Zusätzlich zu Drehzahl und Drehmoment werden die Emissionen auf die zeitliche Ableitung des Saugrohrdrucks bezogen. Für das Verhalten des Katalysators wurde ein Teilmodell entwickelt, für welches die "engine-out" Emissionsdaten als "Inputdaten" genutzt wurden. Es basiert auf dem Sauerstoffablagerungsmechanismus. Die Genauigkeit des Modells und die Parametrierung wurden überprüft, indem diese mit realen Fallstudien verglichen wurden. Es wird gezeigt, dass das Model geeignet ist, die Wirkung des Katalysators unter realistischen Bedingungen vorherzusagen und das es folglich für Emissionsmodellierungen verwendbar ist.

Contents

1. Introduction

During the past decades, the environmental effect of burning fossil fuel has become an important issue. Smog, greenhouse effect, acid rain and toxic particles are consequences of the increasing traffic, heating and industrial thermal processes. Under stricter legislation, fuel consumption and vehicle emissions per distance have been reduced, but the increase of vehicle fleet and of average distance travelled have counteracted these measures.

Due to the quantity of information necessary to determine the different parameters related to the traffic emissions, direct measurement becomes impractical and expensive. Therefore, models for predicting emissions, although difficult to develop, represent an alternative to direct measurement.

1.1. The pollutants and the environment

The impact of traffic air pollution is high. Air pollution represents the presence of undesirable material in the air, in quantities which are large enough to cause harmful effects, both to the environment and to the human health. Road transport is one of the major sources of air pollution. Since human population is close to the sources of emissions from road transport, vehicle emissions contribute to the personal exposure even more than expected from their share on total emissions ([40], [77]).

The majority of the vehicles use a spark ignited gasoline engine. Gasoline mixture represents a blend of paraffins and aromatic hydrocarbons which combust with air at a very high efficiency. The simplified combustion reaction is:

$$gasoline + O_2(in\ air) \rightarrow CO_2 + H_2O + heat \tag{1.1}$$

Carbon dioxide (CO_2) and water (H_2O) are the desired products of the fuel combustion. However, due to the imperfect combustion process, the following

undesired compounds result as exhaust components[1] ([24]):

- carbon monoxide (CO, at the range of 0.1-6 vol. %);
- unburned hydrocarbons (HC, at the range of 500-5000 ppm);
- nitrogen oxides (NO_x, at the range of 100-4000 ppm);
- hydrogen (H_2, at the range of 0.17 vol. %);
- carbon dioxide (CO_2, at the range of 10-13.5 vol. %);
- water (H_2O, at the range of 10-12 vol. %);
- oxygen (O_2, at the range of 0.2-2 vol. %).

Beside the gasoline vehicles, diesel cars are increasingly used due to the economy of operation and decrease of greenhouse gases, especially of CO_2. In this case, the fuel is injected into a highly compressed charge of air where the temperature is high enough for the combustion to occur. Thus, diesel engines are based on a compression-ignited process. Due to the nature of this combustion process, some quantities of unburned fuel, lubricating oil emissions and large numbers of dry soot particles result. Beside the desired components O_2, CO_2 and H_2O, the exhaust emissions of diesel engines consist of:

- solid exhaust: soot particulate matter (PM);
- gaseous exhaust: carbon monoxide (CO), hydrocarbons (HC) and oxides of nitrogen (NO_x);
- liquid exhaust: soluble organic fraction (SOF: unburned fuel and lubricating oil) and liquid sulfates.

Carbon dioxide

All the carbon present in the fuel will be eventually transformed to carbon dioxide in the atmosphere. Even if, due to incomplete combustion, carbon monoxide may result as exhaust, it is ultimately oxidized in the atmosphere to form CO_2. Carbon dioxide is a major source to the greenhouse effect, which leads finally to global warming. CO_2 production is an invariable consequence

[1] N_2 is a remainder

of burning fossil fuel and, at least, the process of fuel burning should be as efficient as possible.

Carbon monoxide

The main source for CO in the atmosphere comes from the exhaust of internal combustion engines, especially of gasoline vehicles [76]. Carbon monoxide is a colourless, inodorous and tasteless gas that is very poorly soluble in water. In the human body, carbon monoxide binds with haemoglobin to form carboxy-haemoglobin (COHb), causing a reduction in the oxygen carrying capacity of the blood. This determines headache, dizziness or nausea and, at high level of COHb, becomes lethal [39].
Carbon monoxide is produced mainly during rich combustion situations, when there is insufficient oxygen to burn completely all the hydrocarbons from the fuel into CO_2. Some of these rich situations appear during transient engine operations like acceleration or high torque demand. Also, when the engine is cold, it is necessary to enrich the air/fuel mixture, causing high levels of CO until the engine is warmed-up.
In microenvironments in which combustion engines are used under conditions of insufficient ventilation, like underground car parks or road tunnels, the mean levels of carbon monoxide can rise to values much higher than those from the ambient outdoor air, becoming thus extremely dangerous for the human health and hence, relevant for the ventilation design.

Hydrocarbons

In the vehicle exhaust there is a large variety of unburned hydrocarbon compounds. The most important are paraffins, olefins, acetylenes and aromatics. As for CO, hydrocarbons are caused by the lack of oxygen when the air/fuel mixture is rich. Beside that, other reasons for hydrocarbon emissions are: flame quenching at the walls, filling of crevices with unburned mixture, absorption by oil layers, incomplete combustion (partial burning or misfire), bulk quenching and evaporative emissions [38].

Due to their variety, the hydrocarbons have different impacts on human health and on the environment. Benzene, for example, can lead to leukaemia and it is carcinogenic to humans [68]. In the troposphere, hydrocarbons react with nitrogen dioxide (NO_2), forming ozone and photochemical smog. Ozone causes cough, throat irritations, pain on deep breath, chest tightness and, sometimes, headache and nausea [36]. Additionally, ozone determines the damaging of vegetation.

Oxides of nitrogen

Oxides of nitrogen are either direct products of the combustion in engines, like nitric oxide (NO) and nitrogen dioxide (NO_2), either a product of the catalytic converter like nitrous oxide (N_2O). The first two species are collectively denoted as NO_x. They are produced during combustion when oxygen reacts with nitrogen due to a high combustion temperature ($> 1500°C$).
Nitric oxide (NO) is colorless, inodorous, tasteless and relatively non-toxic for humans. Similar to CO, nitric oxide is eventually oxidized in the atmosphere to form NO_2.

Nitrogen dioxide (NO_2) is reddish-brown in colour, extremely toxic and has a harsh odor. Nitrogen dioxide has effects on human pulmonary functions, causing damages of lung tissue, couching, bronchitis, etc. Beside the health effects, NO_2 is extremely important to monitor because: (a) it is also an absorber of visible radiation which could have a direct role on the global climate change if its concentration were to become too high; (b) it is a key factor in the formation of ozone in the troposphere and (c) it is, along with atmospheric sulfur oxides, responsible for acid rains [60].

Particulate matter

Airborne particulate matter (PM) represent a combination of organic and inorganic substances. Gasoline vehicles with or without catalyst, diesel cars and heavy-duty trucks, all emit particles mainly in the range of 0.1-0.2 μm in diameter. Gasoline cars equipped with three way catalytic converters emit much lower particle masses than those without, while diesel cars emit about 100 to 1000 times the particle mass of a gasoline car equipped with a catalytic converter.

Diesel particulate matter is almost pure carbon and exists as a sub-aggregate of ultra-fine carbon spheroids with aerodynamic diameters of around 0.1 μm [69]. Apart from the presence of this unburned carbon in the exhaust, which is a consequence of incomplete combustion and implies therefore lower efficiency, the particulate matter may cause lung diseases. Significant relationships between particulate air pollution and human health have been found by epidemiological studies [64]. The particulates are usually denoted by $PM_{2.5}$, which represents "particulate matter of size less than 2.5 μm".
However, the subject of particulate matter measurements and modelling will not be discussed in this paper, but excellent research on this topic can be found in [53], [52], [54].

Sulfur oxides

Both, gasoline and diesel fuels, contain sulfur in different amounts. This sulfur is oxidized during combustion and produces sulfur dioxide (SO_2). Oxidation of sulfur dioxide leads to the formation of sulfurous and sulfuric acids, which can be deposited to the earth by rain. This is called "acid rain" and has caused deforestation in Europe and North America and serious damages to buildings. Current regulation on sulphur oxide emissions are very strict and are presently fulfilled.

1.2. Legislation

Motor vehicle traffic is one of the most important sources for air pollution throughout the world. The investigation in [51] indicates that motor traffic is the major source for air pollution in megacities, in half of them being the single most important source. Since 1950, the global vehicle fleet has grown ten times and it is estimated to double again within the next 20-30 years [56]. As cities expand, more people will drive more vehicles over greater distances and for longer time. Emissions caused by motor traffic are thus important to be monitored and controlled.

In Europe, several directives for the tightening of emission levels have been issued. The first passenger car emissions regulation was the directive 70/220/EEC and for heavy duty vehicle emissions the first directive was issued in 1998. The first mandatory European vehicle emission levels was set by the Euro-1 standards introduced in the 91/441/EEC directive. Consequently, the Euro-2 standard was set within the 94/12/EEC directive and the Euro-3 standard by the 98/69/EG directive. Presently, the Euro-4 standard is going to come in power in 2006.

In Switzerland, the first emission limits were introduced in 1971, by adopting the ECE/UNO regulations. In order to achieve the air quality targets conform to the ECE regulations, stricter emission limits were introduced in 1982. These regulations for the limits were developed within the framework of the EFTA's "Stockholm group". In 1987 the next regulations, called FAV1, were enforced by setting first emission limits for diesel vehicles and by requiring three-way catalytic converter for gasoline vehicles. Stringent requirements for particles of diesel vehicles were set in 1998 within FAV2. Since 1996, the European legislative levels have been adopted in Switzerland. The evolution of Swiss

Class	Year	CO [g/km]	HC [g/km]	NO_x [g/km]	HC+NO_x [g/km]	Particles [g/km]
Gasoline						
FAV 1	1987	2.10	0.25	0.62	-	-
Euro 1	1991	3.16	-	-	1.13	-
Euro 2	1994	2.20	-	-	0.50	-
Euro 3	1998	2.30	0.20	0.15	-	-
Euro 4	2006	1.00	0.10	0.08	-	-
Diesel						
FAV 1	1987	2.10	0.25	0.62	-	0.370
FAV 2	1998	2.10	0.25	0.62	-	0.124
Euro 2	1994	1.00	-	-	0.70	0.080
Euro 3	1998	0.64	-	0.50	0.56	0. 050
Euro 4	2006	0.50	-	0.25	0.30	0.025
Euro 5	2009	-	0.10	0.08	-	0.025

Table 1.1.: Swiss and European standards for emissions of passenger cars

and European standards for emission levels is given in Table 1.1.

To check the fulfillment of the legislative emission requirements, the vehicles under test are placed on a chassis dynamometer and driven through a specific driving cycle.

The European legislative cycle (known as NEDC - New European Driving Cycle) consists of an artificially created driving speed time series with low dynamics (see Figure 1.1). It contains a synthetic urban driving pattern (called ECE or UDC - Urban Driving Cycle) and an extra-urban driving pattern (known as EUDC - Extra Urban Driving Cycle).

Until the adoption of the Euro-3 standard , the procedure was that the vehicle was started with cold engine and a 40 seconds idle phase was run to warm-up the engine before the start of the measurements. From the introduction of Euro-3, this pre-conditioning warm-up period was eliminated. In this way, emissions are measured from the beginning of a cold-start, making the fulfillment of Euro-3 level much harder to acquire than the Euro-2 standard.

This new cycle, which skips the 40 seconds idle phase, is called NEDC 2000 (New European Driving Cycle 2000) or MVEG (European Motor Vehicle Emissions Group).

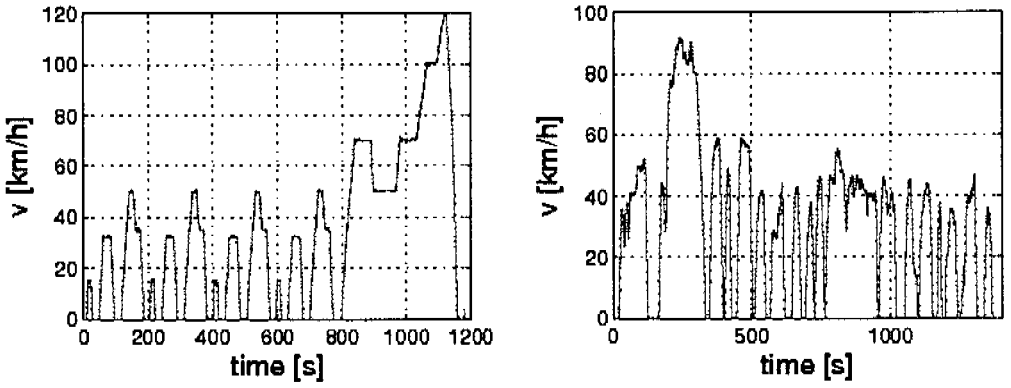

Figure 1.1.: Speed profiles of legislative NEDC (left) and US FTP-75 (right)

In the United States, different emission standards are enforced, with even more stringent requirements for California. The FTP-75 (Federal Test Procedure) cycle is being used in the US as a legislative cycle (Figure 1.1). The first 505 seconds of this test start when the engine is cold and represent the first part of this cycle. The test continues for another 867 seconds, at which point the vehicle is shut off. After a ten minutes interval, the first part is repeated with a warm engine.

Effective model year 2000 vehicles have to be additionally tested on two Supplemental Federal Test Procedures (SFTP) designed to address short comings within the FTP-75 in the representation of: (1) aggressive, high speed driving (US06 cycle) and (2) the use of air conditioning (SC03 cycle).

In California, the LA92 is a dynamometer driving schedule for light-duty vehicles developed by the California Air Resources Board. It is a more aggressive driving cycle then the federal FTP-75. It has higher speed, higher acceleration, fewer stops per kilometer and less idle time.

Most of the real-world emissions are generated during transient phases like strong acceleration, deceleration or gear-shift phases. Both, European and American legislative cycles have rather low maximum speed and acceleration levels, which causes large discrepancies between emissions on certification tests and emissions from real-world situations [21]. Therefore these standard driving cycles are not representative for real-world behaviour and, hence, for their corresponding emission levels.

1.3. Real-world driving cycles

For about 20 years environmental agencies such as the Swiss Agency for Forest, Environment and Landscape (SAEFL), the Environmental Protection Agency (EPA) in the United States, etc., have monitored the success of the emissions regulations. The evolution in vehicle technologies (mainly in the electronic engine control systems) has caused, however, an increase in the difference between emissions in legislation tests and those from real world driving. Thus, legislative cycles are no longer representative for real-world driving behaviour and, consequently, for the assessment of pollutants. The use of real-world driving cycles is therefore one of the key issues in emissions inventories.

Within SAEFL, an extensive measurement campaign has been conducted on Swiss roads in order to determine real-world driving behaviour [22]. Cars equipped with velocity and time logging devices were driven by special drivers, who were told to follow the flow of the traffic. During this measurement campaign 759'299 seconds of driving manner have been recorded and analysed by statistical means.

Recorded data were divided into driving patterns based on the different road characteristics. For that, 14 parameters were defined to describe the road type: mean travel speed, sign of the change of the average speed during driving pattern, standard deviation of velocity, road gradient, percentage of time with constant velocity, percentage of time with velocity zero, length of the driving pattern, etc.

By means of cluster analysis, 12 driving patterns which are most representative for Swiss driving behaviour have been selected to develop a new set of 4 real-world driving cycles. Each of these cycles contains three of these driving patterns. Their corresponding speed time series are depicted in Figure 1.2.

Cycle R1 is composed of three motorway driving situations, AE1R, AE2R and AE3R. Cycle R2 contains a motorway part A4R and two rural driving components, LE1R and LE2sR. Cycle R3 is formed out of rural driving LE2uR and urban driving LE3R and LE5R. Finally, R4 consists of urban driving LE6R, highway and urban stop-and-go driving, StGoHW and StGoUrb.

Within the frame of the European research program ARTEMIS (Assessment and Reliability of Transport Emission Models and Inventory Systems), another real-world driving cycle called Common ARTEMIS Driving Cycle (CADC) has been developed [9]. The goal was to have a common cycle for all the

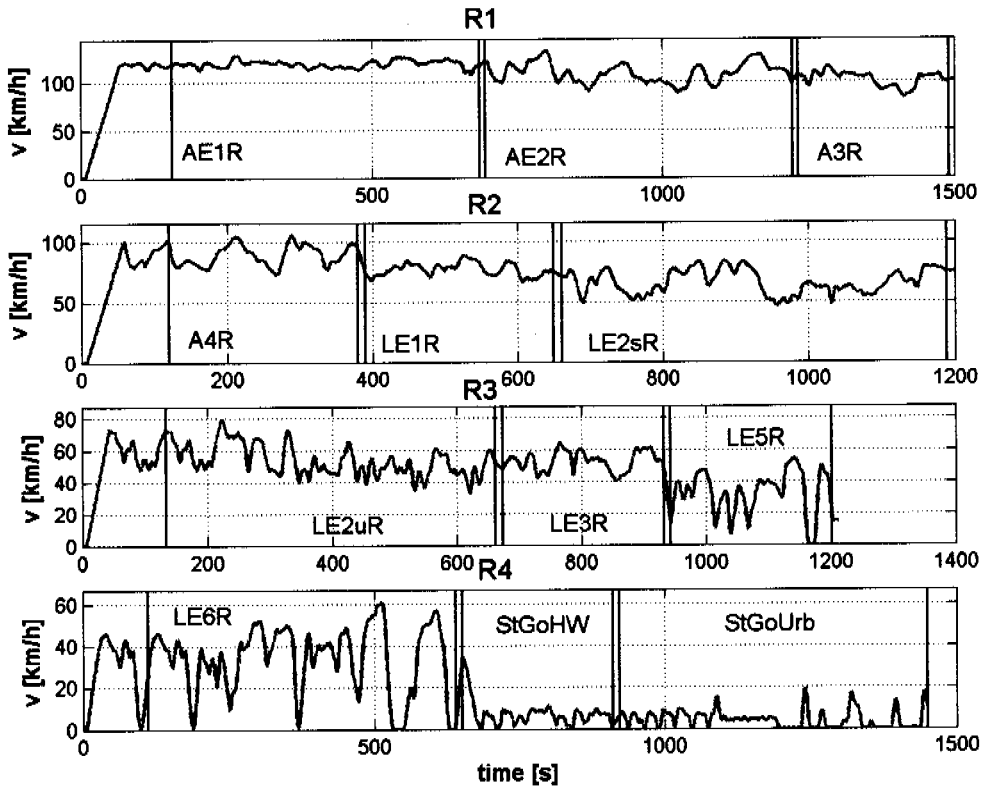

Figure 1.2.: Speed profiles of the Swiss real-world driving cycles R1, R2, R3, R4.

ARTEMIS partners, suitable for both bag and instantaneous measurements and representative for the actual driving conditions of European cars.

Using the Swiss data, the data from another multinational project ([10]) and additional data recorded in Naples, 14 European driving patterns have been identified by factorial analysis and clustering tools: congested urban, urban dense, urban with low speed, urban with free flow, urban unsteady, secondary roads unsteady, secondary rural roads, rural roads with steady speed, main-road unsteady, main-road with steady speed, motorway unsteady and motorway with steady speed.

CADC is divided in three main parts which account for the aggregated road categories: urban, rural (i.e. extra-urban) and highway (Figure 1.3). Each of these parts contain 4 or 5 sub-cycles that can be attributed to a specific road "sub-category", allowing thus disaggregation of the emission levels at various driving conditions. The three main parts are independent from one another and each of them includes a pre- and a post-conditioning phase.

Unlike R1-R4 cycles which follow the NEDC's fixed, predefined gearshift

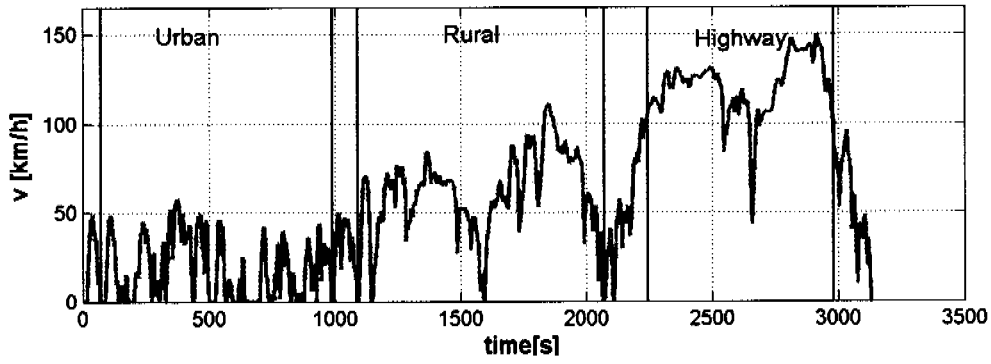

Figure 1.3.: Speed time series of the CADC cycle

strategy, the CADC considers four strategies for the gearshift depending on the technical characteristics of the vehicles (power, mass, transmission ratios).

Kinematic characteristics and description of the Swiss and of the CADC cycle are given in Appendix A.1.

Similar real-world driving cycles are the modal emission cycles (MEC01) developed by a research team from California [16], the cycle for the area of Hong Kong [74] or the Istanbul urban driving cycle [27].

Although the real-world cycles represent a significant improvement towards representative emissions factors, they cannot take into account driving style distribution, different loadings of the vehicle or gradients of the road. Therefore, models that are able to predict the emissions generated by these contributory aspects are of increasing interest.

1.4. Overview of the emission models

From 1995 until 2000, in Switzerland, the total vehicle-km of all road vehicles has increased by about 7 percent [44]. This growth is likely to continue in the future and, by the year 2010, the increase in total vehicle-km relative to 1995 is expected to be about 19-20 percent [44].

Both, the increased vehicle fleet and larger distance covered yearly per vehicle have counteracted the improvements generated by the stricter legislation.

Using test bench measurements, emission models are developed to obtain regional, national or international emission inventories and to predict the impact

of different traffic related measures. Emission models can be split into two categories:

- Fleet emissions models: they use emission factors of different measured cycles and compute a weighted sum that is multiplied to fleet statistics to generate fleet emission models.
- Vehicle emission models: they allow to calculate emissions for any speed pattern, for any combination of vehicle load, slope or gear-shift strategy out of a limited set of measured test cycles.

Vehicle emissions depend on a large set of input parameters: traffic situation, vehicle loading, gradient of the road, driving behaviour, etc. Due to the quantity of information necessary to determine the different combinations related to the traffic emissions, direct measurement becomes impractical and expensive. Therefore, models for predicting emissions represent an alternative to direct measurement.

For more than a decade attempts have been made to store or map emission measurements of test on chassis dynamometers or engine test benches in a neutral way, such that emissions of other driving conditions can be calculated out of them without additional measurements.

There is a variety of vehicle emissions and fuel consumption models derived for different spatial and temporal scales. These models can be categorised into three main groups with increasing level of complexity: (a) average speed models, (b) traffic situation models and (c) instantaneous (modal) models.

1.4.1. Average speed models

The average speed models relate emissions and fuel consumption to the average speed of each driving cycle. The emission and fuel consumption rates are generated from chassis dynamometer measurements for a variety of simulated cycles at different average speed levels.

An example of this type of the model is the COPERT III computer program developed by the CORINAIR Working Group on behalf of the European Commission [59]. COPERT III uses linear regression to express emission factors as function of the average travelling speed (Figure 1.4).

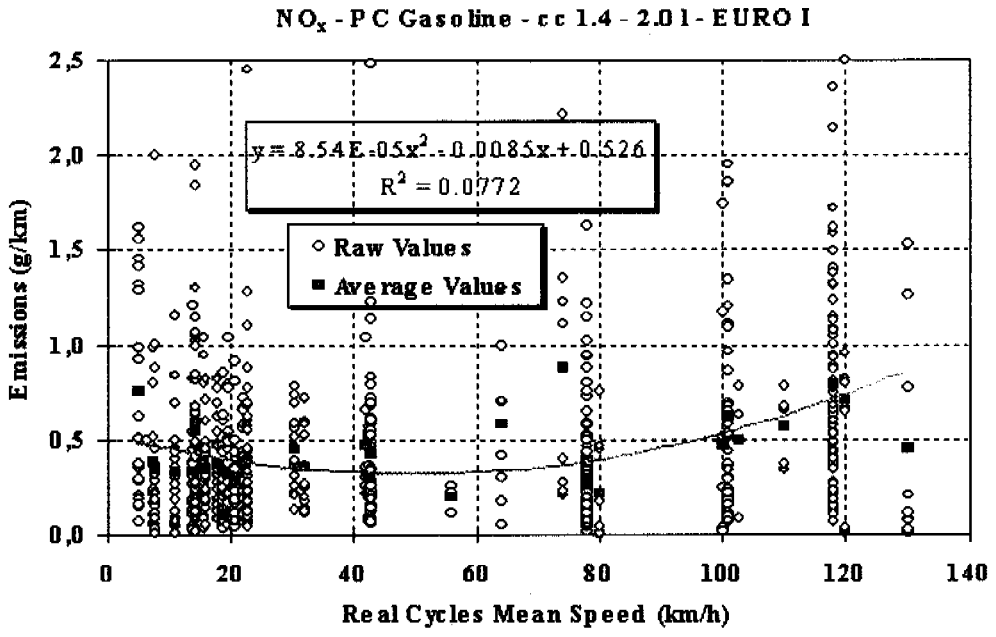

Figure 1.4.: Calculation of NO_x emissions for Euro-1 gasoline vehicles as function of the average speed (source COPERT III)

The prediction quality of the emission factors decreases dramatically from pre-ECE vehicles (since emissions were high and presented good correlation with mean speed) to Euro-1 vehicles (where emissions become lower and more scattered between vehicles and operating conditions). The Pearson coefficient R^2 for the quality of CO estimation drops from 0.924 (for pre-ECE vehicles) to values between 0.133 and 0.159 (for Euro-1 cars), depending on the engine capacity (Table 1.2).

In 2003, about 15 European countries were using the COPERT III model for official emission estimates, among them Belgium, Denmark, France, Greece, Ireland, Italy and Spain. Emission factors for Euro-2, Euro-3 and Euro-4 vehicles were derived from the Euro-1 emission functions using reducing factors.

An evaluation of the COPERT III model was performed by on-road optical remote sensing measurements in Sweden [26] with the results showing not so favorable agreement for CO and HC emissions and better quality for NO_x emissions.

In the US, the MOBILE5 model developed by the U.S. Environmental Protection Agency [15] and the EMPAC model developed by the California Air Resources Board (CARB) [20] attempt to determine the overall emission levels,

Vehicle Class	Engine capacity [l]	Speed [km/h]	CO emission factors [g/km]	R^2 [-]
pre-ECE	all capacities	10-100	$281\ V^{-0.63}$	0.924
	all capacities	100-130	$0.112\ V + 4.32$	-
ECE 11-00/01	all capacities	10-50	$313\ V^{-0.76}$	0.898
	all capacities	50-130	$27.22 - 0.406V + 0.0032V^2$	0.158
ECE 15-02	all capacities	10-60	$300\ V^{-0.797}$	0.747
	all capacities	60-130	$26.62 - 0.44V + 0.0026V^2$	0.102
ECE 15-03	all capacities	10-19.3	$161.36 - 45.62\ln(V)$	0.790
	all capacities	19.3-160	$37.92 - 0.68V + 0.00377V^2$	0.247
ECE 15-04	all capacities	10-60	$260.788\ V^{-0.91}$	0.825
	all capacities	60-130	$14.653 - 0.22V + 0.0011639V^2$	0.613
Improved Conventional	CC<1.4 l	10-130	$14.577 - 0.294V + 0.002478V^2$	0.781
	1.4<CC<2.0	10-130	$8.273 - 0.1511V + 0.00957V^2$	0.767
Open Loop	CC<1.4 l	10-130	$17.882 - 0.377V + 0.00283V^2$	0.656
	1.4<CC<2.0	10-130	$9.446 - 0.23012V + 0.00203V^2$	0.719
EURO 1	CC<1.4 l	5-130	$9.846 - 0.2867V + 0.0022V^2$	0.133
	1.4<CC<2.0	5-130	$9.617 - 0.245V + 0.001728V^2$	0.145
	CC>2.0 l	5-130	$12.826 - 0.2955V + 0.0018V^2$	0.159

Table 1.2.: Speed dependency of CO emission factors for gasoline passenger cars. V represents average driving cycle speed in [km/h] (source COPERT III)

predictions over time and effects of strategies for emissions control. Similar to the European version, these models use average speed as the only variable characterising emissions behaviour.

A further update of MOBILE5 is the MOBILE6 version. Although several improvements were implemented in MOBILE6 regarding cold start emissions, air conditioning, fleet characterisation, idle emissions, etc. [37], the main approach based on average cycle speed was kept. Some additional correction functions for average speeds other than the speed of the FTP-75 cycle used for vehicle type approval were also included in MOBILE6.

However, the dominant parameter, which is the average speed, statistically smoothes the effect of acceleration and deceleration [14]. Two cycles for the same vehicle can have the same average speed, but completely different instantaneous characteristics and, thus, different emissions and fuel consumption levels [42]. Moreover, as Table 1.2 shows, the effectiveness of average speed at describing the emission rates of vehicles is quite poor for modern cars equipped with exhaust gas after treatment systems.

Average-speed models are often used for medium and large scale emission estimates. This type of approach has the clear advantage of being simple and easy to apply in emission estimations. However, since the emission factors are based on average driving situations, this model is not sensitive to the vehicle's operating modes such as idling, accelerating, cruising and decelerating. Thus, major disadvantages appear when used on micro- or meso-scale level, like for traffic management schemes or emission estimates for quarters, cities, etc.

1.4.2. Traffic situation models

Traffic situation models use single emission factors for individual categories of vehicles operating in a specific type of traffic conditions (i.e. urban congested, urban with stop-and-go, rural, motorway, etc.). The emission factors are derived as a mean value of repeated measurements of total emissions over a particular driving traffic situation and are usually expressed in terms of mass of pollutant per unit distance travelled (i.e. g/vehicle-km).

The Georgia Tech's GIS-based mobile emissions model [1] as well as the CHINA-MOBILE emission model developed in China [33] are of this type. In Europe, several traffic situation models were developed at national level, such as the Urban Road Model in Denmark [17], LEEM or AEEM model in UK [50], or

Motor Vehicle Inventory Model in Ireland [67]. In Switzerland, Germany and Austria, the Handbook Emission Factors for Road Transport (HBEFA) is the corresponding traffic situation model [45].

The approach for most of the traffic situation models considers the description of each traffic situation by kinematic parameters, such as acceleration, total stop time, total accelerating time, number of stops, relative positive acceleration, positive kinetic energy, etc. Measurements on test-benches provide data for basic cycles, which are used as a "source" for the further emissions forecasting. In the case of HBEFA, the twelve most important driving patterns which have been selected to represent the real world driving as described in Section 1.3 were used as basic cycles in the model development.

For the forecasting of emission factors produced in unmeasured traffic situations, speed profiles must be provided and their kinematic parameters are afterwards computed. Linear combination of basic cycles which best describes the set of kinematic parameters is then used to determine the corresponding emission factors.

The HBEFA model is able to predict the emission factors with an average absolute error of 8% for CO_2 and fuel consumption, 20% for NO_x, 42% for CO and 41% for HC. The bias, which is a measure of the systematic error, is -3% for CO_2 and fuel consumption, 4% for NO_x, 17% for CO and 21% for HC [23].

Another traffic situations model is the VERSIT+ LD emission factor model [72]. This approach offers the possibility to determine emission factors of passenger cars as a function of driving cycle characteristics. The model consists of a set of statistical representations that are constructed using least-squares multiple regression analysis. The validation exercise performed for the NO_x emission factors gives 15%-36% relative error for a Euro-2 gasoline vehicle.

Traffic situations models provide better emission estimates than the average speed models. This type of modelling is also used for macro- or meso-scale level, such as for regional and national level. However, these models are also based on average emissions of a 5-15 minutes cycle, making their use for micro-scale level inappropriate. Moreover, traffic situations models are not able to include non-standard conditions like different road gradients, gearshift strategies or various loads of the car. Especially for modern catalyst-equipped gasoline vehicles the influences of these conditions should be accurately predicted for reliable emission inventories.

To account for the additional effect of load, slope or gearshift strategies, some traffic situations models include correction functions. However, these correction functions are based on a small number of measurements with few vehicles which may not be representative for the emissions behaviour. Moreover, the combination of these correction factors (i.e. when a vehicle drives uphill with a full load) can be extremely dangerous, since each correction function is developed independently.

1.4.3. Instantaneous emission models

The terms "instantaneous", "modal", "continuous", "online" emission models are used as synonyms. The instantaneous emissions and fuel consumption models operate at a higher level of complexity. They are designed to provide an estimation technique at a micro-scale level. Extensive vehicle measurements are necessary to provide vehicle operation, emissions and fuel consumption data at a high time resolution (typically second by second). The data are then analysed in terms of vehicle's events (modes) such that instantaneous emissions and fuel consumption rates can be estimated on a second by second basis.

Usually, instantaneous emission modelling maps the emissions at a given time to their generating "engine state", like speed, acceleration, engine power, etc. This makes it possible to integrate new, unmeasured driving patterns over the model and calculate their emission factors without further measurements. Thus, emission factors for a large number of driving situations can be determined from the same number of measurements. Beside that, contributory aspects like load, gradient, gear shift strategies can be included, without introducing ambiguous correction functions like in the case of previously mentioned models (Subsection 1.4.1 and Subsection 1.4.2).

Examples of instantaneous emission measurements on engine test benches for heavy-duty engines can be found in [41] and [12]. An instantaneous emission model for heavy-duty vehicles is the PHEM model described in [34].

One approach for characterising vehicle modal events is to set up a speed-acceleration matrix ([83], [46], [32] and [78]) . This matrix provides the instantaneous emissions and fuel consumption for different combinations of instantaneous speed and acceleration. For each cell of speed and acceleration, the emission or fuel consumption rates are averaged to give a mean value.

Other researchers ([42], [11]) used the product of speed and acceleration in-

stead of the acceleration rate. The MODEM emission model is developed by this method [42]. Emissions and fuel consumption data are classified into different classes of speed and speed times acceleration (Figure 1.5). Instantaneous emissions and fuel consumption are then estimated by selecting values from the corresponding combination of speed and speed times acceleration.

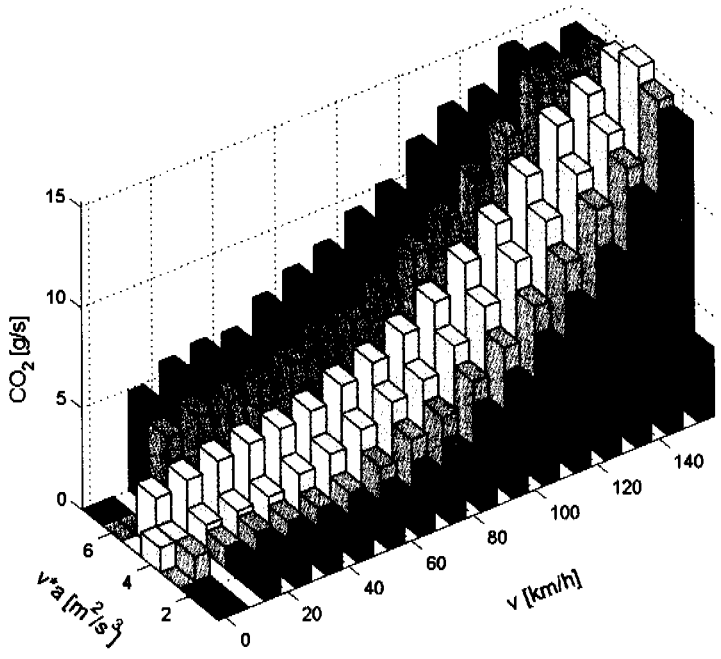

Figure 1.5.: Typical CO_2 map based on speed and speed times acceleration

The errors of this modelling range from -51% to +57%, depending on the driving cycle and the vehicle type [43]. These models are hardly more precise than the average speed models and have the disadvantage of being much more complex to develop. The reasons for this bad quality arise from the fact that the data used come from measurements on a 1 Hz basis, altough experience showed that at least 10 samples per second are needed [79]. Additionally, the variable time-shift of the measurements was not properly compensated. Another drawback of the models based on vehicle speed and acceleration is that they do not include other variables such as road gradient and cannot take into account different gear shift scenarios or load variations.

In a different approach, emissions were modelled as a combination of linear, quadratic and cubic speed and acceleration terms [2]. The main problem of this model is that the coefficients were calibrated once for all vehicle types. In this

way, the distinction between different vehicle categories was not considered. This division was considered in the VT-Micro (Virginia Tech microscopic) model [66], which was included in the MOBILE6 emission inventory. The model categories for the vehicles were determined using classification and regression tree algorithms, but the approach to predict emissions based on speed and acceleration remains practically unchanged.

Emissions models based on engine power and engine speed may prove to be more effective than the emissions functions based on speed and acceleration, as the ones mentioned before, because the effects such as the road gradient can be properly taken into account ([14], [81]).

In [65] another instantaneous emissions model (named POLY) based on vehicle speed and acceleration was developed. However, in this model the road gradient and vehicle loading were additionally considered by including variables like grade of the road segment and vehicle specific power. For this approach, least-square regression models were employed to take into account the effects of acceleration, deceleration and road gradient. The emissions $e(t)$ for each vehicle category and at each moment in time were determined according to:

$$\begin{aligned} e(t) &= a_0 + a_1\, V(t) + a_2\, V^2(t) + a_3\, V^3(t) + b_1\, T_1(t) + b_2\, T_2(t) + \\ &\quad + \sum_{i=0}^{9} c_i\, A(t-i) + d_1\, W(t) \end{aligned} \tag{1.2}$$

Here $V(t)$ represents vehicle speed, $A(t)$ is a variable which contains both acceleration and road gradient, $T_1(t)$ and $T_2(t)$ are used to make the distinction between acceleration and deceleration and $W(t)$ is the specific power relating to the vehicle's kinetic power.

The data employed for this study is the same with the data used in the Comprehensive Modal Emissions Model (CMEM) which was described in [14]. In CMEM, the emissions were expressed as a function of engine demand and other physical parameters related to vehicle operations. The model consists of six modules that predict engine power, engine speed, air-to-fuel ratio, fuel use, engine-out emissions and catalyst pass fraction. This approach provides explanation for the variations in emissions among various parameters and can potentially handle all the factors in the vehicle operating environment that affect emissions. However, this model is highly complex due to the large amount of data required. There are a large number of physical variables for different vehicle types to be determined (engine friction factor, catalyst pass fractions, enrichment threshold and strength, thermal efficiency, etc.). Moreover, too high

degree of parameterisation may complicate the modelling process and can substantially accumulate errors.

The comparison between POLY's and CMEM's performance showed that mean square error is generally smaller for the POLY model for all emissions. When the criterion of correlation is considered, the CMEM model performed better for CO and HC. The prediction errors range from -48 % to +12 %, depending on the considered emission, driving cycle, or vehicle type.

The VeTess computer program developed within the DECADE project by a European consortium represents another instantaneous emission model which is based on measurements made on the engine test benches for three cars. In this approach, four maps are needed for the emissions simulation: steady-state emissions map, jump fraction emissions map, time constant emissions map and additional transient emissions map. However, although this method tries to take into account the transient generation of emissions, the prediction quality is not satisfactory. Moreover, since the engine has to be dismounted and measured on the test benches, this approach is too expensive and time consuming for a reasonable amount of cars.

1.5. Scope of the thesis

The subject of this work is the development of a dynamic model for the instantaneous emissions of vehicles. More specific, the goal was to develop an instantaneous emission model able to predict vehicle fuel consumption and emissions for a given speed profile, for various vehicle loads, slopes and gear shift scenarios using just a limited number of measurements.

Many advantages can appear if it is possible to simulate emissions for any driving situation from the data recorded on a small number of measured cycles:

- The set-up of emission inventories would become much cheaper and flexible.
- The effects of different road gradient, of different loads of the vehicles or of various gear-shift strategies could be predicted without performing expensive additional measurements.
- The impact of traffic control schemes like, for example, the emplacement of traffic lights on road networks and, thus, change of driving behaviour,

could be easily assessed and it would help the traffic decision makers.

The basic idea of this work is to use a statistical model based on the physical mechanism of emissions generation. We used a bottom-up approach, i.e. a simple model was considered and more complexity was added when results were unsatisfactory.

Since the emission scatter from one vehicle to another is extremely large, the instantaneous emissions model was developed at the vehicle level. The resulting emission factors were averaged only afterward, for each vehicle category. The goal of the work was to obtain a 20% prediction quality for each pollutant (CO, HC, NO_x, CO_2) and for each vehicle category.

The main parts of the research were: modeling and compensation of the exhaust gas transport dynamics (Chapter 2), development of a static and dynamic instantaneous emissions model (Chapter 3 and Chapter 4), development and inclusion of a catalyst model (Chapter 5). The Chapters are structured as follows:

In Chapter 2 the exhaust gas transport systems are modelled using signal processing approaches. The goal is to reconstruct the emission signals at their location of formation (catalyst-out or engine-out) from the signals recorded at the analyzers.

Using the reconstructed emission signals, a static instantaneous emission model is developed in Chapter 3. The comparison with old approaches is performed and the ability to predict emission factors for various vehicle categories is also checked.

A further development of the model represents the inclusion of a dynamic variable, able to describe the transient generation of emissions. This dynamic model is described in Chapter 4. The model generates the engine-out emissions of gasoline and diesel vehicles on an instantaneous (10 Hz) basis. Validation of the model for different vehicle loads, for various gradients of the road and for different gear-shift strategies is also verified.

In order to estimate the catalyst-out emissions for gasoline vehicles with after treatment systems, a simplified catalyst model is developed in Chapter 5. This model considers oxygen release and adsorption phenomena as mainly features of the catalyst's behaviour and generates conversion efficiency based on the relative oxygen level in the catalyst.

Finally, some conclusions are drawn and future steps in the research are rec-

ommended.

1.6. Contribution

In this thesis, several personal contributions to the field of emissions modelling have been introduced. First, the modelling of the exhaust gas transport systems by means of linear time-varying approaches was performed with excellent results. The approach is straightforward and can be easily implemented by any emission laboratory.

A second contribution is given by the mapping of emissions based on engine speed and torque, unlike old speed-speed times acceleration maps. It is demonstrated that this type of mapping is capable of predicting the emissions of pre Euro-1 gasoline and of diesel vehicles under different real-world situations.

For gasoline cars equipped with a three way-catalyst, a more complex model is developed. This model generates the engine-out emissions based on a transient 4D engine model. Further on, a catalyst model based on the oxygen storage dynamics is developed to predict the catalyst-out emissions. Although the influence of the catalytic converter on emissions does not represent a novelty in this field, there are no functional simple catalyst models able to reproduce the exhaust pollutants under realistic transient situations.

The catalyst model used here represents a simplification of a more detailed model developed in [13]. Using this simplified catalyst sub-model, the overall emission model proved to be capable of forecasting the generated catalyst-out pollutants for different real-world conditions, concluding in significantly higher accuracy than most other known emission models.

Unlike most of the existing approaches, which try to make the best out of the available data, our approach aimed to answer the question "what do I need for a certain quality?". We used a bottom-up technique, starting with a simple model based on a standard set of investigations. This model was enhanced with more complexity and additional measurements were performed in the cases when the problem could not be successfully solved with the simplified assumptions.

The efforts made during these four years of work were concluded in several presentations at international conferences [8], [5], [7], together with a number of papers published in well known scientific journals, [4], [3], [6], [80].

Seite Leer /
Blank leaf

2. Modelling of the exhaust gas transport systems

2.1. Introduction

The testing of vehicles for environmental emission factors measurement and calculation are usually made on chassis dynamometers and engine test benches. Bag measurements represent the legislative way to determine the mass of emissions (CO, CO_2, HC, NO_x) produced over a legislative cycle. This procedure consists in drawing the entire content of the tailpipe exhaust into a constant volume sampling (CVS) system, where it is diluted with fresh air and, afterwards, a representative sample is put into bags. The analysis of the bags gives a single overall figure for each emission, representing the total mass of emission produced over the driving cycle. The emission factors per kilometer travelled are afterwards determined by division to the total distance.

Bag measurements have their limitations, because they do not provide any information regarding the emissions produced at a specific event. Instantaneous emission measurements become therefore increasingly normal, since much more information about the formation conditions can be extracted than from bag values. When integrated over a driving cycle, the instantaneous emissions data should be equivalent to the bag results. The bag measurements generally act as a verification towards the total sum of instantaneous measurements. The instantaneous measurements always start at the beginning of the cycle and end at the end.

A complete exhaust gas measurement system is capable of measuring concentrations of CO, CO_2, HC, NO_x and O_2. Common devices for the measurement of the exhaust gases are non-dispersive infrared analysers for CO and CO_2, flame ionization detectors for HC, photochemical luminescence detectors for NO_x and paramagnetic sensors for O_2. These common exhaust gas analysers allow measurements at a rate of one to ten samples per second. This gives the impression of having the information of the emitted emission with that chrono-

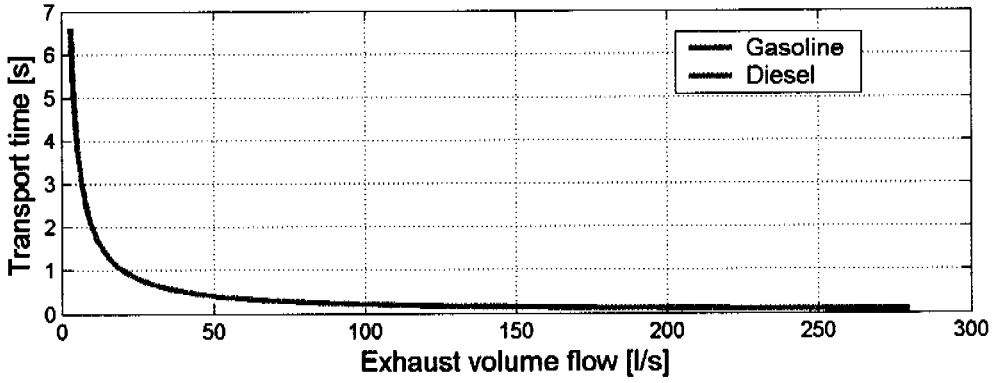

Figure 2.1.: Relation between transport time and exhaust volume flow for a characteristical vehicle with 1.6 l displacement volume and 20 l exhaust volume.

logical precision. It has been shown however [79] that beside the reaction time of the analysers, the dynamics of the gas transport in both the exhaust system of the car and the measurement system last significantly more than one second.

Although transport dynamics and, consequently, incorrect time alignment of emission data is a measurement issue well known in the area of vehicle emissions testing and modelling, the aspects of correcting these misalignments do not appear to have been widely published in the literature. The transport time delay has been, until now, taken into account only by shifting backward the measurement data with a constant number of time steps [35], [47].

However, the actual time delay is not constant. Significant changes in the transport time delay can occur during a transient cycle, due to the varying speed of the exhaust gas flow. Generally speaking, a slow exhaust gas flow at low rpm and low load causes a large delay, while a quick flow at high rpm and high load causes a short delay. This variation in transport times is particularly high for light-duty vehicles with gasoline engines, since the gas volume flow becomes significantly low when the throttle is closed at idle or near-idle conditions, while it reaches its maximum when the throttle is fully opened at full load. Diesel vehicles have no throttle located in the intake manifold. As a consequence, the fresh air is sucked into the cylinders without any big resistance. Thus, the changes of exhaust gas volume flow due to the variable engine speed and engine load are much lower than those for gasoline vehicles.

Figure 2.1 sketches the difference in the transport time variation for a diesel and a gasoline passenger car with a displacement volume of 1.6 l and a typical volume for the exhaust system of 20 l. While for the diesel car the transport

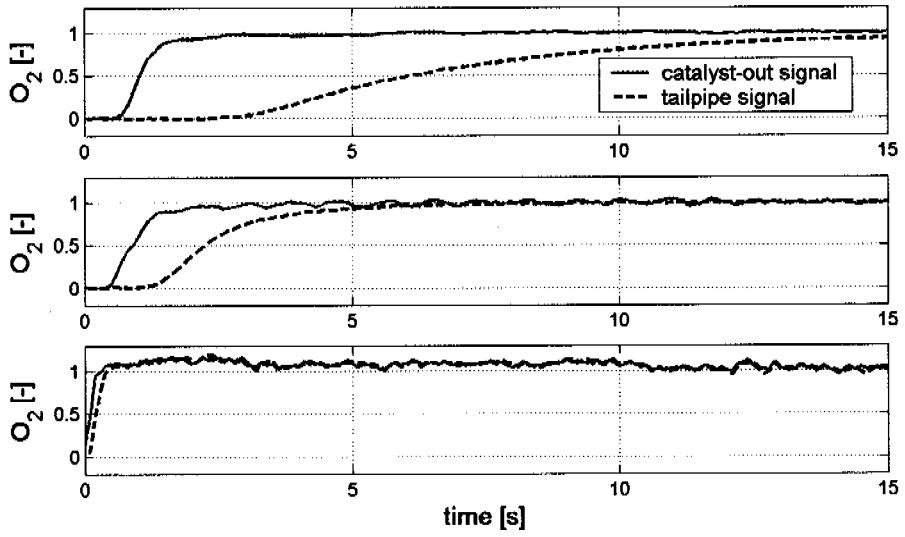

Figure 2.2.: Normalised oxygen signals at the catalyst outlet and at the tailpipe, at different constant loads and speeds of the engine (from top): idle 800 rpm, 2000 rpm with street load (3rd gear) and 4000 rpm with full load.

time varies between 0.078 and 1.3 s, it varies for the gasoline vehicle from 0.071 to 6.6 s.

In addition to this delay, the exhaust gas is convoluted by turbulence during the transport. This causes the smoothing of momentary emission signals (peaks, steps), and these dynamics of mixing also depend on the exhaust volume flow. Variations of, both, transport delay and mixing dynamics in the exhaust system of the car are highlighted in Figure 2.2. It can be seen there that the rise time of the signal at idle lasts more than 10 seconds, while at full load it takes barely 0.1 seconds.

In instantaneous emissions modelling, the emission signals are often statically related at each time span to their causative variables such as vehicle speed, acceleration, torque, engine speed, etc. [83], [42], [14]. If emissions are to be correlated to the actual driving conditions, the variable time delay and the smoothing must be compensated for. Therefore, reconstruction of the original transient data at their location of formation (catalyst-out or engine-out) from the signals recorded at the analysers is necessary.

In some laboratories, the exhaust gas is collected directly after the tailpipe and analyzed at one to ten samples per second (raw gas analysis). In other laboratories, the exhaust gas is first diluted with fresh air and then analysed (diluted or CVS gas analysis).

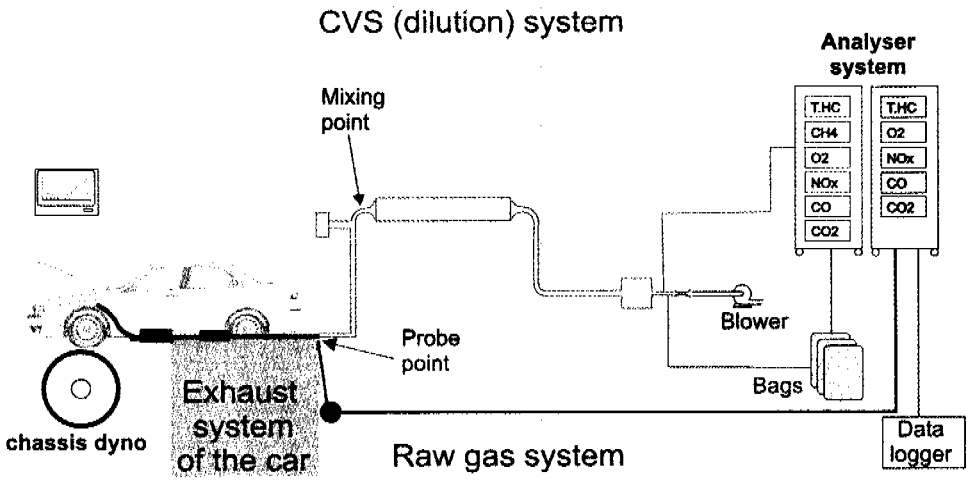

Figure 2.3.: Exhaust gas transport systems.

For the modelling purposes, the exhaust gas transport of both the above cases may be split into three parts, with increasing level of complexity (see also Figure 2.3):

- The first system modelled is the raw gas analyser system. Since, in this case, the volume flow is kept constant by a pump, the parameters of this system can be considered time-invariant.
- The second model describes the exhaust system of the vehicle. Here the transport delay varies typically between 0.1 seconds at high load and several seconds at idle, depending on the exhaust volume flow and on the exhaust system of the vehicle (Figure 2.2). In addition, the exhaust gas is mixed, particularly in the silencer, causing the flattening of the emission peaks. This dynamic of mixing also depends on the exhaust volume flow.
- The third system to be modelled is the dilution (CVS = Constant Volume Sampler) system. This system is a measurement alternative to the raw gas analyzer system and its gas transport is far more complex than the raw gas system. The behaviour of the dilution system also depends on the volume flow, as for the exhaust system of the car. The process through the dilution system has to be modelled by a non-linear, time-varying structure.

The method presented here has been already published in [3], and [6], with some minor modifications made since then.

2.2. Methodology of the model

2.2.1. Basic model

In general, the non-stationary gas transport in tubes, filters, pumps, etc. should be described by the Navier-Stokes equation [82]. This three-dimensional partial differential equation is, however, difficult to solve in practice as it would require the tremendous knowledge of the boundary conditions and the geometry of the entire system. This equation is usually solved by finite elements simulation and the question that arises is how many elements such a simulation needs to provide satisfactory results.

Therefore, in a simplified approach, it is assumed that the basic gas transport system can be modelled as the combination of a thin tube with no friction, where all gas molecules are moving at the same velocity (piston flow), and one or more chambers, where there is so much turbulence that the concentration within the chamber(s) is always homogeneous, and perfect mixing thus takes place. It will be shown consequently that one or two of these basic elements are sufficient for the problems here.

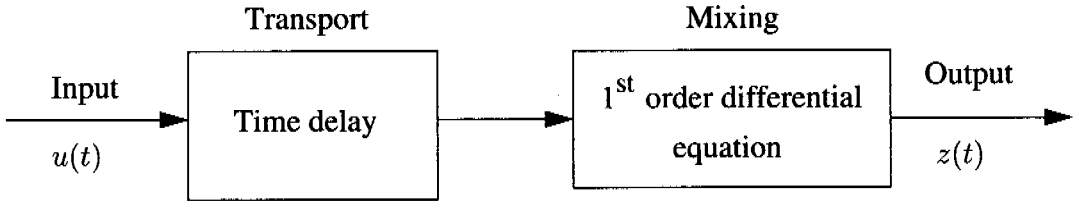

Figure 2.4.: Block diagram of the basic gas transport system

The first part gives a time delay $T_d(t)$, the second results in a linear differential equation of order one (in the case if a single mixing chamber), with the time constant $T_m(t)$ (see Figure 2.4). The sum of these parameters is known as the total delay, $T_t(t)$. The combination results in Equation 2.1, where $u(t)$ denotes the input (the concentration of any gas component at the entrance of the system) and $z(t)$ the output (gas concentration at the exit) of this basic transport model:

$$T_m(t)\dot{z}(t) + z(t) = u(t - T_d(t)) \tag{2.1}$$

Assuming that the volume flow, $\dot{V}(t)$, is a continuous function of time, the total delay generated by the transport of the gases through a system of volume V_{sys}

can be calculated out of mass conservation law as:

$$V_{sys} = \int_{t}^{t+T_T(t)} \dot{V}(\tau)d\tau \tag{2.2}$$

where

$$T_T(t) = T_d(t) + T_m(t) \tag{2.3}$$

If the exhaust volume flow is constant, the total delay can be easily determined as:

$$T_T = \frac{V_{sys}}{\dot{V}} \tag{2.4}$$

According to the above equations, the knowledge of the volume flow is vital for the model parameterization. Approaches for the determination of the exhaust volume flow will be discussed consequently.

In addition, for a gas transport system which also includes analysers (raw or dilution measurement line), the dynamics of the analysers have to be put in series with the gas transport model of Equation 2.1. For the determination of the analysers' model structure, pre-tests were executed with steps as input signals created by switching between zero and different calibration gases. Since all step responses are proportional to each other and their final value was linear to the one of the input, the analysers can be considered as linear time invariant systems. The step responses of most analysers are continuously differentiable, and it thus follows that the description of the analysers is at least of order two. Therefore, the relation linking the input u_a and the output y of the analyzer system is described by the equation:

$$\ddot{y}(t) + a_1\dot{y}(t) + a_0\, y(t) = u_a(t) \tag{2.5}$$

Each analyser for the different components (CO, CO_2, HC, NO_x, O_2) has a unique response characteristic and, consequently, different coefficients.

Approaches for the determination of the exhaust volume flow are discussed next. Afterwards, with the discussed basic elements, the models for the three different gas transport schemes displayed in Figure 2.3 will be developed and validated.

2.2.2. Evaluation of the exhaust volume flow

As stated in Section 2.2.1, the knowledge of the exhaust gas volume flow is vital for the modelling. This variable is calculated directly from the measured

exhaust mass flow, pressure and temperature. Several methods are possible for the measurement of the exhaust mass flow:

- Measuring intake air flow and fuel flow of the car and building the sum.
- Measuring dilution air and the total CVS flow and forming the difference.
- Direct measurement of the exhaust mass flow with ultrasonic flow meter systems or similar [31].

While pressure in the gas transport system is closed to the ambient pressure and can be considered constant, the temperature is a function of both time and location. The temperature within the gas transport system cannot be measured at every point, but a good approximation is the mean of the temperatures at the input and the output of the transport system considered [57].

Even with this approximation, for the exhaust system of the car, the temperature signal at the catalyst outlet cannot be easily measured for economical and technical reasons. A model for the average temperature based on the temperature at the tailpipe is therefore more appropriate.

For that purpose, several steady-state tests were performed with different cars placed on the chassis dynamometer (BMW 318i, displacement volume of 1.8 liters; Nissan Micra, displacement volume of 1.3 liters; Mercedes A140W, displacement volume of 1.4 liters). Table 2.1 shows the values obtained for the tests performed with the Nissan Micra vehicle. For the other two vehicles only 4 tests with constant speed and load were performed.

Nr	Test	$T_{cat-out}$ [K]	T_{pipe} [K]	T_{mean} [K]
1	Idle 800 rpm	520	356	438.0
2	1400 rpm, overrun	458	342	400.0
3	1500 rpm, street load	462	339	400.5
4	2000 rpm, 2nd gear	507	352	429.5
5	2000 rpm, 3rd gear	524	355	439.5
6	2500 rpm, 3rd gear	580	381	480.5
7	3000 rpm, 3rd gear	654	412	533.0
8	4000 rpm, full load	952	694	823.0

Table 2.1.: Steady-state tests for the exhaust system model for Nissan Micra

The mean temperature was simulated using the temperature at the tailpipe of the car simply by linear regression:

$$Temp_{mean} = b_0 + b_1 \cdot Temp_{tailpipe} + b_2 \cdot Temp^2_{tailpipe} \quad (2.6)$$

The result of the model calibration using the steady-state tests is presented in Figure 2.5.

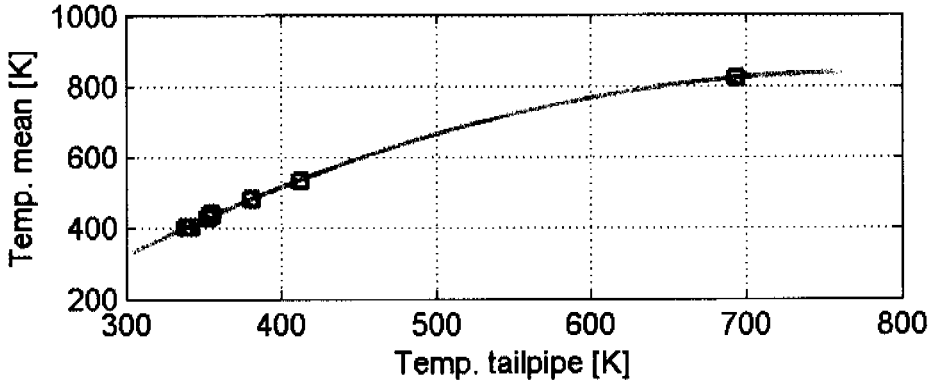

Figure 2.5.: Linear regression model for the exhaust temperature for the Nissan Micra vehicle.

For the validation of the identified coefficients, a transient FTP-75 test was run using the same vehicle. Temperatures at the catalyst-output and at the tailpipe were recorded on a 10 Hz basis. Mean temperature at each moment of time was determined using Equation 2.6 and the results were compared to the values obtained from the measurements. Similar, the exhaust volume flow was calculated using modelled and measured temperatures and the result showed excellent agreement (Figure 2.6).

The same procedure was employed to determine temperature coefficients for the other two vehicles and the same validation method was performed. The regression coefficients were found to be quite similar for the three cars studied.

2.2.3. Raw gas system model

Model structure

The technical system linking the raw gas probe at the end of the tailpipe and the output of the analyser (Figure 2.3) can be regarded as having two parts: one

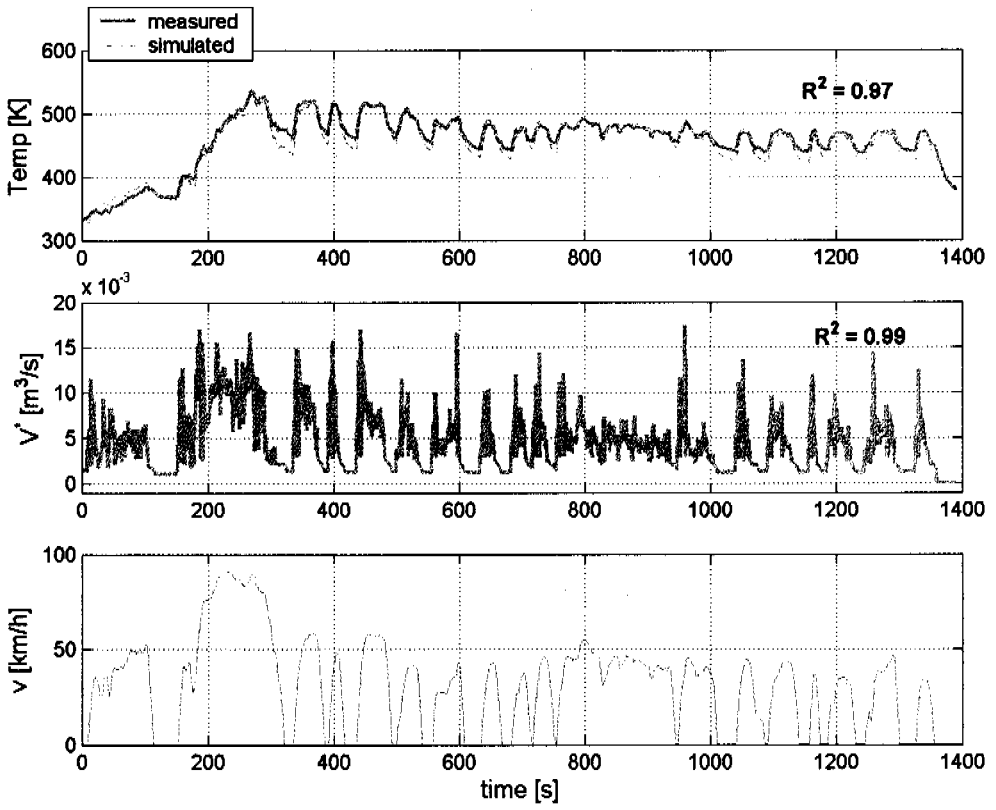

Figure 2.6.: Validation of the temperature model for an FTP-75 test.

part is determined by the transport line of the exhaust gas to the analysers and the second part contains the analyser dynamics. The first part can be described using the basic transport model specified in Section 2.2.1, the second part is modelled as a second-order linear system using Equation 2.5. Therefore, the simplest approach for the whole raw gas measurement system is a linear differential equation of order three (see also Figure 2.7).

Since the data logger protocols the emission signals discretely (up to ten samples per second), this differential equation can be transformed into a difference equation (where y is the concentration signal at the analyser output, u is the concentration signal at the end of the tailpipe and nt is the time delay divided by the sampling rate):

$$y_n = b\, u_{n-nt} - c_1\, y_{n-1} - c_2\, y_{n-2} - c_3\, y_{n-3} \tag{2.7}$$

If the analyser is well calibrated, u and y will have the same value in stationary conditions and thus,

$$b = 1 + c_1 + c_2 + c_3. \tag{2.8}$$

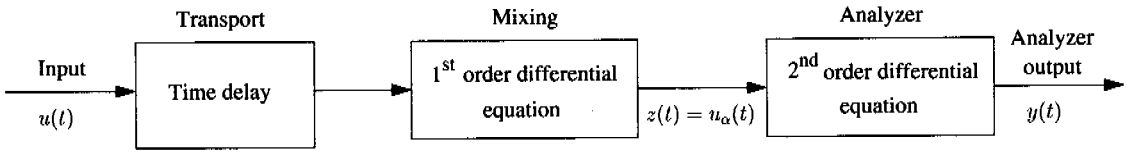

Figure 2.7.: Block diagram of the raw system model

Parameterization and validation

In the parameterisation of the system, two things must be done: first, it has to be proved that this third order approach is sufficient, and second, the parameters c_1, c_2, c_3 and nt have to be identified.

For the parameterisation, measurements can be done using a gas injection inlet installed directly at the probe point (see Figure 2.2 and Figure A.1). A pressure reduction valve and an electrical valve (on/off) are installed between a calibration gas bottle and the injection inlet. Using this system, emission step signals are created at the probe point and the corresponding step responses are measured at the analyser output. This procedure has to be repeated for each analyser.

Parameter estimation can be accomplished through a variety of methods. One prevalent method is the use of prediction of error minimization. The aim of prediction error minimization is to utilize a *least-square criterion* of the form:

$$V_N = \frac{1}{N} \sum_{i=1}^{N} (y_i - \hat{y}_i)^2 \tag{2.9}$$

with $\hat{y}_i$ denoting the estimated output signal.

The parameters of the model can be found numerically by iterative Gauss-Newton algorithm of the specified least-square criterion, since an analytical solution would be impossible to find [49].

Therefore, step responses simulated numerically with Equation 2.7 are matched to the measured step responses. The model parameters are estimated by minimizing the square error V_N. Figure 2.8 shows the measured and fitted step response for the raw oxygen analyser.

Once the representative set of parameters have been determined, the model must be tested in order to determine if it is representative to the actual dynamics of the system. Several techniques are possible to assess the validity of the

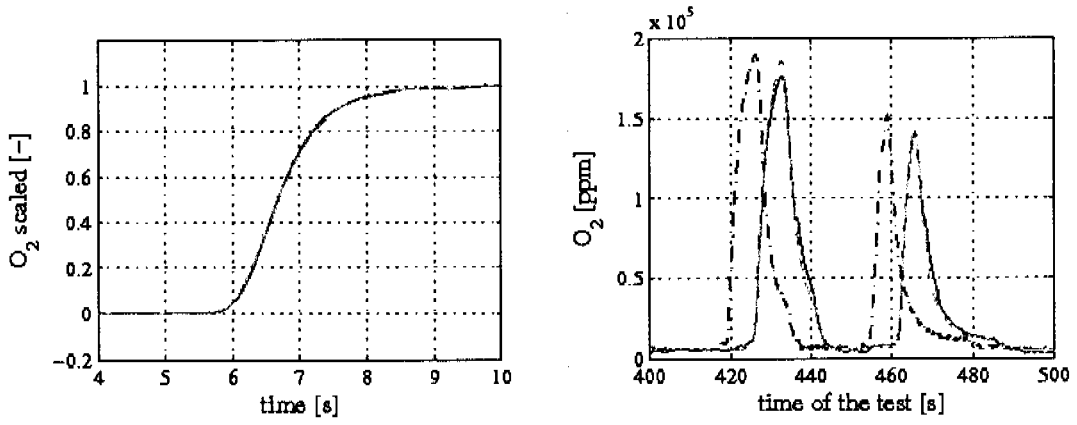

Figure 2.8.: Left graph: measured (solid) and fitted (dashed) step response of the raw oxygen system. Right graph: validation of the transport model for the raw gas system in the FTP-75 test. Note: dash-dotted: signal at the tailpipe, $u(t)$, dashed: simulated analyzer signal, $\hat{y}(t)$, solid: measured analyzer signal, $y(t)$.

model [49]. One such direct approach is to observe how well the model simulates the system output based on a given input.This method of simulation is a commonly applied procedure that compares the actual measured output of a system to the simulated output from the model.

For the validation of the developed raw system model, a transient FTP-75 test was run, using a vehicle mounted on the chassis dynamometer. A continuous lambda sensor (ETAS LSU) was mounted at the end of the tailpipe and was calibrated as an oxygen sensor, having a fast response time of 20 ms. This sensor was used to measure the input signal $u(t)$. In addition, the raw gas signal $y(t)$ was recorded at the analyzer.

Using the measured input $u(t)$ of the raw system (oxygen signal at the tailpipe) and the identified parameters of Equation 2.7, the corresponding output (analyser signal), $\hat{y}(t)$, is simulated and compared to the measured output, $y(t)$. In Figure 2.8 the excellent agreement between measured and simulated output can be checked.

2.2.4. Exhaust system of the car

The exhaust system of the car can be modelled, using the basic model described in Section 2.2.1, as a perfect delay and a first order system. Additional complexity arises here since the volume flow of the exhaust gas may vary by a factor of fifty, depending on the engine load. Therefore, the simple approach used in Section 2.2.3 must be extended.

The transport of the exhaust gas from the catalyst outlet location to the tailpipe goes with the volume flow of the exhaust gases. This volume flow varies between 3 l/s and 150 l/s for a typical 2000 cm^3 car. For an exhaust system of 20 liters, the total delay varies between 0.1 and 6 seconds (Figure 2.2).

Therefore, the parameters of Equation 2.1 become time-varying. In consequence, the sequence of the subsystems becomes important here. The results are different if the transport time delay is considered before or after the mixing chamber. Following the geometry of the exhaust transport system, the time delay should be split ideally into two parts (corresponding to the pipes), with the dynamic part in between (corresponding to the silencer).

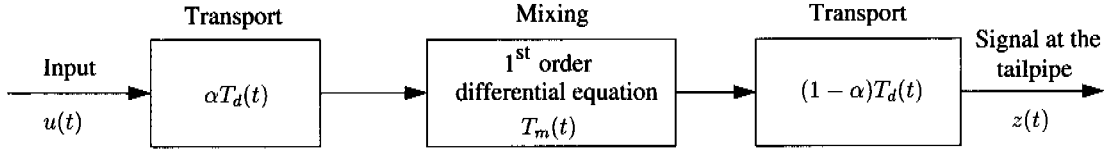

Figure 2.9.: Block diagram of the exhaust system model

Again it was found by least squares optimization that the time delay can be split into two equal parts ($\alpha = 0.5$), thus:

$$T_m(t)\,\dot{z}\Big(t+\frac{T_d(t)}{2}\Big)+z\Big(t+\frac{T_d(t)}{2}\Big)=u\Big(t-\frac{T_d(t)}{2}\Big) \qquad (2.10)$$

This result was tested for two different vehicles with completely different shapes of the tailpipe systems.

The parameters of Equation 2.10, $T_d(t)$ and $T_m(t)$, are now functions of the volume flow and shall be determined according to Equations 2.2 and 2.3. Introducing an additional parameter p, the coefficients of the system can be obtained as:

$$T_d(t)=p\,T_T(t), \qquad T_m(t)=(1-p)\,T_T(t), \qquad 0\le p\le 1 \qquad (2.11)$$

where $T_T(t)$ represents the solution of Equation 2.2. For the model parameterization, the factor p has to be identified.

The following set-up was used for that purpose. A gas bottle inlet was installed directly in front of the catalyst of a BMW 318i, 1.8 liters car, mounted on the chassis dynamometer. This vehicle was driven at different constant states, such as idle, overrun, medium loads and full load (Table 2.2). During these steady states, oxygen step signals were created by closing and opening the gas bottle. Both input and output of the exhaust system of the vehicle were recorded using fast oxygen sensors (Figure 2.2).

Test	T_d $[s]$	T_m $[s]$	p $[-]$	V_{sys} $[l]$
Idle 850 rpm	1.980	4.344	0.66	19.3
Overrun 1400 rpm	1.823	3.525	0.65	19.7
1500 rpm with street load, 3rd gear	0.905	1.609	0.64	20.1
2000 rpm with street load, 3rd gear	0.567	0.999	0.66	20.7
3000 rpm with street load, 3rd gear	0.190	0.323	0.63	18.6
4000 rpm with full load	0.041	0.074	0.64	18.8

Table 2.2.: Estimated parameters of the exhaust system model from different stationary tests for BMW 318i.

For these steady state cases, Equations 2.4 and 2.11 yield:

$$T_d = p\,\frac{V_{sys}}{\dot{V}_{exh}}, \qquad T_m = (1-p)\,\frac{V_{sys}}{\dot{V}_{exh}} \tag{2.12}$$

Here V_{sys} denotes the relevant volume of the exhaust system of the car. However, the volume of the exhaust system that actually participates to the flow is just a percentage of the physical volume, since the pipes and the silencer may contain internal insulation and metal parts causing dead zones for the flow (Figure 2.10).

Therefore, V_{sys} cannot be precisely estimated by external geometrical measurements, due to the unknown flow and the geometry inside it. In the parameterization step, both p and V_{sys} have to be determined and, to avoid more complexity, it has to be verified that neither p nor V_{sys} are functions of the volume flow.

Following the same procedure as for the raw analysing system, the parameters T_d and T_m were estimated by least squares method in each of the steady state

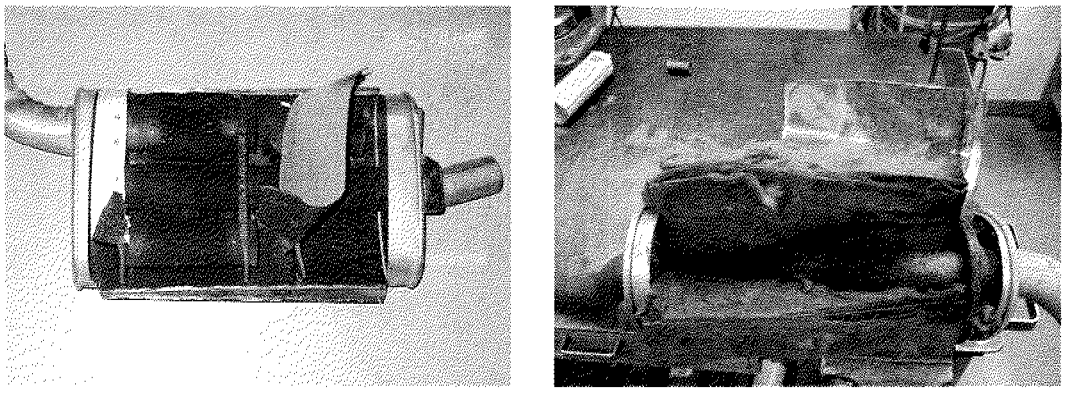

(a) (b)

Figure 2.10.: Interior of a silencer for two different vehicles

cases. Since the volume flow was also recorded, the parameters p and V_{sys} were determined in each case using Equation 2.12.

Table 2.2 shows that, beside some measurement uncertainties, both p and V_{sys} can be considered constant for a given vehicle.

The global parameters of the exhaust system of the analysed vehicle are calculated as the average value of the values estimated in the steady state cases:

$$p[-] = 0.647, \qquad V_{sys}[l] = 19.5 = 0.84\, V_{sys,m} \tag{2.13}$$

Here $V_{sys,m}$ denotes the physically measured exhaust volume of the vehicle.

The additional problem that arises is that these global parameters (p and $\frac{V_{sys}}{V_{sys,m}}$) may vary from vehicle to vehicle. To analyze that, similar tests were performed with a different vehicle (Nissan Micra, displacement volume of 1.3 liters). The same approach was used for the model parameterization. The global parameters found in this case were:

$$p[-] = 0.656, \qquad V_{sys}[l] = 0.87\, V_{sys,m} \tag{2.14}$$

Thus, both the parameter p and the correction factor between measured and relevant exhaust volume are similar for the two cars studied. This leads to the hope that these parameters may be used generally.

For the model validation, a transient FTP-75 test was run. At the input and output of the investigated system, the oxygen concentrations were again instantaneously logged using fast lambda sensors.

Since the volume flow is no longer constant here, the total delay $T_T(t)$ must be determined from Equation 2.2. To solve this equation the exhaust volume flow must be known at all moments in time. However, the available measurements contain only discrete values of the volume flow. For this reason the integral from Equation 2.2 is approximated numerically by the sum:

$$V_{k,N} = \sum_{i=k}^{k+N} \dot{V}_i \, \Delta t = \sum_{i=k}^{k+N} \Delta V_i \tag{2.15}$$

where $N \in \{0, 1, 2, 3, \ldots\}$ and Δt is the sampling rate.

The total delay at the k-th moment ($T_T(k)$) is determined by linear interpolation between the closest approximations ($V_{k,N}$ and $V_{k,N+1}$) of V_{sys} as:

$$T_T(k) = N \cdot \Delta t + \frac{V_{sys} - V_{k,N}}{V_{k,N+1} - V_{k,N}} \cdot \Delta t \tag{2.16}$$

With the determined $T_T(k)$ and parameter p identified as described above, the time delay and time constant of the system, $T_d(k)$ and $T_m(k)$, are determined using Equation 2.11. Further, the output of the system is simulated using Equation 2.10. Figure 2.11 shows the excellent quality of the simulated tailpipe signal when compared to the measured one.

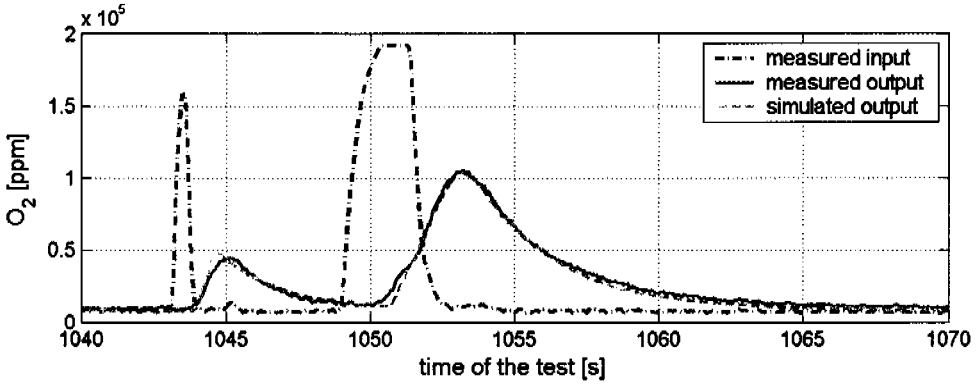

Figure 2.11.: Validation of the transport model for the exhaust system in a dynamic FTP-75 test. Note: dash-dotted: oxygen signal at the catalyst outlet, solid: measured signal at the tailpipe, dashed: simulated signal at the tailpipe.

2.2.5. Dilution system model

Model structure

An alternative method to the raw system for measuring emissions is the Constant Volume Sampling (CVS) system where the entire content of the tailpipe exhaust is diluted with fresh air. The model for the dilution system has to be

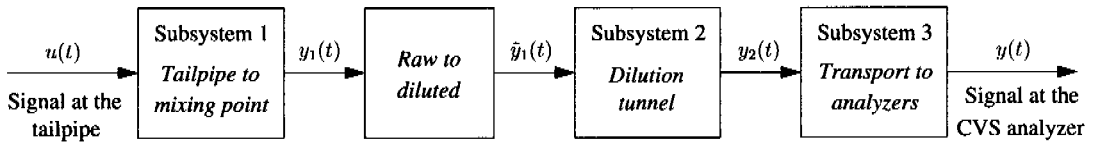

Figure 2.12.: Block diagram of the dilution system model

split up into subsystems as described in Figure 2.12 (see also Figure A.3 in Appendix A.2):

- In most CVS systems, the point where the raw exhaust gas is mixed with the dilution air is some meters away from the tailpipe (Figure 2.3). The transport of gas from the tailpipe to the mixing point goes with the volume flow of the exhaust gases. As explained in Section 2.2.4, this volume flow varies between 3 l/s and 150 l/s for a typical 2000 cm^3 car and, thus, the total delay varies between 0.3 and 16 seconds for a pipe system of 50 liters as in our case. Hence, the first subsystem, which describes the transport between the tailpipe and the mixing point, varies with time. This subsystem is modelled by applying again the basic model. It results in a varying time delay (divided in two parts as for the exhaust system of the car) and a turbulent mixing system composed of two similar mixing chambers, set in series. Two first-order systems, with the same time constant, therefore result. With $u(t)$ denoting the input signal (gas concentration at the tailpipe), $y_1(t)$ the output of this part (gas concentration right before the mixing point), $T_{d,1}(t)$ the time delay and $T_{m,1}(t)$ the time constant of the system, the description of the first subsystem becomes:

$$T_{m,1}^2(t)\cdot\ddot{y_1}\Big(t+\frac{T_{d,1}(t)}{2}\Big)+2\cdot T_{m,1}(t)\cdot\dot{y_1}\Big(t+\frac{T_{d,1}(t)}{2}\Big)+ \\ +y_1\Big(t+\frac{T_{d,1}(t)}{2}\Big)=u\Big(t-\frac{T_{d,1}(t)}{2}\Big) \quad (2.17)$$

- The processing of the raw gas concentrations at the mixing point is nonlinear: the raw concentration values (in ppm) have to be multiplied by

the (time varying) exhaust volume flow (in m^3/s) to calculate the diluted concentration. The volume flow balance gives:

$$\tilde{y}_1(t) = \frac{y_1(t)\dot{V}_{exh}(t) + y_{dil}(t)\big(\dot{V}_{CVS} - \dot{V}_{exh}(t)\big)}{\dot{V}_{CVS}} \tag{2.18}$$

Here $\tilde{y}_1$represent the gas concentration of the exhaust gas species after the mixing and y_{dil} is the concentration of the gas species in the ambient air. Since no big variations are recorded in the dilution tunnel, the CVS volume flow is treated as constant.

- After this static non-linearity, the second subsystem describes the transport through the dilution tunnel. This subsystem is modelled again as a time delay and a second-order dynamic for the turbulence. Since the transport speed variations in the dilution tunnel due to temperature changes are negligible, the parameters of this subsystem can be considered as time-invariant. With $\tilde{y}_1$ denoting the input of this subsystem, $y_2(t)$ the output (diluted gas at the end of the dilution tunnel), $T_{d,2}$ the time delay and $T_{m,2}$ the time constant of the system, we obtain:

$$T_{m,2}^2\,\ddot{y}_2(t) + 2\,T_{m,2}\,\dot{y}_2(t) + y_2(t) = \tilde{y}_1(t - T_{d,2}(t)) \tag{2.19}$$

- Finally, the same approach is used for the transport in the small tubes carrying the gas from the CVS tunnel to the analyzers and the analyzers dynamic is added. This is the third part and it is sufficient to be modelled as a time delay and a second-order linear system:

$$a_1\,\ddot{y}(t) + a_0\,\dot{y}(t) + y(t) = y_2\big(t - T_{d,3}\big) \tag{2.20}$$

As a consequence, the model for the gas transport through the dilution system becomes a *non-linear* time varying system of order *six*.

Parameterization and validation

For the model parameterization, similar gas bottle tests, as described for the previous systems, were performed. Concentration step signals were generated by injecting calibration gases at the input of each of the subsystems of the dilution system and the emission step responses were logged at the corresponding output by fast sensors.

Test	$\dot{V}_{exh}$ [l/s]	$T_{d,1}$ [s]	$T_{m,1}$ [s]	p_d [-]	p_m [-]
Idle, 850 rpm	3.89	12.39	1.344	0.82	0.090
2000 rpm, street load, 3rd gear	8.19	5.95	0.610	0.83	0.085
4000 rpm, street load, 3rd gear	22.72	2.07	0.259	0.80	0.100

Table 2.3.: Estimated parameters of the first subsystem of the dilution model using different stationary tests.

Since the first subsystem of the dilution system has time-varying coefficients, several steady state tests at different vehicle loads are needed. The following set-up was used for that purpose: A gas bottle inlet was installed directly at the tailpipe of the BMW 318i, 1.8 liter car, mounted on the chassis dynamometer. The car was driven at different constant states, such as idle, medium load and full load (Table 2.3). During these steady states, oxygen step signals were created by closing and opening the gas bottle. Both, signals at the tailpipe and at the mixing point were logged using fast oxygen sensors.

The model coefficients for the first subsystem can be determined using Equation 2.3 as:

$$T_{d,1}(t) = p_d\, T_{tot}(t),\ T_{m,1}(t) = p_m\, T_{tot} \tag{2.21}$$

where T_{tot} represents the total time delay of this transport subsystem and:

$$p_d + 2\, p_m = 1. \tag{2.22}$$

The factor 2 in the previous equation derives from the two mixing chambers considered in the model description.

For these steady-states, T_{tot} is determined using Equation 2.4. In this case, the system volume represents the volume of the pipes between the tailpipe to the mixing point and is evaluated by physically measuring the geometry of the pipes.

For the identification of the model parameters, the same approach as for the exhaust system of the car was followed.

Table 2.3 shows that, beside some measurement uncertainties, both p_d and p_m can be considered constant for this subsystem. Therefore, the global parameters of this subsystem are obtained as the average value of the values determined in the steady state cases:

$$p_d[-] = 0.8167,\ p_m[-] = 0.0917. \tag{2.23}$$

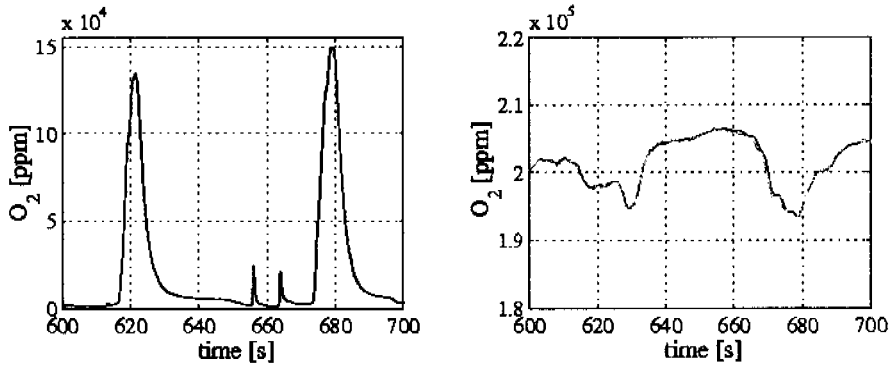

Figure 2.13.: Result of CVS model validation. Note: left: measured oxygen at the tailpipe, $u(t)$, right: measured (solid), $y(t)$, and simulated (dashed), $\hat{y}(t)$, oxygen signal at the dilution analyzer.

The second and third parts of the dilution system have time invariant coefficients; therefore, only one gas bottle test was necessary for the identification of these parameters in each case. The same procedure as explained above was used to determine the time delay and time constant of each of these subsystems.

For the validation of the identified parameters, an FTP-75 test cycle was run again. No gas was injected, but the *natural* concentration signal of the exhaust specie was measured at the tailpipe by fast sensors to log the input signal, $u(t)$. Additionally, the dilution analyzer signal, $y(t)$, was also recorded.

The simulation of the model was performed subsystem by subsystem. Figure 2.13 shows the quality of the simulation,$\hat{y}(t)$, compared to the measured signal at the analyzer, $y(t)$.

2.2.6. Overall validation

Until now the modelling and validation for each of the exhaust gas transport system has been presented. However, the goal is that the overall system, from the catalyst-outlet to the analyser, to be modelled. The models of the measurement line and exhaust system of the car are therefore connected. Figure 2.14 shows the quality of the simulation of the analyser signal using as input the signal at the catalyst outlet.

As an additional observation, the plateau seen at the oxygen signal at the catalyst-

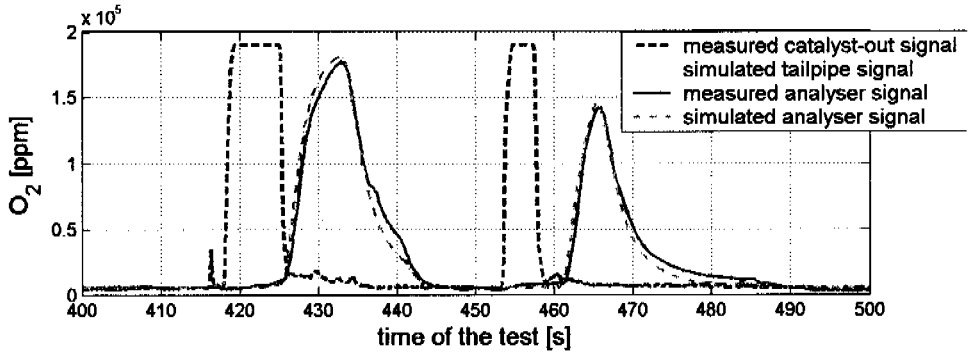

Figure 2.14.: Overall validation of the system from the catalyst-out to the raw analyser.

out location is not a measurement error, but arises from the fact that oxygen has attained its limit of 21 percent in the air during an overrun fuel cut-off situation.

It has been, therefore, shown that it is possible to model the exhaust gas transport systems for typical chassis dynamometer test equipment. Obviously, the easiest part is the modelling of the raw gas system, i.e. the transport from the raw probe point (at the tailpipe) to the raw analyser output, since this leads to time-invariant models. Modelling the dynamics in the exhaust system of the car is a more complex step, since the system is time variable, and the most difficult task of all is to model the dilution system, since it is a combination of the other two problems and, additionally, includes a non-linear static relation. Moreover, the knowledge of the exhaust volume flow is necessary here. This is in contrast to the standard CVS measurement procedure, were no information about the volumetric flow is considered necessary.

Several details have to be addressed in order to make this modelling ultimately useful. These are:

- The exhaust volume relevant to the gas transport is estimated by measuring geometrically the exterior volume of pipes and silencer. A correction factor between this exterior volume and the actual volume relevant for the flow has to be determined. For the two cars measured, this correction factor was found to be similar (85 percent of the measured exhaust volume).
- Also the parameter p corresponding to the division of the exhaust system of the vehicle was found to be similar for the two cars studied (0.65). More cars nevertheless need to be studied for complete validation.

The overriding goal is that no holes must be drilled into the car's exhaust system, so that cars from private owners can be taken for emission inventories without incurring major costs. For this reason, the signals at their location of formation should be reconstructed from the signals at the analysers. Therefore, after the step of modelling described here, the identified models must be inverted. This is the subject of the Section 2.3.

2.3. Methodology of the inversion

2.3.1. Basic inversion model

To achieve the final reconstruction of the emission signals at the catalyst outlet location, the models developed in Section 2.2 must be inverted. This means that, for a basic transport system, the model Equation 2.1 must be solved for the input, $u(t)$. Doing this, $u(t)$ becomes a linear combination of the output $y(t)$ and its derivative(s). As the output $y(t)$ is a measured signal, it is always overlaid by some noise (random error), which is highly amplified by building the derivatives. A low-pass filter is therefore necessary for the noise reduction in $u(t)$.

There are many different approaches for efficient filter parameterization. Most of these methods are designed to achieve good qualities in the frequency response, i.e. a sharp drop-off at the cut-off frequency, zero-noise amplification in the stop band, etc [48]. However, they create fairly damped step responses with overshoots, which cannot be accepted for concentration signals (for example, concentration signals that are below zero are meaningless).

Filters were therefore created by the author which show maximally sharp cut-off behavior (to minimize noise without *distorting* too much the true signal), but with no overshoot for signals with no noise. A pole placement method was applied here. The transfer function of the filter necessary for the inversion is:

$$F(s) = \frac{1}{T_f\, s + 1} \tag{2.24}$$

with T_f being the filter time constant.
Consequently, the transfer function of the inversion is given by:

$$\tilde{G}(s) = \frac{T_m\, s + 1}{T_f\, s + 1} \tag{2.25}$$

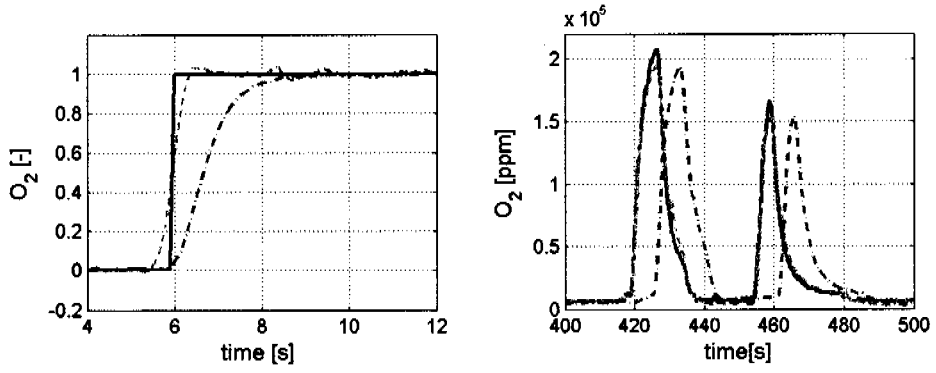

Figure 2.15.: Result of the inversion (left) and validation of inversion (right) of the oxygen raw system. Note: measured (solid) *u(t)* and reconstructed (dashed) $\hat{u}(t)$ emission signals at the tailpipe, dash-dotted: measured analyzer signal *y(t)*.

This basic inversion is applied subsequently for the different systems of exhaust gas transport.

2.3.2. Inversion of the raw gas analyzer system

Since the raw gas system is described by a third-order linear difference equation, a third-order filter was chosen. The damping was set to avoid overshoot, and the time constant was searched for optimal noise suppression, which resulted in the filter time constant being four times shorter than the time constant of the model. This can be interpreted that the area between the delayed input unit step and corresponding step response is circa four times larger than the area between the same unit step and the inverted signal (Figure 2.15). Afterwards, the time delay is easily compensated by shifting back the inverted signal.

The choice of the filter time constant depends on the noise level of the measurement signals, and thus on the quality of the analyzers. The factor four used here for the filter time constant refers to a signal-to-noise-ratio of about 20 dB.

For the validation of the developed inversion, an FTP-75 test was run, using a vehicle mounted on the chassis dynamometer. A continuous lambda sensor (ETAS LSU) was installed at the end of the tailpipe and was calibrated as a fast oxygen sensor. This sensor was used to measure the input signal $u(t)$. In addition, the raw gas analyzer signal $y(t)$ was recorded. The comparison between the reconstructed and measured signal at the tailpipe ($\tilde{u}(t)$ and $u(t)$,

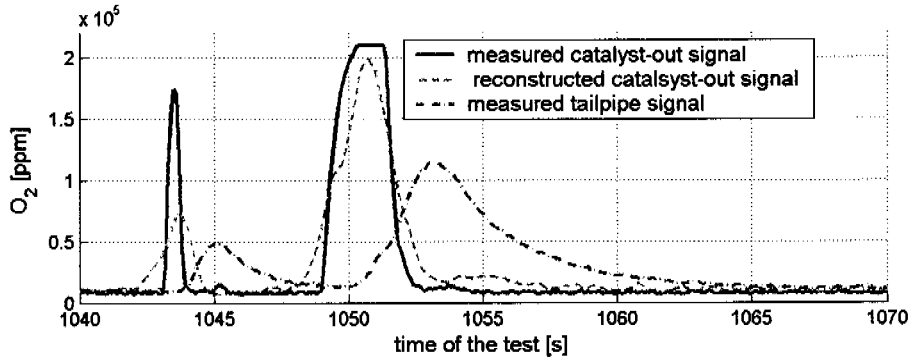

Figure 2.16.: Inversion of transport dynamics for the exhaust system. Note: measured (solid) and reconstructed (dashed) oxygen signal after the catalyst, dash-dotted: measured signal at the tailpipe.

respectively), is presented in Figure 2.15. As it can be seen, the quality of the reconstruction is excellent.

2.3.3. Inversion of the exhaust system of the car

To achieve the reconstruction of the emission signals at their location of formation using the signal at the tailpipe, the exhaust system model has to be inverted, i.e. Equation 2.1 must be solved for $u(t)$. This again necessitates a filter.

Since that model has a time varying coefficient $T_m(t)$, the filter time constant, $T_f(t)$, must also be adapted. For that purpose, the same steady-state situations used for the model parameterization were considered. In each of these cases, the best filter time constant was determined, following the same optimization criterion as for the raw gas system. The time-varying parameter of the filter was then determined by regression as a function of the model time constant. A second order polynomial function fits best the data points:

$$T_f(t) = f_0 + f_1\, T_m(t) + f_2\, T_m^2(t) \tag{2.26}$$

Due to the limited sampling rate of 0.1 seconds, a filter is needed only when the system time constant $T_m \geq 0.04$ ($T_{90} \geq 0.1$ seconds), which means that for dynamics faster than 0.04 seconds, the inversion may be switched off.

While in the time invariant case the time delay can be easily compensated by shifting back the signal, a more complex algorithm has to be used for the case

here. The total delay has to be determined as the solution of Equation 2.2, and the composing time delay and time constant of the system are afterwards estimated from Equation 2.11.

The inversion must also follow the geometry of the exhaust system (Figure 2.9) and therefore in the case of a transient test the inversion is made in three steps:

- First, the variable time delay from the tailpipe to the silencer is compensated, using as delay $0.5\,T_d(t)$.
- In a second step, the first order system is inverted, using the filter whose time constant was already determined by regression.
- Third, the last part of the variable time delay from the silencer to the catalyst out location is compensated and the reconstruction of the signal at the catalyst-out is achieved.

Figure 2.16 illustrates the quality of this time-varying inversion of the exhaust system dynamics. A perfect reconstruction cannot be achieved due to the filter inclusion and to the inherent uncertainties in the mass flow measurements. The signal at the catalyst out location can be reconstructed from the signal at the tailpipe with a time quality of about 0.5 seconds.

2.3.4. Inversion of the dilution analyser system

To achieve the reconstruction of emission signals at the tailpipe from the signal at the dilution analyzer, the overall CVS model must be inverted. This inversion is made subsystem by subsystem. In each case the input of the subsystem must be determined from its output.

Since the second and the third subsystems of the CVS model have time-invariant characteristics, the same approach as for the inversion of the raw gas system is followed.

For the part between the car's tailpipe and the mixing point a time varying filter is designed, analogous to the one used for the exhaust system.

Beside the inversion of these subsystems, the nonlinear Equation 2.18 corresponding to the dilution of raw exhaust gases at the mixing point has to be solved for y_1. However, for signals such as oxygen, which is contained in both

the exhaust gas and dilution air, this step is not possible, because the signal-to-noise ratio of the measurement is too small.
For this reason, the NO_x signal was preferred for the validation of that model inversion. Since no measured NO_x signal at the tailpipe was available, the reconstructed NO_x signal using the raw gas line was used for comparison. The quality of the overall CVS inversion is presented in Figure 2.17.

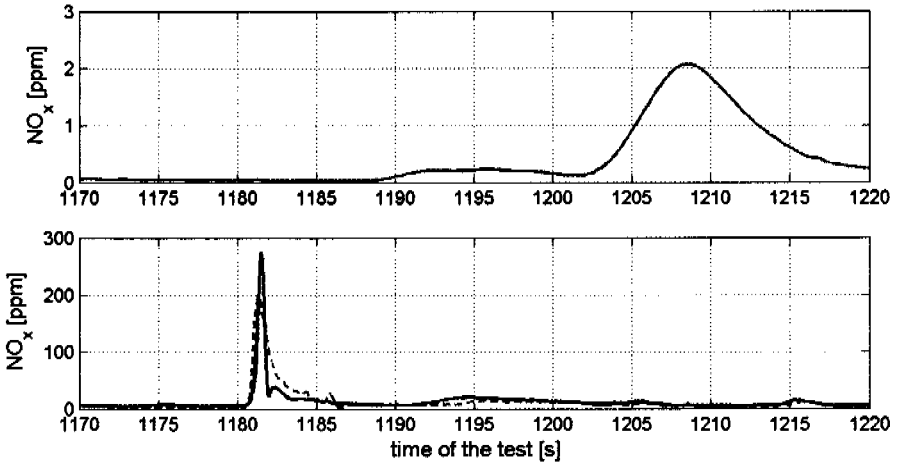

Figure 2.17.: Inversion of the dilution system model. Top figure: NO_x signal at the dilution analyzer. Bottom figure: reconstructed signal using the model of the dilution system (dashed) and reference signal at the tailpipe, obtained from the raw gas measurements (solid).

The measured peak, which lasted more than twelve seconds in the diluted measurements can be reconstructed to a peak of about 3.5 seconds duration. This is a very good result in itself. However, the quality is roughly half as good as for the raw gas system inversion, whose peak lasts just 1.7 seconds.

2.3.5. Overall inversion

So far, the modeling, inversion and validation of each of the exhaust gas transport systems have been presented. However, the final goal is that no holes have to be drilled into the car's exhaust system, so that cars from private owners can be taken without incurring major costs for emission inventory measurements. For this reason, the signal at the catalyst-outlet location should be reconstructed from the signal recorded at the analyzer. The inversion models for the measurement line and exhaust system of the car are therefore connected.

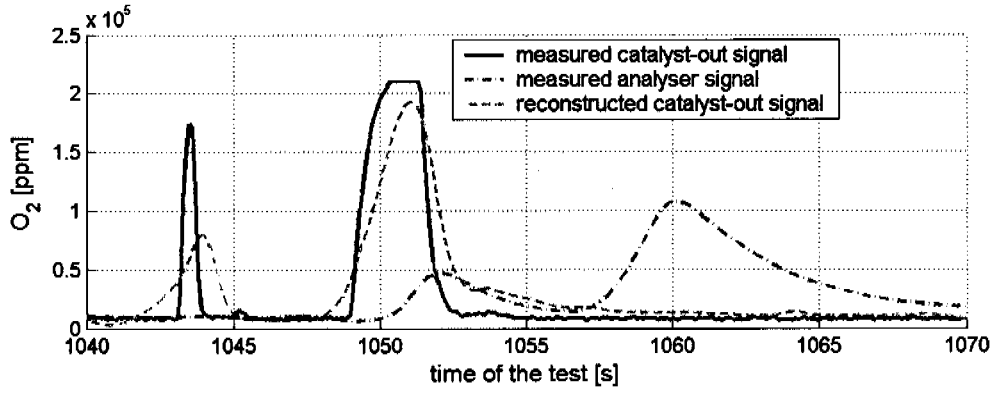

Figure 2.18.: Inversion from the analyzer until the catalyst-out

Figure 2.18 shows the quality of the reconstructed oxygen signal at the catalyst outlet from the analyzer signal. The time quality of this overall reconstruction is about 0.8 seconds, when raw gas measurements are used.

Moreover, the integral value (i.e. the sum) of the reconstructed emission data has been compared to the integral value of the measured emissions at the catalyst outlet and a deviation of less than 1.5 percent has been found, which is considered to be excellent for the emission inventories.

Using signals from the diluted measurements, the quality of the reconstructed signals shows maximal time errors of 2.5 seconds, which is significantly better than using the original signal with up to 25 seconds uncertainty, but which is notably worse than using the raw line.

In addition, it is essential for the reconstruction process to know the exhaust volume flow. Thus the original advantage of CVS measurements, of not needing the exhaust volume flow signal, is lost.

3. Static instantaneous emission model

3.1. Introduction

The availability of vehicle emission models has improved significantly in the last decade. However, there are still problems that can affect the prediction quality of the existing approaches. Most of these problems appear due to the lack of data on emission measurements for different types of vehicles, vehicle operational modes, inaccuracies in the measurements due to the gas transport dynamics and difficulties inherent in accurately predicting vehicle usage under real driving conditions.

Emission models based on bag data such as average speed models or traffic situations models are often inadequate to assess the emissions impact of various transportation management schemes, transportation control strategies or inspection/maintenance programs contained in most air quality management plans. What is needed besides these macroscale models is an emission model which takes into account the modal operating conditions of the vehicles (i.e. emissions that relate directly to the vehicle operating situations such as idle, acceleration, deceleration, etc).

The influence of speed fluctuation on emission levels is important for microscale applications, like emission modelling applied to the level of single streets. Such an instantaneous emission model would have a significant role in evaluating microscale traffic scenarios (like the emplacement of traffic lights, signal coordination, impact of traffic calming or speed limitations on emission levels, etc.). Moreover, this type of modelling could also improve macroscale or mesoscale emission inventory predictions by managing to forecast non-standard effects as load, slope or gear-shift strategies onto emissions level.

For the development of instantaneous emission models, emission measurements on chassis dynamometers with a high time resolution are needed. In most of the instantaneous emission models, the exhaust gas signals and all

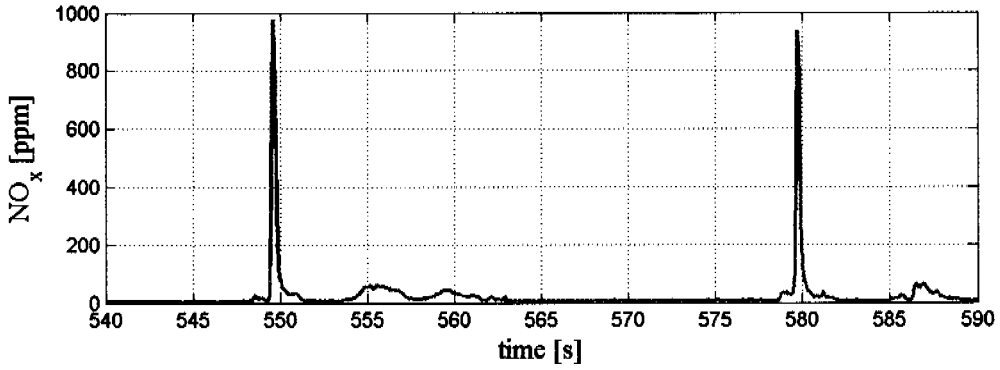

Figure 3.1.: NO_x emissions on a transient cycle for a three-way catalyst vehicle.

other information from the tests are collected at a rate of one to ten samples per second.

From the analysis of emission signals measured with fast sensors (lambda sensors for oxygen, NO_x sensors, fast FID (flame ionization detector) for hydrocarbons) it follows that the "emission peaks" last less than one second (Figure 3.1). Their frequency content is up to 5 Hz. Some engine related signals, like torque or manifold pressure, may also change significantly within a few tenths of a second [79]. From signal theory it is well known that by sampling a signal with a frequency f all information above $f/2$ is lost [48]. Thus, a significant part of the frequency content of the signals is lost at the usual sampling rate of 1 Hz. For this reason, it is advisable to collect the emissions and engine signals on a 10 Hz basis or faster.

The mapping of instantaneous emissions is mostly performed by statically relating the emission signals at each time span to their causative variables, such as vehicle speed, torque, engine speed, etc [83], [42], [14]. As a result of this static approach, the emission values can be correlated to the correct engine state of the car only if they are at the correct location on the time scale. But the original signals measured in a test are delayed in relation to their location of formation, due to the transport from the the engine to the analysers. If these dynamic aspects of the exhaust transport are neglected, the emission events are correlated to "the wrong second", resulting in incorrect engine status in emission modelling. Therefore, it is critical to reconstruct the emission signals at their location of formation by means explained in Chapter 2.

In conclusion, two pre-conditions have to be fulfilled for accurate instantaneous emission modelling:

- Frequency of the measurements: emissions and all other related engine signals should be collected on a 10 Hz basis, due to their frequency content.

- The transport dynamics from the engine to the analysers must be compensated by time-varying approaches.

Another aspect which has to be considered is the scatter of emissions from car to car, even for vehicles belonging to the same vehicle category.
From the Euro-1 legislation, which requires the presence of a three-way catalyst together with a lambda sensor, the advances in vehicle technologies have improved considerably. As a result of the different concepts used for different makes and models, large discrepancies between emissions behaviour of various vehicles can be observed. This can be considered natural, since vehicles from different manufacturers with different exhaust gas after treatment systems are measured. Moreover, for each car model the control logic in the ECU is tuned differently. But for instantaneous emissions modelling these differences are important to consider, since, in old approaches, emission data from many different vehicles were binned in the same emission matrix. Hence, very large standard deviations within this matrix were obtained.

As an example, Figure 3.2 depicts the time series of CO emissions from three different Euro-3 gasoline vehicles (see Table 3.1 for details about vehicles) during the same period of the CADC cycle. As it can be seen, although the cars have similar characteristics (legislation level, mass, power, displacement volume, mileage), the differences in emissions at the same speed profile are considerable. This behaviour is possibly determined by internal causes such as different response times of the lambda sensor, ageing of the catalytic converter and, mainly, by different control logic in the ECU.

Therefore, it becomes advisable to develop the instantaneous emission model at vehicle level and to average the resulting emission factors as a last step, for each vehicle category. The model developed here was described in [4], but some modifications and new results have been acquired since then.

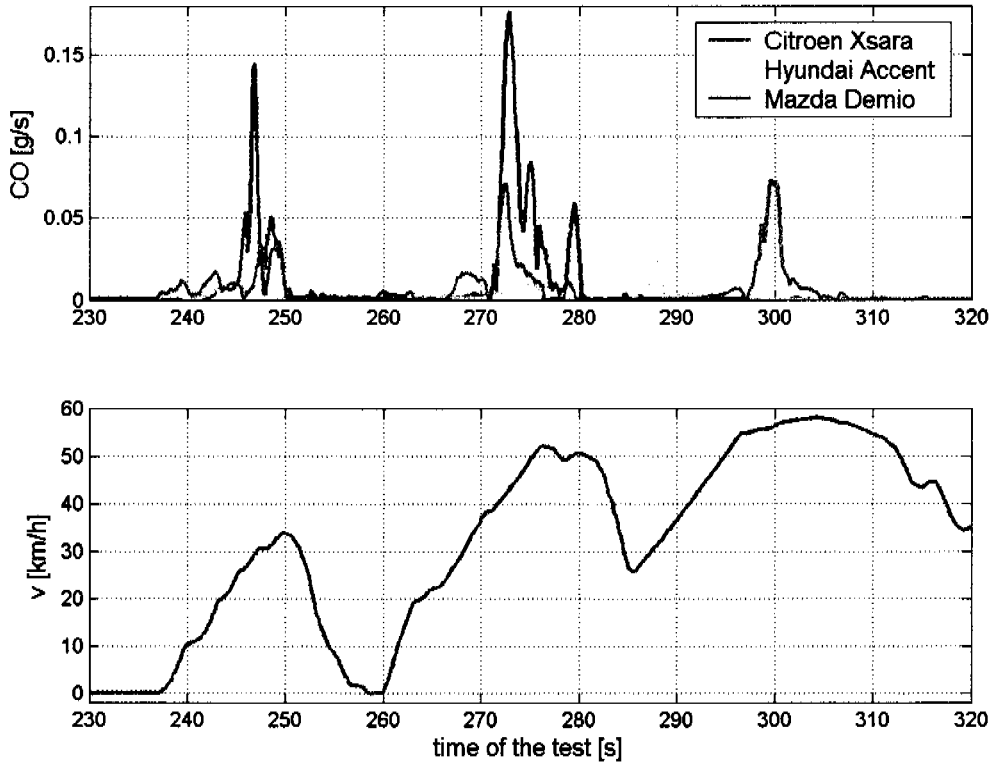

Figure 3.2.: Comparison of CO emissions from three Euro-3 gasoline vehicles for the same speed profile

3.2. Methodology

3.2.1. Measurement procedure

For the Swiss emission factors inventory programme, measurements conducted at EMPA are available for a total of 20 vehicles, which are divided into three vehicle groups: 3 vehicles are gasoline passenger cars from pre Euro-1 generation, 10 vehicles are gasoline passenger cars from Euro-3 generation and 7 are diesel passenger cars conforming to Euro-2 standards. Tables 3.1-3.3 list individual and average vehicles for these categories.

The cars were chosen out of the Swiss official sales statistics, with the aim of getting a representative engine-sizes, manufacturer distribution and gearbox type. For the sake of representativity, the measurements were performed with the vehicles brought directly from the traffic without any initial maintenance. All vehicles were measured in the real-world driving cycles (R1-R4 and CADC) which were described in Section 1.3 and in an additional cycle

Not.	Make	Model	Mass [kg]	Engine cap. [l]	Mileage [km]	Power [kW]	1st reg. year
PB0-02	Opel	Kadett D 1300	995	1.296	128,400	50	1984
PB0-03	VW	Golf	985	1.595	165,000	55	1984
PB0-05	Peugeot	505 GTI	1310	2.164	57,800	96	1984
		Average	1093	1.685	117,067	67	1984

Table 3.1.: Sample of pre Euro-1 gasoline passenger cars

(BAB=Bundes-Autobahn) representing a highway driving pattern [70] (see also Appendix A.1).

The measurements were performed in a vehicle test cell equipped with a chassis dynamometer (Schenk manufacturer, 60 kW power capacity), humidity control of the combustion air, full-flow dilution of the vehicle's exhaust gases using the CVS system for the bag measurements and raw line measurements for the instantaneous emission data (Figure 2.3). For each vehicle, measurements were available on the emissions of NO_x, CO, HC, O_2 and CO_2. Fuel consumption was calculated from the emissions of CO_2, HC and CO. Beside the exhaust emissions, all relevant parameters (e.g. vehicle speed, manifold pressure, engine speed, temperatures, etc.) were recorded on a 10 Hz basis.

For each vehicle, the exhaust gas transport dynamics from the engine- or catalyst-out to the analysers were compensated by means explained in Chapter 2.

3.2.2. Model development

A first step in improving the existing models, which allocate emissions to a speed-speed times acceleration matrix on 1 Hz measurements, is to fulfill the pre-conditions explained in Section 3.1. This is done by taking 10 Hz measurements and by compensating for all the transport dynamics.

As it was already explained in Section 1.4, speed and acceleration based models cannot properly take into account other variables which can affect emissions, such as road gradient, use of accessories or changes of gear-shift strategy. Some correction factors can be used to compensate these effects, but their use can be problematic and misleading.

Not.	Make	Model	Mass [kg]	Engine cap. [l]	Mileage [km]	Power [kW]	1st reg. year
PB3-01	Toyota	Yaris	975	0.998	37,300	50	2000
PB3-03	Citroen	Xsara	1191	1.360	21,100	55	2001
PB3-04	Hyundai	Accent	1070	1.341	22,300	62	2001
PB3-05	Mazda	Demia	1100	1.498	20,500	55	2001
PB3-07	Renault	Megane	1195	1.598	20,400	79	2001
PB3-08	Fiat	Punto HGT	1095	1.747	21,500	96	2000
PB3-09	Peugeout	306	1245	1.761	18,700	81	2001
PB3-12	Honda	Accord	1500	1.997	28,400	108	2000
PB3-13	Renault	Megane Scenic	1400	1.998	80,400	100	2001
PB3-15	Ford	Mondeo	1460	1.999	31,700	107	2001
		Average	1223	1.630	30,230	79	2000.7

Table 3.2.: Sample of Euro-3 gasoline passenger cars

Not.	Make	Model	Mass [kg]	Engine cap. [l]	Mileage [km]	Power [kW]	1st reg. year
PD2-01	Ford	Focus 1.8 TD	1348	1.753	35,800	66	2000
PD2-02	Seat	Ibiza	1180	1.896	31,143	81	1999
PD2-03	VW	Passat	1450	1.896	103,320	81	2001
PD2-04	Peugeot	406	1440	1.905	93,610	66	1997
PD2-05	Opel	Zafira	1505	1.995	68,639	60	1999
PD2-06	Alfa Romeo	156	1485	2.387	70,980	100	1998
PD2-08	Mitsubishi	Pajero	2065	2.835	59,320	92	1999
		Average	1496	2.095	66,116	78	1999

Table 3.3.: Sample of Euro-2 diesel passenger cars

For this reason, the mapping variables are changed to brake mean effective pressure (*bmep*) and engine speed (*n*). Brake mean effective pressure can be considered as "scaled" engine torque size since:

$$bmep = \frac{T_e \, 4\pi}{V_d} \tag{3.1}$$

where, V_d denotes the displacement volume of the engine, T_e is the engine torque and 4 is the number of strokes per engine cycle. Thus brake mean effective pressure is equal for different engines when running in similar operating points (unlike torque) and is useful for the comparison of different cars. Since the mapping of emissions is performed at vehicle level, engine torque could be used instead of *bmep*. However, we decided to map using this scaled variable, because this approach allows comparison between emission maps of cars with different engine sizes.

The advantage of this new alternative of mapping derives from the fact that the influences of vehicle loading, gradient, use of accessories or gearshifts onto emissions may be taken directly into consideration. The gearshift strategies as well as the actual loading of the car have a considerable effect on emission levels [30]. This is why *n* and *bmep* seem to be more appropriate variables for the description of emissions behaviour. Additionally, the fuzziness of different gear settings at the same velocity is avoided.

Another advantage of the considered approach is that data used for the model development come from real-world driving cycles. In this way, the model is not restricted to pure steady-state emission maps and transient correction functions as for some other approaches [61]. Therefore, emission events that are related to the transient operation of the vehicles can be more appropriately modelled.

The emissions, with the right time and dynamic correction, as described in Chapter 2, were mapped onto *bmep* and *n*, on a 10 Hz basis. All recorded data are put into bins, i.e. intervals of instantaneous *bmep* and *n*. Each of these two-dimensional cells represents a value in the "emission matrix". In this way, a *bmep-n* matrix for each emission (CO, CO_2, HC and NO_x) is set-up. In each cell of the *bmep* and *n* matrix, the emission rates are averaged to give a mean value.

The size of the grid within the matrix has a considerable influence on the results. The finer the cells are, the better is the allocation of emission information to their generating driving conditions. The weak point is that by fine griding many fields of the emission matrix would remain empty (without recorded values) or would contain very few points (which would be dangerous when calculating

the mean value within the cell). On the other hand, the coarser the increments are, the smaller the number of empty cells, but the less accurate will be the correlation of the emissions to the driving conditions. Therefore, a compromise has to be found.

The chosen approach was to consider a 16x16 matrix, with coarser cells at the extremes and finer in between. The size of the cells was determined based on the measured *bmep* and *n* values collected from all "source" cycles. The procedure to determine the increments is as follows:

- Determine mean values (μ_n and μ_{bmep}) and standard deviation(σ_n and σ_{bmep}) from the available input data.
- Determine the increments on the x-axis (engine speed) as:
  $x_1 = min(n)$,
  $x_i = \mu_n - 2\,\sigma_n + \frac{4\,\sigma_n}{14} \cdot (i-1), i = 2 \ldots 16$,
  $x_{17} = max(n)$.
- Determine the increments on the y-axis (brake mean effective pressure), using the same procedure as described above.

In this way, the first cell contains points which are outside the $\mu - 2 \cdot \sigma$ range and the last cell contains points which have values higher than $\mu + 2 \cdot \sigma$. The rest of the cells are equidistant. With this approach, cells at the extremes are larger since they contain points outside of the range of $\pm 2 \cdot \sigma$ around the mean, while cells in the middle are finer. The reason for this choice of increments is that if normal distribution is assumed for the *bmep* and *n*, then 95.5% of the points are within $\pm 2 \cdot \sigma$ around the mean. If any other distribution with finite mean and variance is assumed, *Tchebychev's Inequality* states that at least 75% of the points are included within this range [28]. Figure 3.3 depicts the development of the grid cells for a particular vehicle.

It has to be mentioned here that a fix grid approach has been also tried, but this has the inconvenient that the grid has to be selected individually for each car. The results with this method were comparable to the results obtained when the grid was chosen by the manner explained above. Hence, this automatic technique of grid determination was preferred.

For the prediction calculation, instantaneous emissions and fuel consumption data are generated from the emission matrices by considering different combinations of *bmep* and *n*. At each discrete moment in time, the appropriate cell

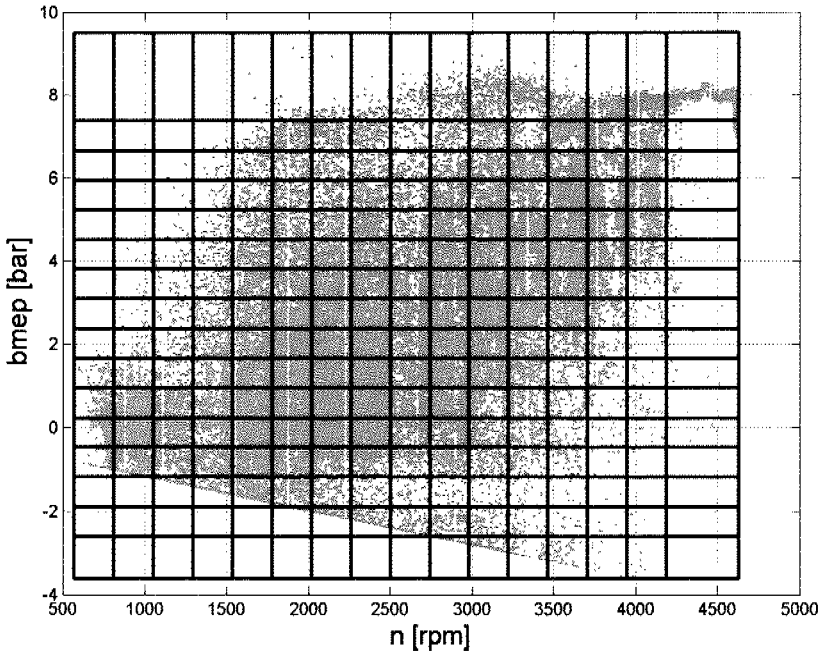

Figure 3.3.: Grid choice

in the emission matrix is determined based on the instantaneous values of the input data.

Since the matrices store the emission information in particular increments, the interpolation scheme used to calculate the values between the grid points attains a certain significance. The procedure chosen was the bilinear interpolation between the 2x2 neighboring grid points. The emission value in a point $E(x,y)$ is given by:

$$E(x,y) = (1-t)(1-u)E_{i,j} + t(1-u)E_{i+1,j} + (1-t)uE_{i,j+1} + tuE_{i+1,j+1} \tag{3.2}$$

where $x_i < x < x_{i+1}$ and $y_i < y < y_{i+1}$, and

$$t = (x - x_i)/(x_{i+1} - x_i)$$

$$u = (y - y_i)/(y_{i+1} - y_i)$$

Other methods of interpolation, like nearest neighbour interpolation or Shepard interpolation were tested, but since the bilinear interpolation gave the best results, this method was preferred.

Even though time series of emissions may be predicted using this approach rather accurately, the goal was not to have a good prediction at each time step. Just the integrated emission results of a cycle of several minutes duration should

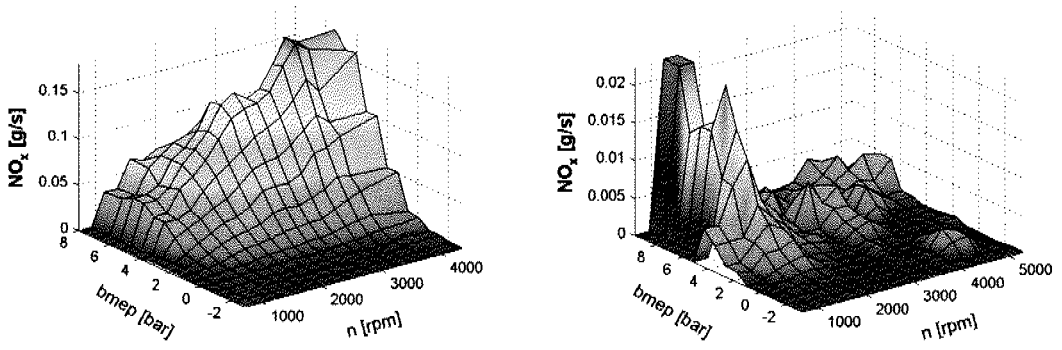

(a) (b)

Figure 3.4.: NO_x emission maps for a pre Euro-1 vehicle (a) and for a Euro-3 car (b). Note different scales on all axis.

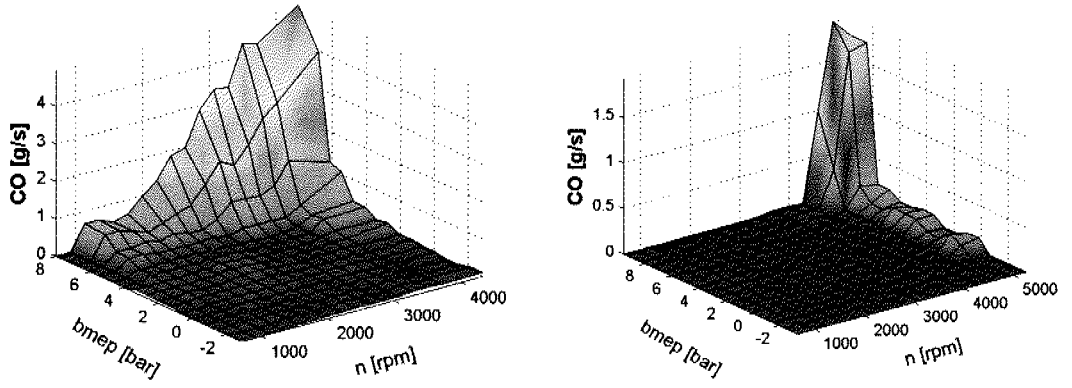

(a) (b)

Figure 3.5.: CO emission maps for a pre Euro-1 vehicle (a) and for a Euro-3 car (b). Note the different scales.

be reasonably accurate. The total emissions (in [g]) for the cycle in question are determined as the time integral of the forecasted instantaneous values. Consequently, the corresponding emission factors (in [g/km]) are calculated by dividing to the total distance driven in the cycle.

Figures 3.4-3.7 depict as examples NO_x, CO, HC and CO_2 emission maps for a pre Euro-1 gasoline (VW Golf, see Table 3.1) and for a Euro-3 gasoline vehicle (Toyota Yaris, see Table 3.2). While the pre Euro-1 NO_x emission map has a smooth behaviour, it becomes completely irregular for the Euro-3 engine, with high values at low engine speed accounting, most likely, for the imperfect combustion. The CO map has high values overall on the full load curve for the pre Euro-1 vehicle, but in the Euro-3 case high values are obtained only at high engine speeds when most likely the vehicle goes into enrichment regime.

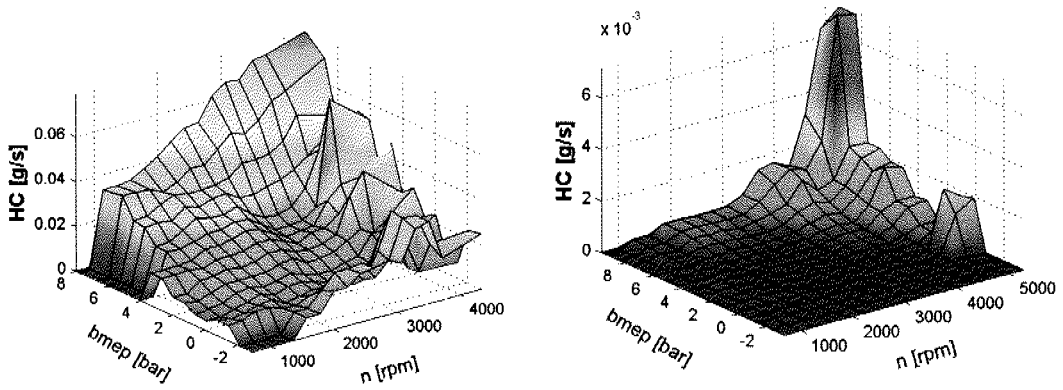

(a) (b)

Figure 3.6.: HC emission maps for a pre Euro-1 vehicle (a) and for a Euro-3 car (b). Note the different scales.

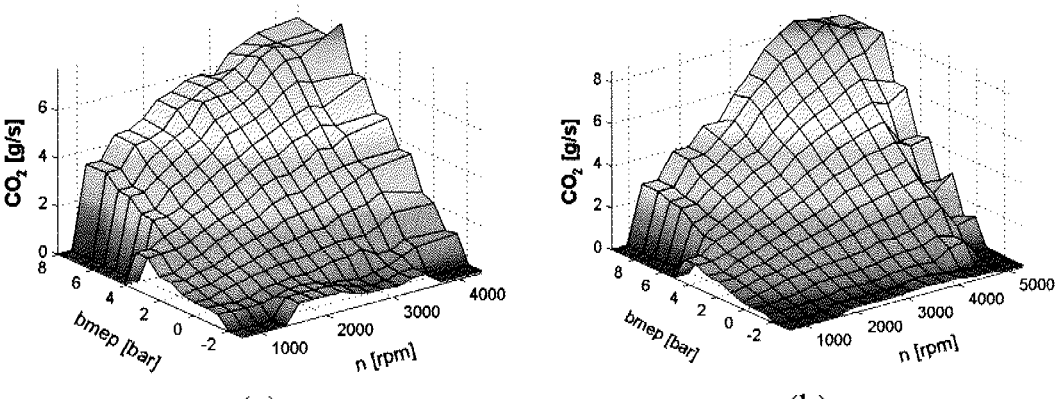

(a) (b)

Figure 3.7.: CO_2 emission maps for a pre Euro-1 vehicle (a) and for a Euro-3 car (b). Note the different scales.

Similar behaviour can be observed in the case of the HC emission maps. As expected, for the CO_2, there is not much difference between the two vehicle technologies, the emissions are increasing with high torque and high engine speed since they relate to load and fuel consumption strongly.

3.3. Validation

For the verification of the model quality and robustness, a cross validation method was used. Fifteen of the measured driving patterns were used to develop the vehicle emission maps and the remaining sixteenth cycle was used for the verification of the model. Thus, its emission factors were determined from the model and compared afterwards to the measured values. Hence, the model had to be run 16 times for each vehicle, since each time there is a different validation cycle. The forecasted and measured emission factors were averaged for each of the three vehicle categories obtaining thus the results for the average vehicle at each vehicle class.

The comparison between measured and predicted with $bmep - n$ method emission factors together with the corresponding limits for the factor 2 of prediction are shown in Figures 3.8-3.10. The results are given for the average vehicle at each vehicle category. Excellent prediction quality is reached for pre Euro-1 gasoline vehicles; the average of absolute relative error is 1.5% for CO_2, 9% for CO and NO_x, and 8% for HC. For the average Euro-2 diesel vehicle the average of absolute relative error is 2% for CO_2, 13% for CO, 14% for HC and 2% for NO_x. The slightly higher error in the prediction of CO and HC is mostly determined by the smaller values of these pollutants for the diesel engines, which are very close to the detection limit of the analysers. As for the average Euro-3 gasoline vehicle, the values obtained are 1.5% for CO_2, 21% for CO and 36% for HC and NO_x.

To check if the considered modelling approach gives better results than the older instantaneous emission models, the emission signals were also mapped onto classical speed-speed times acceleration map on a 1 Hz data. In this case the emission signals measured at the analyser were not dynamically corrected by means explained in Chapter 2, but just a constant time delay was considered as in the old approaches.

The overall numerical qualification of the both models is performed by calculating several statistical measures for each vehicle class:

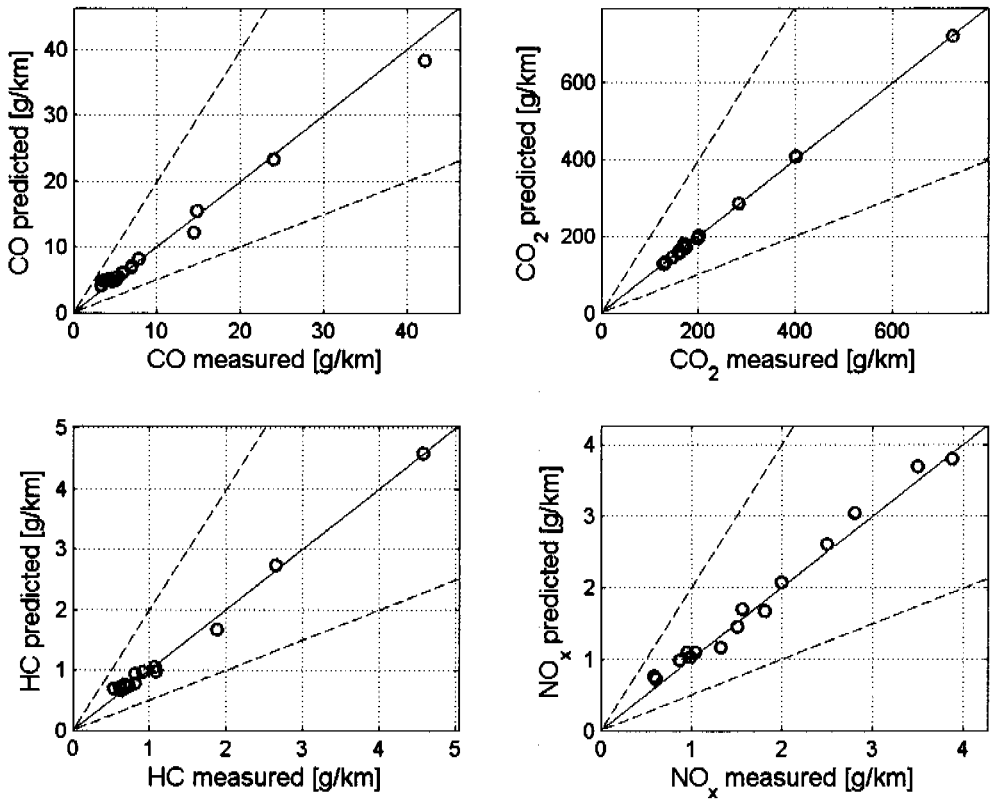

Figure 3.8.: Comparison between predicted with *bmep-n* map and measured emission factors for the average pre Euro-1 vehicle

- the normalised mean square error: $NMSE = \frac{\overline{(E_m - E_p)^2}}{\overline{E_m} \cdot \overline{E_p}}$
- the fractional bias: $FB = \frac{\overline{E_m} - \overline{E_p}}{0.5\left(\overline{E_m} + \overline{E_p}\right)}$
- the coefficient of determination: $R^2 = \frac{\overline{\left(E_m - \overline{E_m}\right) \cdot \left(E_p - \overline{E_p}\right)}^2}{(\sigma_m \cdot \sigma_p)^2}$
- the fraction of predictions within a factor two from measurements: $FAC2$.

Here E_m and E_p represent the measured and predicted emission factors, $\overline{E_m}$ and $\overline{E_p}$ denote the mean values and σ_m and σ_p are the corresponding standard deviations for each of the average vehicle.

The statistical measures presented above, $NMSE$ (which is a measure for the average error, i.e. the scatter), FB (which is a measure of the systematical error, i.e. the bias), R^2 (which is a measure of the common variance) and $FAC2$ are listed in Tables 3.4-3.6. The results show that the prediction quality

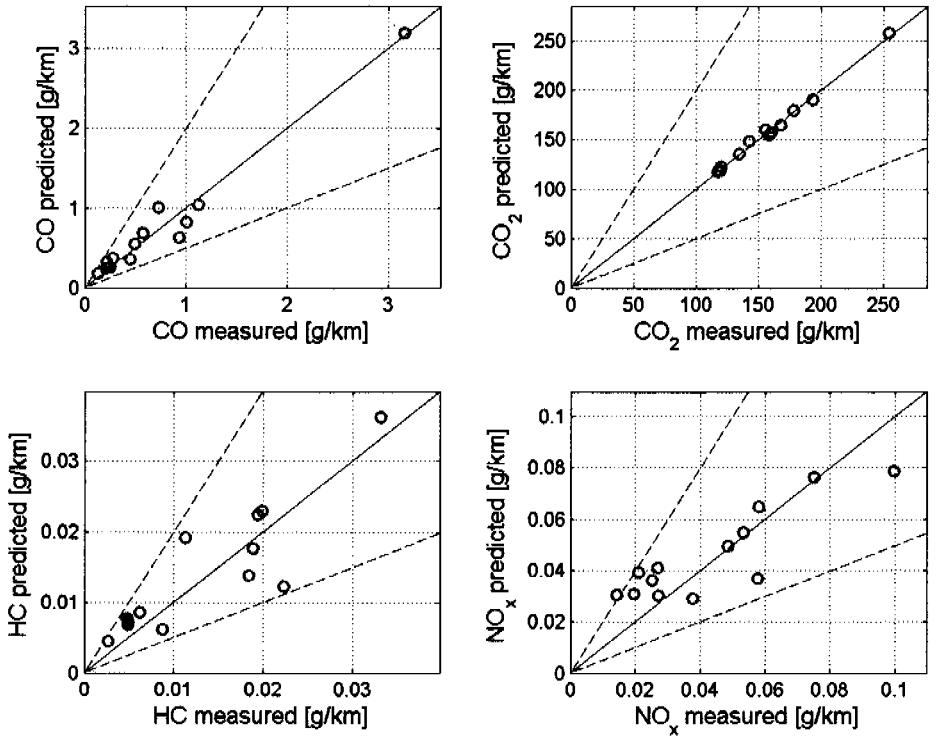

Figure 3.9.: Comparison between predicted with *bmep-n* map and measured emission factors for the average Euro-3 vehicle

improves significantly from the old to the new approach. Mapping with time corrected data and onto *bmep-n* leads almost always to a better prediction in the sense of lower average error (smaller $NMSE$ and FB value) and a higher correlation (higher R^2). The changes in $FAC2$ are less pronounced for the pre Euro-1 gasoline and for the Euro-2 diesel vehicles, but they are obvious in the case of the Euro-3 gasoline cars.

A statistical analysis was also performed to determine if the observed improvement in the coefficients of determination was statistically significant. For that, confidence intervals have been calculated using the bootstrap resampling method for the differences between the coefficients of determination obtained with the two models. The bootstrap resampling procedure is mainly used if the distribution of an investigated variable is not known. In [29] it was confirmed that the standard statistical formulas for the confidence intervals may be inappropriate since model performance measures such as R^2 are not necessarily normally distributed. A good introduction to this technique can be found in [25]. The procedure considers the sampling with replacement of hundreds sets from a given data set. This technique has the advantage of not depending on

	Map used	CO	CO_2	HC	NO_x
$NMSE$	$v - v \cdot a$	0.042	0.006	0.033	0.130
	$bmep - n$	0.016	0.000	0.006	0.006
FB	$v - v \cdot a$	-0.026	-0.030	-0.045	-0.117
	$bmep - n$	0.009	-0.004	-0.014	-0.033
R^2	$v - v \cdot a$	0.966	0.996	0.962	0.694
	$bmep - n$	0.994	0.999	0.993	0.986
$FAC2$	$v - v \cdot a$	100%	100%	100%	93.3%
	$bmep - n$	100%	100%	100%	100%

Table 3.4.: Statistical performance measures for the average pre Euro-1 gasoline vehicle. Perfect match would results in $NMSE = 0$, $FB = 0$, $R^2 = 1$ and $FAC2 = 100\%$.

	Map used	CO	CO_2	HC	NO_x
$NMSE$	$v - v \cdot a$	0.089	0.003	0.472	0.138
	$bmep - n$	0.036	0.000	0.099	0.079
FB	$v - v \cdot a$	-0.074	-0.017	-0.085	0.018
	$bmep - n$	-0.008	-0.004	-0.053	-0.058
R^2	$v - v \cdot a$	0.783	0.934	0.112	0.247
	$bmep - n$	0.966	0.994	0.776	0.770
$FAC2$	$v - v \cdot a$	76.9%	100%	61.5%	84.6%
	$bmep - n$	100%	100%	100%	92.3%

Table 3.5.: Statistical performance measures for Euro-3 gasoline vehicles

	Map used	CO	CO_2	HC	NO_x
$NMSE$	$v - v \cdot a$	0.434	0.005	0.096	0.012
	$bmep - n$	0.117	0.001	0.070	0.002
FB	$v - v \cdot a$	0.104	-0.010	0.028	-0.001
	$bmep - n$	0.098	-0.005	0.053	-0.020
R^2	$v - v \cdot a$	0.832	0.982	0.959	0.980
	$bmep - n$	0.975	0.991	0.963	0.990
$FAC2$	$v - v \cdot a$	100%	100%	100%	100%
	$bmep - n$	100%	100%	100%	100%

Table 3.6.: Statistical performance measures for Euro-2 diesel vehicles

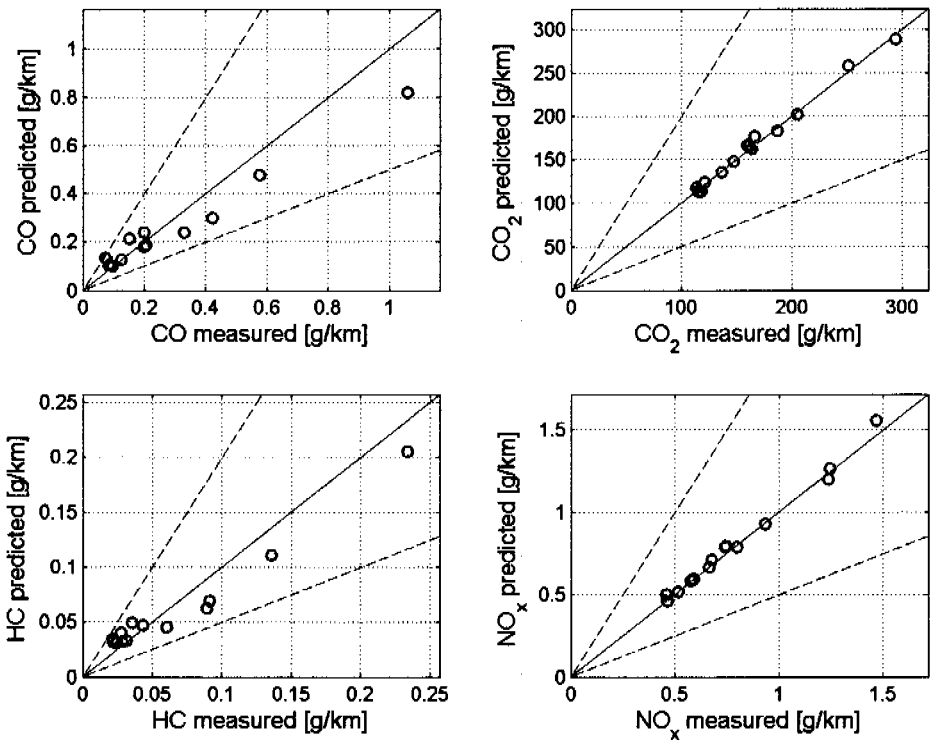

Figure 3.10.: Comparison between predicted with *bmep-n* map and measured emission factors for the average Euro-2 vehicle

the form of the underlying distribution function.

In our case, 95% confidence limits are desired for the difference between the coefficient of determination obtained with the first map ($v - v \cdot a$) and the one obtained with the second map ($bmep - n$), ΔR.

In the bootstrap technique, a new set of N values (with $N = 16$ in our case) of E_m, E_{p1}, E_{p2} is randomly drawn from the original set. Each drawn sample is replaced into the original set before the next draw. For each resampled set of size N, the difference ΔR is calculated. This procedure is repeated m times, with m chosen in this case to be 1000. Based on the m values of ΔR the 95% confidence intervals are determined from the 2.5 and 97.5% quantiles of the distribution of the samples statistics.

These 95% confidence levels on ΔR for all emissions and for all vehicle categories are presented in Figure 3.11. The results show that, with the exception of CO for Euro-3 gasoline and Euro-2 diesel vehicles, ΔR is signigicantly different from 0.0, which implies that R^2 with model $v - v \cdot a$ is significantly different than R^2 with the model $bmep - n$. Moreover, since the difference is significantly negative, it implies that the correlation is higher when using the

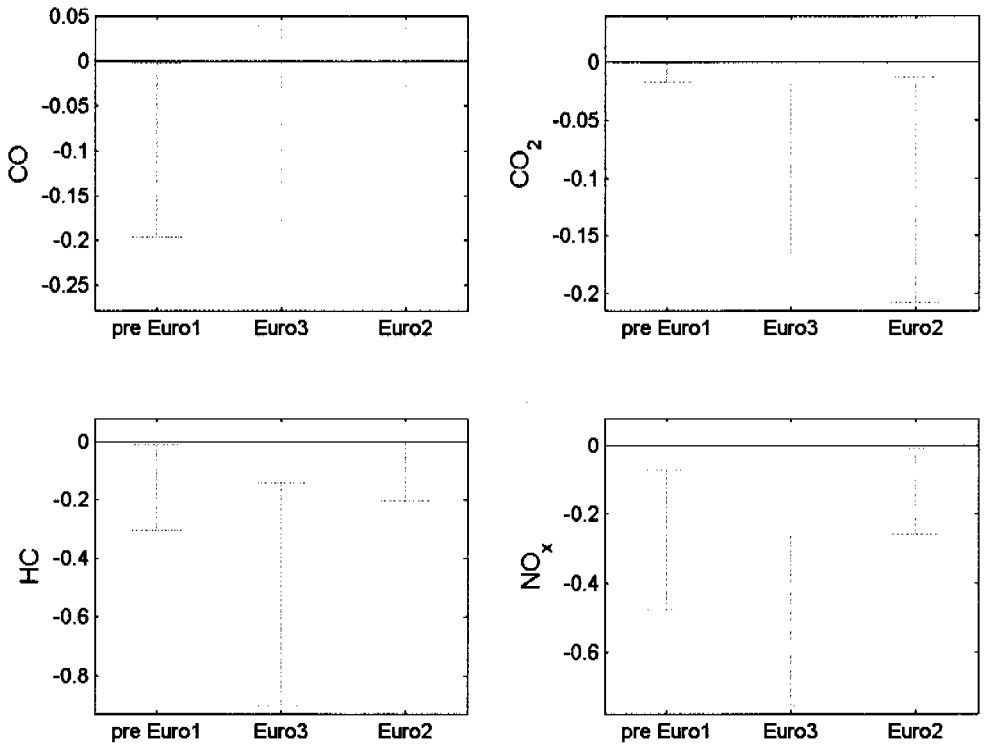

Figure 3.11.: 95% confidence intervals on differences in R^2 (ΔR) between old ($v - v \cdot a$) and new ($bmep - n$) models. If the confidence interval does not overlap 0.0, then we have 95% confidence that the R^2 for the two models is different.

second method than when using the first method.

This shows that emissions map based on engine speed and brake mean effective pressure and using 10 Hz dynamically corrected emissions data gives significantly better results than the $v - v \cdot a$ map developed with 1 Hz statically time-shifted data.

3.4. Conclusions

To improve the existing instantaneous emission models, two preconditions have to be fulfilled: the emission signals should be measured on a 10 Hz basis and the transport dynamics from the engine to the analysers must be compensated by time-varying approaches. Additionally, since emissions show a scattered and nonlinear behaviour from vehicle to vehicle, the emissions maps should be developed at the individual vehicle level and, afterwards, the resulting emission

factors for the considered driving pattern have to be averaged at each vehicle class.

Based on these observations, emission maps founded on engine speed and brake mean effective pressure and using 10 Hz dynamically corrected signals have been developed at vehicle level. Three different vehicle categories were under study. The results show that this new mapping gives significantly better results than the existing speed and speed times acceleration map, based on 1 Hz statically corrected data. The prediction quality of the new mapping is excellent for pre Euro-1 gasoline vehicles, Euro-2 diesel cars and CO_2 emissions of Euro-3 gasoline vehicles, but only moderate for CO, HC and NO_x of gasoline vehicles with after treatment systems. This was expected, since for these cars high emissions often arise during the transient manoeuvres. Rapid changes in emissions can occur even during constant speed cruising, due in part to small changes in throttle position that affect manifold pressure without affecting vehicle speed.

Thus, since both these static models do not include the dynamic behaviour of the engine, a dynamic emission model is necessary.

Nonetheless, when comparing the results for all the cars, it results that no single parameter can be derived to explain the differences between the simulated and measured emission factors absolutely satisfying for all the vehicles. Neither the displacement, nor the mileage or some other variable aren't obviously correlated with the quality of the simulation.

4. Dynamic instantaneous emission model

4.1. Introduction

The technologies applied in the new vehicles and advancing insights in dynamic vehicle emissions have put the emission factors under strain. The cars become cleaner and transient emission peaks become more and more important for the average emission factors. The emissions of modern passenger cars equipped with three-way catalytic converters show to be on a low level for large periods, with short but high peaks in between (Figure 3.1). For real-world driving, up to fifty percent of the entire emissions can result during these short peaks, which occur during dynamic situations, like gear changing, load changes or high power intervals.

As already seen in Chapter 3, for catalyst cars, a static map is not capable to accurately describe this transient generation of emissions. In a static map, emissions from both transient and steady-state situations would be mixed in the same cell, causing, when predicting, the underestimation of dynamic emissions and the overestimation of the non-transient emissions. For these reasons, it follows that the emission map should be extended by using an additional variable expressing these dynamics. Such a dynamic variable might be the derivative of the manifold pressure ($\dot{p}$) or the derivative of torque. Here, $\dot{p}$ was chosen because the manifold pressure signal is more accurate (less noisy) than the torque signal (who is, additionally, an artificial signal, not a directly measured one).

Furthermore, it has to be taken into account that all these variables, n, *bmep* and $\dot{p}$, describe the engine behaviour and, hence, the engine-out emissions. But engine-out emissions are highly reduced through the three-way catalyst (TWC). Therefore, a model describing the catalytic conversion efficiency should be also incorporated in the overall model.

As a consequence, for the catalyst equipped gasoline vehicles, the model is split into two parts, following the physical configuration. A sketch of the model

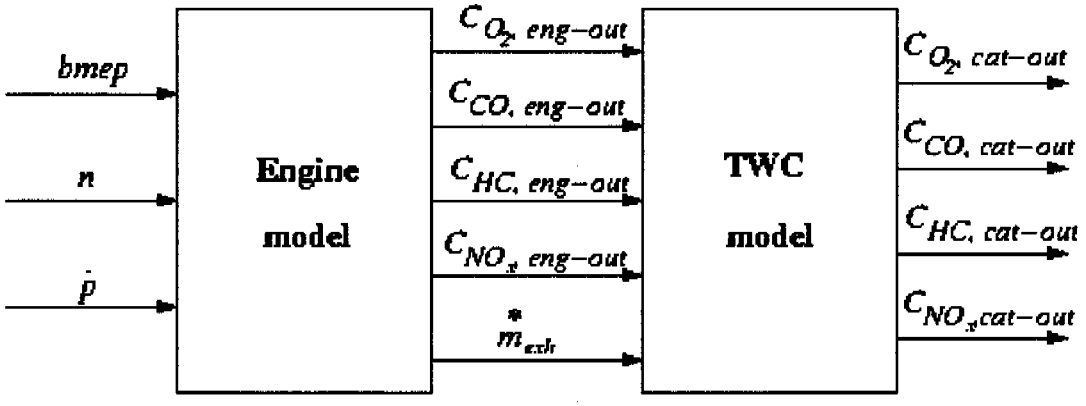

Figure 4.1.: Sketch of the overall emissions model for TWC vehicles

structure is presented in Figure 4.1.

The first part represents a dynamic engine model, where engine-out emission concentrations (CO, HC, NO_x, O_2) and exhaust mass flow are determined using *bmep*, *n* and $\dot{p}$ emission maps (*bmep-n-*$\dot{p}$ map). The second part is the actual three-way catalyst model, where relative oxygen level (ROL) is calculated and, based on this variable, the outlet concentrations are determined using static functions. No cold start effect is taken into consideration, since only emissions from warm cycles are, presently, the subject of the model. CO_2 is not considered in this extended model, given that the prediction quality for this pollutant is already excellent with the static approach.

In this chapter, the dynamic engine model is described and validated. Moreover, the capability of the model to predict the engine-out emissions for different contributory aspects like various gear changing strategies, different loads of the car, various road gradients and combinations of them is also checked.

The dynamic catalyst model is the subject of the Chapter 5.

4.2. Dynamic engine model

The chemistry of the combustion process has as output the emission signals as concentration [ppm]. The emission factors are determined as integration over time of the instantaneous mass flow emissions divided by the total distance. Mass flow emissions are obtained by multiplying the measured concentration

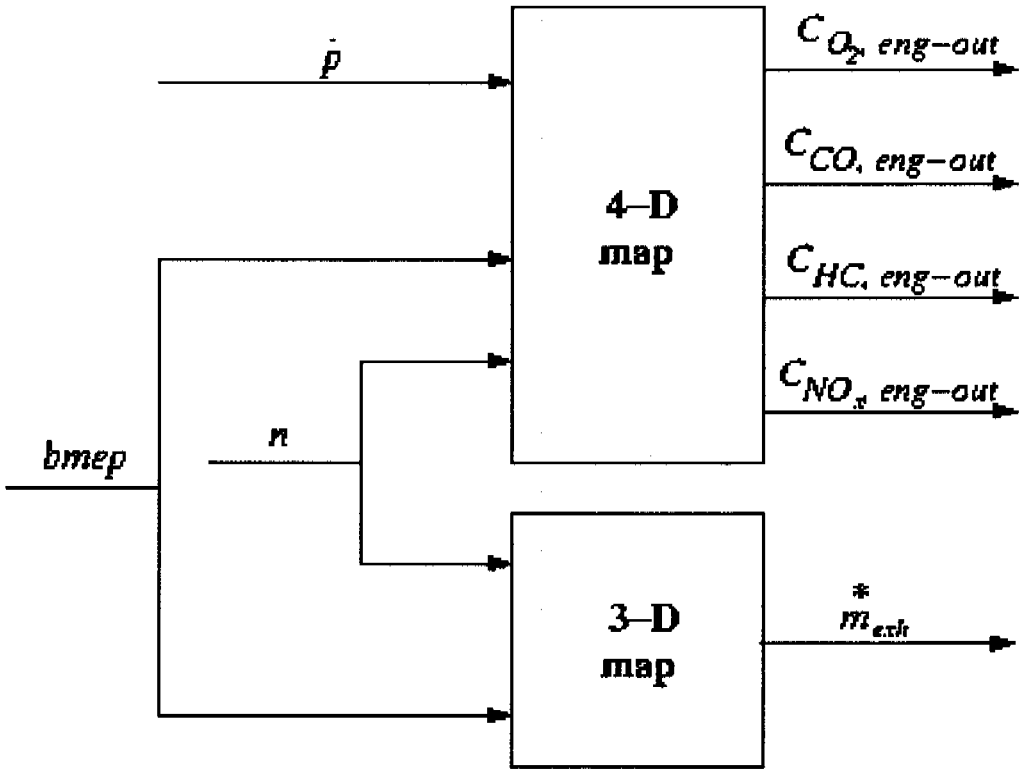

Figure 4.2.: Sketch of the dynamic engine model

of the exhaust gas [ppm] with the exhaust mass flow [g/s].

$$EF_i = \frac{\int_{beg.\ test}^{end\ test} c_i(t) \cdot \dot{m}(t)\ dt}{total\ distance} \tag{4.1}$$

Due to the non-linearity of this problem, an extension of the engine model is the use of a map for the simulation of the exhaust mass flow and of another separate map for the emission concentrations (Figure 4.2). As explained in Section 4.1, a dynamic map has to be used for the modelling of engine-out emission concentrations.

Detailed measurements were performed with five gasoline vehicles, all of them equipped with three-way catalytic converters. Technical details about the measured vehicles are given in Table 4.1.

Emission signals at the engine-output and after the catalyst were both recorded on a 10 Hz basis. The exhaust gas transport dynamics were compensated by means explained in Chapter 2, such that pollutant information was reconstructed at the emissions location of formation. Beside the pollutants, relevant signals like air-fuel ratio upstream and downstream of the catalyst, manifold pressure, vehicle speed, engine speed, exhaust mass flow, etc. were also instan-

Nr.	Make	Model	Mass [kg]	Engine cap. [l]	Class
1	BMW	318i	1360	1.796	Euro-2
2	Fiat	Ulysse	1700	1.9985	Euro-2
3	Mercedes	A140W	1000	1.397	Euro-3
4	Peugeot	206	1070	1.360	Euro-3
5	Toyota	Yaris	970	0.998	Euro-3

Table 4.1.: Gasoline passenger vehicles used for the validation of the dynamic model

taneously logged. The measurements were performed for the sixteen driving patterns already mentioned in Section 3.2.

The exhaust gas mass flow was simulated using the static $bmep - n$ map by means explained in Section 3.2.2. The engine-out emission concentrations were determined using a dynamic *bmep-n-ṗ* emission map. The approach considered for the development of this 4-dimensional map is similar to the one presented in Section 3.2.2. In this case, an 8 x 8 x 8 matrix was chosen, using the same procedure to determine the increments on each axis based on the mean values and standard deviations of the input data. After simulating mass flow and emission concentrations, the overall emission factors were calculated using Equation 4.1.

Similar to the procedure explained in Section 3.3, a cross validation method was employed to check the model quality. Fifteen of the measured driving patterns were used to develop the engine model and the remaining sixteenth cycle was used to check the accuracy of the model. This validation procedure has been repeated sixteen times for each vehicle, since the validation cycle was different every time.

Figure 4.3 illustrates, as an example, the instantaneous simulated and measured engine-out emissions and mass flow for BMW 318i during a highway driving pattern. Furthermore, to ensure that the right oxygen balance situation has been predicted, the measured air-fuel ratio signal was compared to the one calculated using the forecasted emission signals. The results show that the prediction is conform to the reality, i.e. rich situation is predicted when lambda signal is on the rich side and, subsequently, lean when lambda is on the lean side.

The modelling results have been also numerically validated. The coefficient of determination (R^2) between measured and simulated engine-out emission

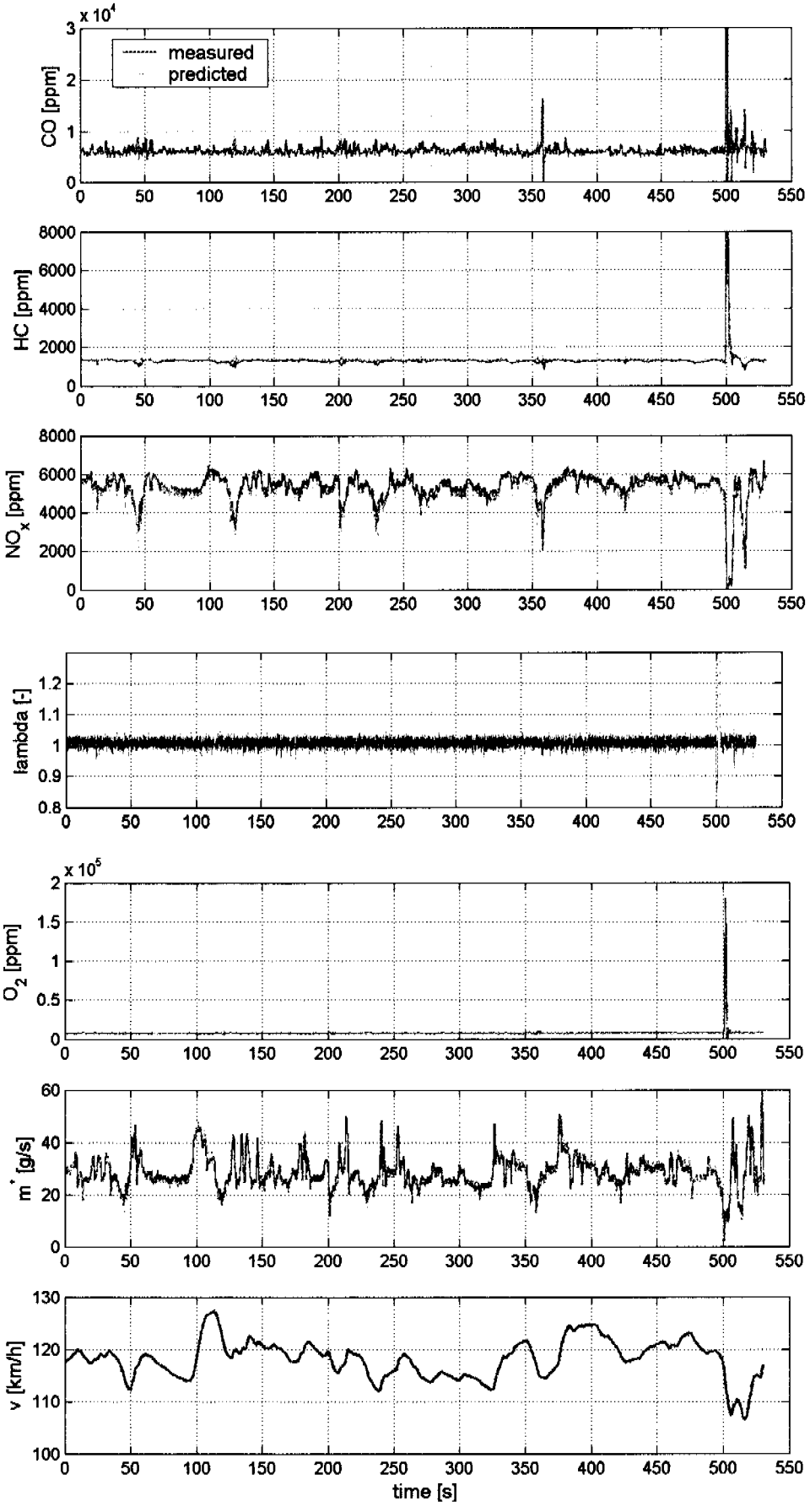

Figure 4.3.: Measured and predicted engine-out emissions and mass flow during a highway cycle

	CO	HC	NO_x
Mercedes A140W	0.94	0.97	0.99
Peugeot 206	0.98	0.97	0.99
Toyota Yaris	0.96	0.98	0.99
BMW 318i	0.98	0.97	0.99
Fiat Ulysse	0.92	0.96	0.96

Table 4.2.: Coefficient of determination between measured and simulated engine-out emission factors (R^2)

factors for the individual vehicles have been calculated. The established results are displayed in Table 4.2. Here only the pollutants CO, HC and NO_x were considered, since the final goal is to have a good prediction quality for the emissions factors of these emissions. The oxygen signal was studied only in connection to the lambda signal and on the instantaneous basis, because no bag values exists for this species.

The quality of the dynamic model is significantly increased. A visual comparison between measured and predicted emission factors for all the individual vehicles is given in Figure 4.4.

Although the sample of cars was quite small, the results were also averaged to determine the quality of the model for the average Euro-2 and, respectively, Euro-3 car. The absolute relative error for both average vehicles was found to be below 5% for all the pollutants (Figure 4.5).

These results indicate a very good agreement in both integrated results and the instantaneous comparison.

4.3. Validation for different loads, slopes and gear-shift strategies

Since contributory aspects like gear-changing, load or slope have a big impact on the resulting emissions, the capability of the model to predict the emission factors for different vehicle loads, for various gradients of the road and for different gear-shift strategies should be also checked.

For that, extensive vehicle measurements of the three Euro-3 gasoline vehi-

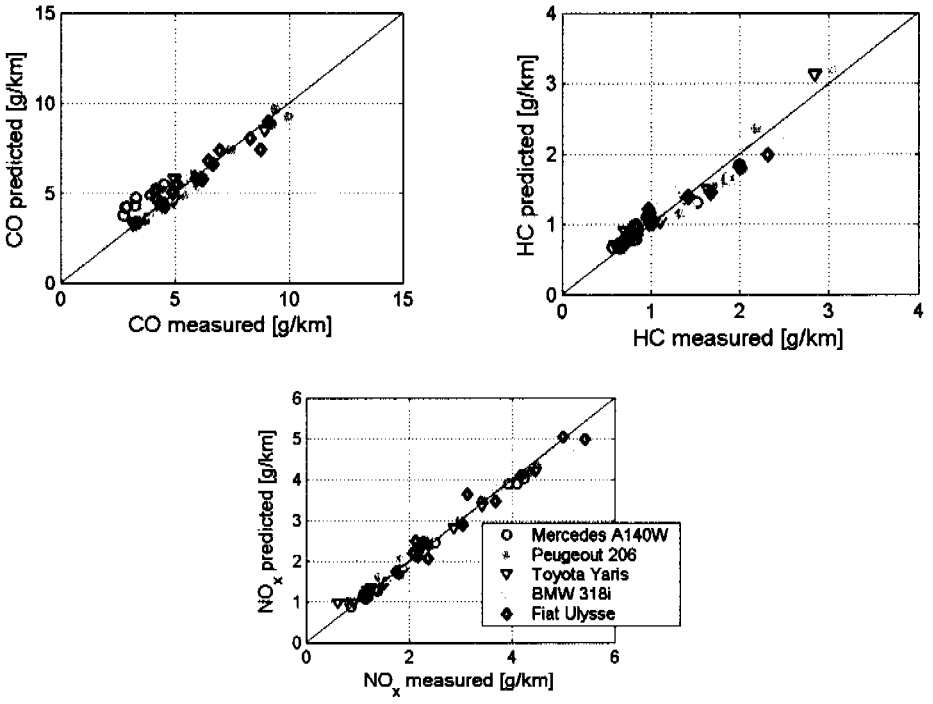

Figure 4.4.: Simulation quality of the engine-out pollutants for the individual TWC-vehicles

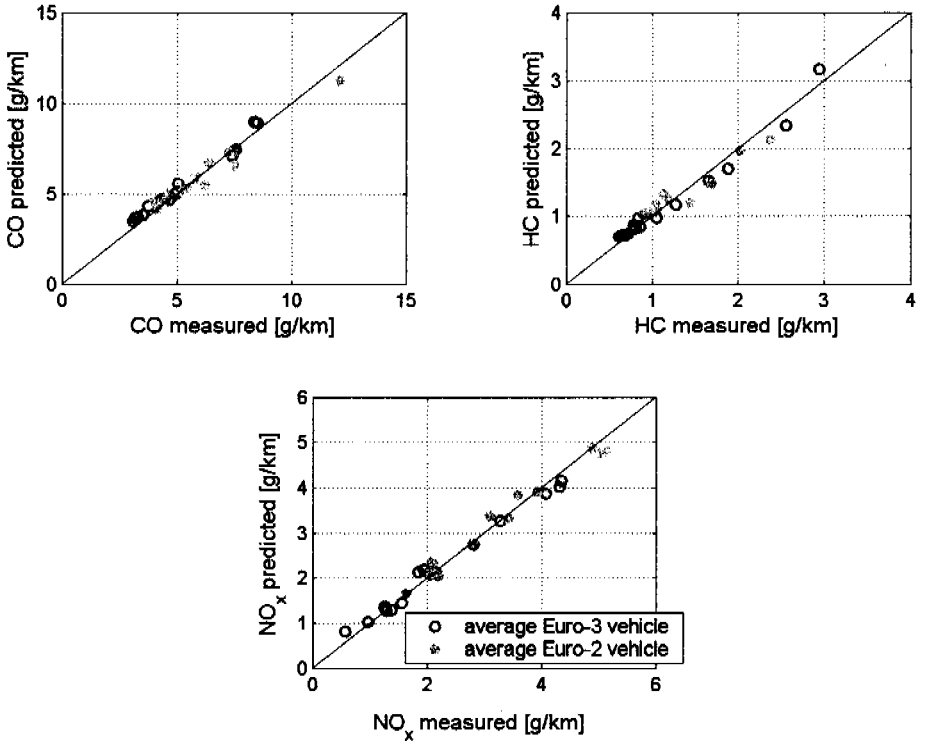

Figure 4.5.: Simulation quality of the engine-out pollutants for the average TWC-vehicles

Test Nr.	Driving pattern	Slope	Load strategy	Gearshift
1-3	CADC, bag 1-3	+3%	50%	normal
4-6	CADC, bag 1-3	-3%	50%	normal
7-9	CADC, bag 1-3	+3%	standard	normal
10-12	CADC, bag 1-3	-6%	standard	normal
13-15	CADC, bag 1-3	0%	full load	normal
16	LE1R	0%	standard	Scenario 1
17	LE2sR	0%	standard	Scenario 1
18	LE2uR	0%	standard	Scenario 1
19	LE3R	0%	standard	Scenario 1
20	LE5R	0%	standard	Scenario 1
21	LE6R	0%	standard	Scenario 1

Table 4.3.: Measurement protocol for the validation of the model for different loads, slopes and gear-shift strategies. Speed diagrams of the driving patterns are given in Section 1.3

cles presented in Section 4.2 and of one Euro-3 diesel car (Hyundai Terracan, displacement volume of 2.9 liters) were available. For each vehicle, the measurement program included the sixteen basic driving patterns which were used to develop the vehicle instantaneous emission model. Beside that, twenty-one traffic situations with different vehicle loadings (no load, medium or full load), different slopes of the road (flat, uphill or downhill), different gear-shift strategies and combinations of them were also measured. Each of this traffic situation accounts also for a different driving pattern like urban, rural, highway driving, etc. This additional measurement program is illustrated in Table 4.3.

The term "normal" for the gear-shift accounts for the standard strategy which is normally used for the CADC and Swiss cycles. "Scenario 1" has the same pre-defined concept as NEDC for the shift of the gears, but the threshold at which the shift is performed is moved with 10 km/h higher.

When checking the coverage of the different cycles onto the map formed using only the basic cycles, it was observed, as expected, that some situations were not perfectly covered by the existing measurements points. This is the case for the CADC cycle, measured at +3% slope of the road and 50% load of the vehicle, which has points at low engine speed and high brake mean effective pressure (Figure 4.6). Similar is the case of the CADC cycle, measured at -3%

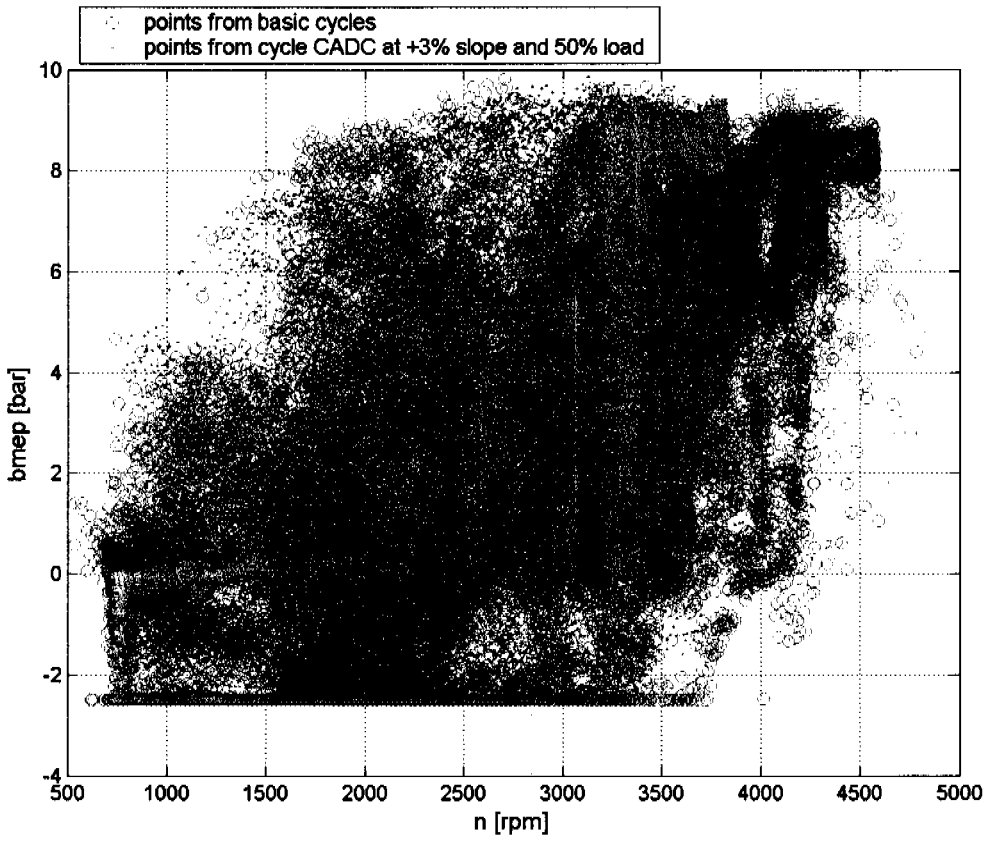

Figure 4.6.: Points of the basic cycles and of the CADC cycle at +3% slope of the road and 50% vehicle load. Note areas where the new situation is not covered by the basic cycles.

road gradient and 50% load of the car. No extrapolation would be possible to establish the emissions at the points not covered in the map, therefore it was decided to include these two cycles to the initial "source" cycles. Later on, a test scenario should be designed to cover the entire possible range of the map points.

4.3.1. Diesel case

Since a static *bmep-n* map already gave excellent results for the prediction of diesel emission factors, this model approach was used to predict the emission factors of the diesel vehicle in the permutation of the 37 validation cycle (each corresponding to the 16 basic and 21 combined situations).

Figure 4.7 depicts the measured and forecasted emission factors of CO, CO_2, HC and NO_x for this vehicle. As it can be seen, the model performs excel-

lent for CO_2 and NO_x, with lower quality for HC and CO. However, this was expected, since CO and HC values are extremely low in the case of diesel vehicles. The CO analyser is calibrated at a range of 50'000 ppm, but more than 90% of the measured CO emissions of this vehicle are typically below 100 ppm, thus significantly lower and very close to the detection limit. Hence, the error in the CO prediction is actually within the measurement error of the analyser. Moreover, as it was shown in [5], the scatter of the results for one car (as for CO in Figure 4.7) is easily reduced if the average of several cars (fleet) is built. Therefore, these errors in prediction can be considered as random and not systematic.

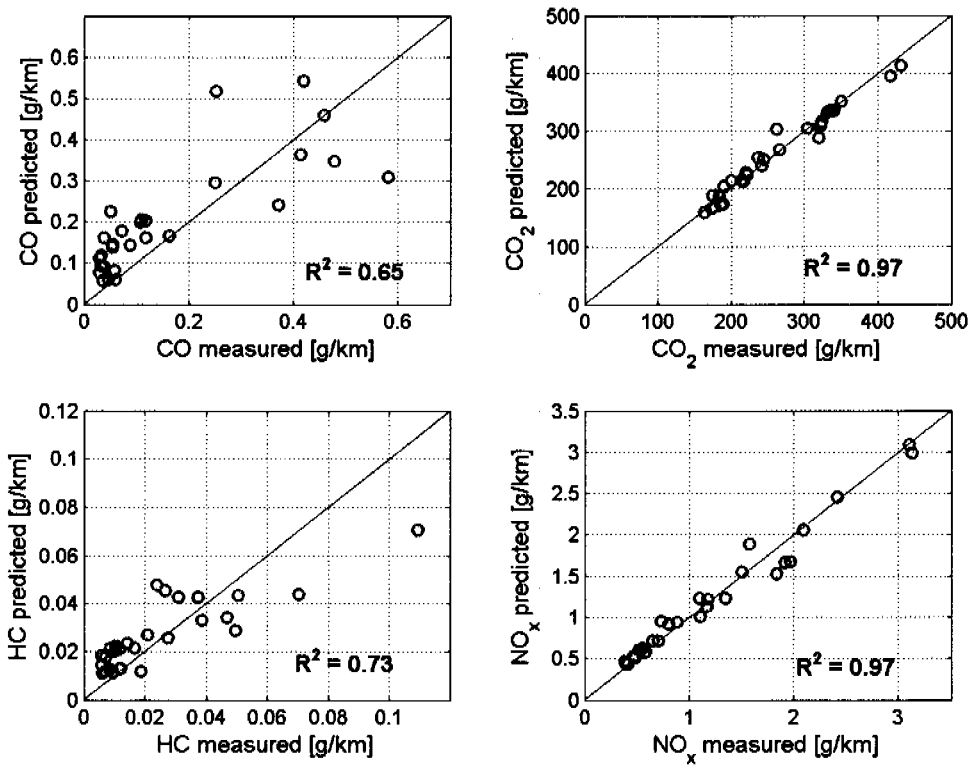

Figure 4.7.: Simulation quality of the emission factors for all 37 situations for the diesel vehicle

When looking at the model capability to forecast different situations, such as a different gear-shift strategies, it can be seen that the model predicts CO_2 emission factors with less than 8% relative error and NO_x emission factors with no more than than 12% relative error (Figure 4.8). As for CO and HC, the model performance quantified in relative error is only satisfactory, but considered in absolute terms the error is less than 0.1 [g/km] for CO and 0.02 [g/km] for HC.

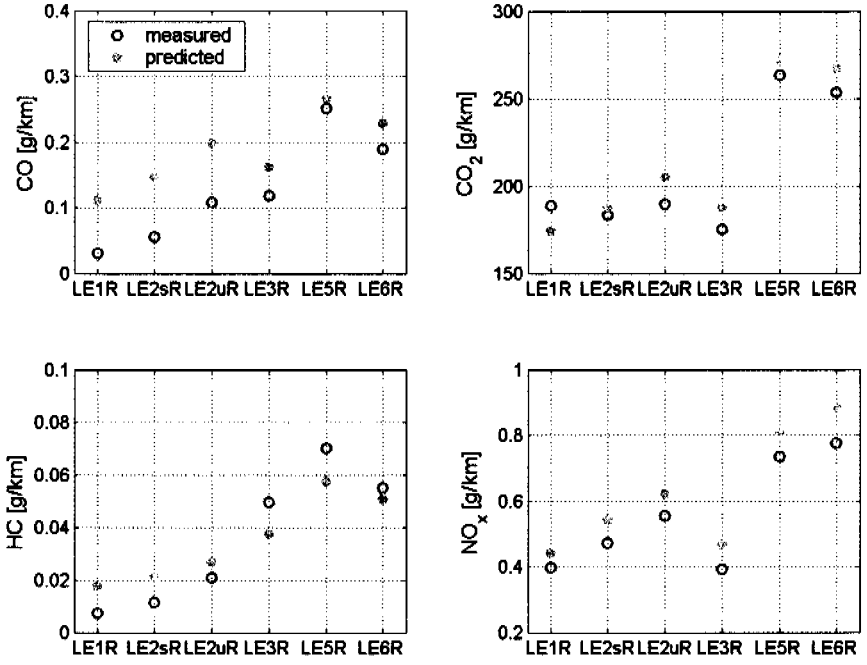

Figure 4.8.: Predicted and simulated diesel emission factors for a different gear-shift strategy (Scenario 1) for several driving patterns.

4.3.2. Gasoline case

For the catalyst cars, the dynamic engine model was employed to generate the simulated engine-out emissions (CO, HC and NO_x) and the catalyst-out CO_2 signal. As Figure 4.9 illustrates, the prediction quality is excellent for all studied cars and for all pollutants.

Moreover, when the average Euro-3 gasoline vehicle is considered, the forecast of engine-out pollutants for different combinations of vehicle loads and road gradients is also remarkable. This result, illustrated in Figure 4.10, confirms that the dynamic engine model is able to accurately predict different situations without the use of any correction functions.

As an additional observation, one should be aware that high value in g/km does not necessarily means high emission value, but a very small distance over the driving pattern. This is, for example, the case of the stop-and-go situations StGoHW and StGOUrb (refer to Figure 1.2 for the speed profiles).

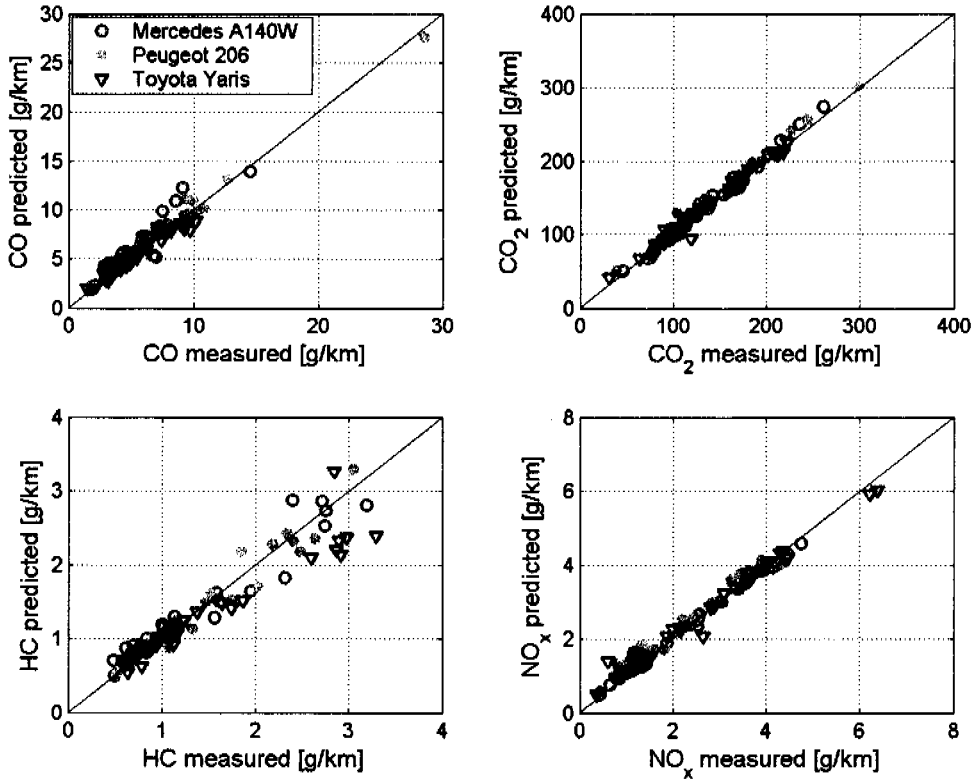

Figure 4.9.: Predicted and simulated engine-out (CO, HC and NO_x) or catalyst-out (CO_2) emission factors for the Euro-3 gasoline vehicles.

4.4. Conclusions

As already concluded in Section 3.4, the instantaneous static model has its limitation when applied to the the modern cars equipped with a three-way catalytic converter. The reason for the (only satisfactory) results obtained is that for this type of vehicles an important share of the exhaust emissions are produced during some very short, but transient situations, like gear changing, accelerations, etc. Moreover, the TWC, with its capability of oxidizing HC and CO and reducing NO_x,plays an important role in the resulting emission factors. Consequently, for catalyst cars the overall model is split into two submodels:

- A dynamic engine model which considers as additional input the derivative of manifold pressure. In this way the transient generation of emissions is properly described. The outputs of this submodel are the engine-out emission concentrations and the exhaust mass flow.

- A dynamic catalyst model, which generates the catalyst-out concentra-

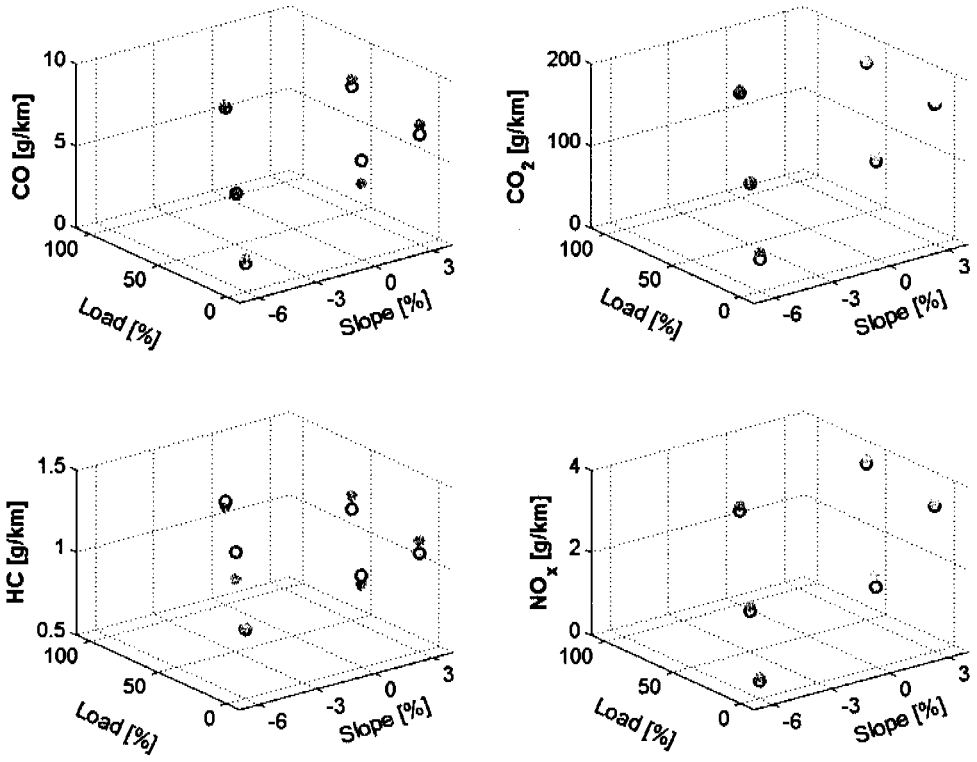

Figure 4.10.: Measured (o) and simulated ($*$) engine-out (CO, HC and NO_x) or catalyst-out (CO_2) emissions for different combinations of vehicle loads and road gradients for the average Euro-3 gasoline vehicle.

tions. This model is described in the next chapter.

The dynamic engine model gives excellent results in the forecasting of the engine-out emissions, both for instantaneous and average emission values. This outcome was tested for several Euro-2 and Euro-3 gasoline vehicles.

Moreover, it has been checked that the instantaneous emission models, although rather complex to develop, are able to include contributory aspects like load, slope or gear-shift strategies without introducing any ambiguous correction functions as it is usual for the bag based models. This can help the emission modellers and the decision makers in the assessment of local emission dispersion models.

No extrapolation of data points is possible in the map which is the basis for the model due to the highly nonlinear character of the problem. Thus, measurements should be designed to add extreme points in the map, in order to be able to predict situations with different slopes of the road and loading of the vehicle.

For a complete validation of the model, more vehicles should be, however, included.

5. Dynamic catalyst model

5.1. Introduction

The three-way catalytic converter (TWC) is an indispensable device for the reduction of CO, HC and NO_x emissions of gasoline engines. Catalytic converters were first used to convert the automobile pollutants into less harmful components starting in 1975. These catalysts were oxidation catalysts (two-way catalysts) because they oxidized CO and HC, converting them to CO_2 and water vapor. In 1980, the catalytic converter was enhanced with the ability to reduce NO_x as well, giving rise to the three-way catalyst. The necessary condition for an optimal conversion is that the engine runs with stoichiometric mixture. A drawback of three-way catalytic converters at the time of their introduction was that a very accurate engine air-to-fuel (A/F) control was necessary to maintain the exhaust mixture at stoichiometry. With the development of exhaust gas oxygen (EGO) sensors, popularly called λ sensors, it was possible to develop a control system that keeps the engine air-to-fuel ratio at stoichiometry.

The main reactions[1] that take place in a warm, properly functioning TWC are summarised in Table 5.1, [73]. These reactions are only the desirable ones, since many other additional reactions could occur such as, for example, reduction of NO_x to ammonia, partial oxidation of HC to give aldehydes and other

[1] Some of the reactions are unbalanced

Oxidation	$2\,CO + O_2 \longrightarrow 2\,CO_2$
	$HC + O_2 \longrightarrow CO_2 + H_2O$
Reduction/three-way	$2\,CO + 2\,NO \longrightarrow 2\,CO_2 + N_2$
	$HC + NO \longrightarrow CO_2 + H_2O + N_2$
Water-gas shift reaction	$CO + H_2O \longrightarrow CO_2 + H_2$
Steam reforming	$HC + H_2O \longrightarrow CO_2 + H_2$

Table 5.1.: Simplified scheme of the reactions occurring on the automotive exhaust catalysts, [73]

toxic components, etc. The reactant species are actually adsorbed on the catalytic washcoat where, with the help of the catalytic substances (palladium, Pd, platinum, Pt, or rhodium, Rh), the formation of the desired products takes place.

Generally, the emissions depend on the air-to-fuel ratio. Tuning the engine to rich feed gives the highest power output, which, however, occurs at the expenses of high fuel consumption and high CO and HC emissions. Under lean conditions, NO_x emission values are rising. With very lean situations, lower combustion temperatures lead to lower NO_x emissions, but, at very high A/F ratio engine misfire appears, leading again to high HC emissions. Under any A/F conditions, catalytic abatement of pollutants is needed to comply with the legislation limits.

Given the nature of the different classes of pollutants, i.e. reducing or oxidizing agents, it is necessary to simultaneously carry out both oxidation and reduction reactions over the catalytic converter. The optimal conversion rates can only be achieved if exactly as much oxygen is available as necessary for the oxidation of CO and HC. At a higher oxygen level, the oxidation process consumes too many reducing agents and NO_x reduction fails. With a shortage of oxygen, all NO_x will be converted, but the removal of HC and CO will be incomplete. Only at stoichiometric conditions appropriate amounts of oxidizing and reducing agents are present in the exhaust to carry out the catalytic reactions as outlined. Under such conditions TWCs effectively remove all pollutants.

The engine management systems are intended to keep the engine operating as close to stoichiometry as possible. However, under real world driving situations, the catalytic converter operates at highly transient conditions. The temperature, flow rate and composition of the exhaust gas flowing through the converter monolith change significantly within seconds according to the driving mode. Under real world driving conditions, the A/F ratio oscillates around the stoichiometric value. Moreover, fuel cutoff during engine overrun, engine misfire or mixture enrichment in acceleration cause more extreme deviations from stoichiometric operation.

In order to cope with the inherent excursions to the lean or to the rich side, an oxygen storage capacity is incorporated in every washcoat [71]. This oxygen storage capacity adsorbs O_2 (up to a certain capacity) during lean operation of the engine and, subsequently, releases O_2 under rich regime. Hence, when the catalyst is operating rich, O_2 is provided (as long as is available) to consume the unreacted CO and HC. The special material used as an oxygen storage component in todays' TWCs is usually ceria, CeO_2, possibly combined with

ZrO_2.

Modelling of the TWC is, thus, of practical interest, as it allows the prediction of the exhaust pollutants under transient situations. Additionally, the TWC model provides a better understanding of the catalyst behaviour during dynamic situations and it would be of tremendous help for the design of economic and efficient exhaust systems. Many detailed chemical and thermodynamic based mathematical models of TWCs have been presented in the literature.

One group of models are "phenomenological" models, which try to identify physical and chemical phenomena occurring in the catalyst based on fundamental chemical and thermo-fluid dynamic principles [18]. Such models are not appropriate for practical applications because of their inherent complexity and because the dynamic effects are not completely described.

Other models use simplified kinetic schemes of the reactions between the various gas components, as well as the dynamics of gas storage on the catalytic surface [75], [13], [63]. Such models are often spatially discretized and can be represented by a set of coupled, differential equations. They contain parameters that have to be estimated by fitting the model to a set of experimental data which characterise the behaviour of the catalyst at different operating points. These models are called lumped parameters models, because all phenomena that are not explicitly considered by the model are lumped into the values of the tunable parameters. This type of approach gives satisfactory results in practical application. The most questionable part of this procedure remains the tuning of the model, which can become extremely complex if the number of the parameters is too high.

A third group of models ([19], [62]) is based on the assumption that the catalyst behaviour is dominated by the dynamics of oxygen storage and that all other kinetics occur over a much shorter and less significant timescale. Models of this type consist essentially of a single nonlinear dynamic element describing these oxygen storage phenomena.

Although the number of studies regarding the modelling of the catalyst is impressive, there is not much to find in the specialized literature about the prediction of the output gas composition or conversion rates of the main pollutants under real-world driving situations. Most of the TWC models have as main goal the development of a control system that can improve the catalyst performance under transient conditions. The prediction of the catalyst-out emissions is under different transient cycles is, however, barely presented.

Beside the three groups of TWC models presented above, an attempt to predict tailpipe NO_x emissions during different transient driving patterns has been made ([58]), based on a model for the conversion efficiency as function of the fuel rate. However, although the authors had limited success in the simulation of NO_x emissions, this model is basically static and has limitations for several transient conditions.

In [63] a designed software (CATRAN - Catalytic Converter Modelling Software) has been used to predict with satisfactory quality the instantaneous CO, HC and NO_x over the NEDC and FTP-75 cycles. This approach, based on a kinetic model containing 10 chemical reactions, has a number of 20 tunable parameters and requires an extensive input database. From the point of view of emission factors modelling, such an approach becomes too complex and difficult to use.

Nevertheless, a model based on simplified kinetic schemes seems to give the best results and, additionally, can be easily generalised. Based on the ideas of [63] and on the work of [13], a simplified catalyst model, equipped with a comprehensive oxygen storage and release submodel, has been here developed. The model has as inputs the inlet concentrations of CO, HC, NO_x and O_2, the mass flow of the exhaust gas and the exhaust temperature. A simplified kinetic submodel generates the relative oxygen level (ROL) in the catalyst on an instantaneous basis. Conversion rates for the main pollutants are expressed as static functions of this variable.

The methodology of the model is presented and its predictive ability is demonstrated in different typical real-world driving conditions. The results of these case studies reveal that the model has an excellent predictive power, suggesting significant steps towards accurate emission models.

5.2. Methodology

5.2.1. Mathematical model

The goal is to develop a simplified catalyst model, able to predict conversion efficiencies under transient situations. We consider a bottom-up approach, trying to keep the model as simple as possible and adding more complexity only when the simple procedure does not give satisfactory results. The structure of the proposed TWC model is presented in Figure 5.1.

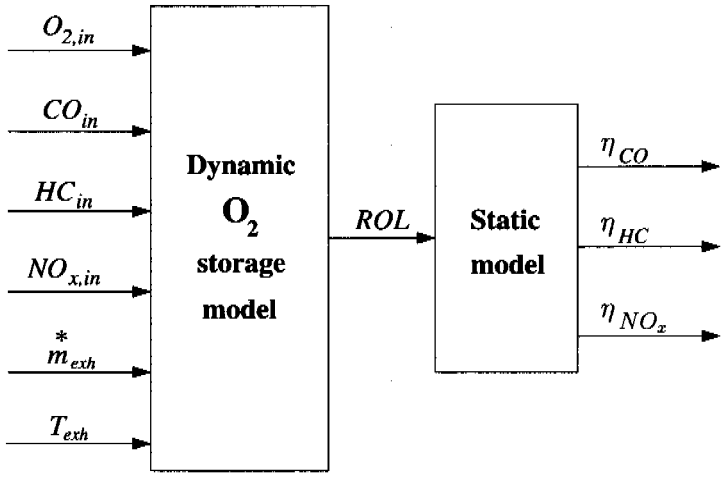

Figure 5.1.: Structure of the proposed TWC model

The basic idea is to decompose the model into two submodels:

- An oxygen storage mechanism that accounts for the departures from the stoichiometric conditions and the imbalance in production and consumption of oxygen which occurs in these situations. The output of this submodel is the relative oxygen level (ROL) in the catalyst.
- A static part describing the conversion efficiency curves as functions of ROL.

Many reactions occur inside a TWC, but comparison with experimental data have shown that a small number of reactions can accurately represent catalytic behaviour. A simplification of the reaction scheme presented in [13] is based on a cumulated chemical approach: CO and HC are aggregated into a virtual reducing species *Red*, O_2 and NO_x are cumulated into a virtual oxidizing species *Oxid*. Therefore, a simplified reaction mechanism is postulated in Table 5.2.

$$\frac{1}{2}\, Oxid + [*] \longrightarrow [O]$$

$$Red + [O] \longrightarrow CO_2\ (or\ H_2O)$$

Table 5.2.: TWC reaction scheme by reactant aggregation. [*] stands for a free site on the catalytic surface, [O] denote an adsorbed oxygen, *Oxid* represents the cumulated oxidising species and *Red* the cumulated reducing species.

The noble metal and ceria surface have been considered as one catalytically

active surface, where oxygen can be absorbed. The first reaction describes this oxygen storage phenomenon. Under the presence of reducing agents, the supply of stored oxygen is used for CO or HC oxidation. This has been accounted for in the second reaction.

The calculation of the reaction rates is straightforward. Both reaction rates constants are determined using standard Arrhenius-type expressions, as follows:

$$r_{ads} = k_1 \cdot c_{Oxid} \cdot (1 - \psi_O) \tag{5.1}$$

$$r_{ox} = k_2 \cdot c_{Red} \cdot \psi_O \tag{5.2}$$

ψ_O denotes the occupancy of the oxygen on the catalytic surface (also named relative oxygen level, ROL), c_{Oxid} and c_{Red} stand for the mole concentrations of oxidising and, respectively, reducing species, whereas k_i represent the reaction rate coefficient and is defined following the Arrhenius equation:

$$k_i = A_i \, exp(\frac{-E_i}{R \cdot T}) \quad i = 1, 2 \tag{5.3}$$

E_i denotes the activation energy and A_i the pre-exponential factor of each reaction, while T represents the exhaust temperature.

Applying the reaction scheme for the two concentrations (c_{Oxid}, c_{Red}) and the oxygen occupancy (ψ_O), the following balance equations are obtained:

$$\frac{\partial c_{Oxid}}{\partial t} = -\frac{\dot{V}}{\epsilon \cdot V_c} (c_{Oxid} - c^{in}_{Oxid}) + OSC \, \frac{1}{2}(-r_{ads}) \tag{5.4}$$

$$\frac{\partial c_{Red}}{\partial t} = -\frac{\dot{V}}{\epsilon \cdot V_c} (c_{Red} - c^{in}_{Red}) + OSC \, (-r_{ox}) \tag{5.5}$$

$$\frac{\partial \psi_O}{\partial t} = r_{ads} - r_{ox} \tag{5.6}$$

V_c denotes the total volume of the TWC, ϵ is a constant representing the volume fraction of the gas phase, $\dot{V}$ denotes the volumetric flow of the exhaust gas, whereas OSC stands for the oxygen storage capacity of the TWC in $\mathrm{mol/m^3}$.

Generally, is has been found that the dynamics of the gas species are much faster than the ones of the oxygen storage and release. Therefore, the mass balance equations (5.4) and (5.5) can be applied as static equations. This can be done by setting the left-hand side of the two equations to zero. After some

algebra, the following terms are obtained for both c_{Oxid} and c_{Red} concentrations:

$$c_{Oxid} = \frac{\dot{V} \cdot c_{Oxid}^{in}}{\dot{V} + 0.5 \cdot \epsilon \cdot V_c \cdot OSC \cdot k_1 \cdot (1 - \psi_O)} \tag{5.7}$$

$$c_{Red} = \frac{\dot{V} \cdot c_{Red}^{in}}{\dot{V} + \epsilon \cdot V_c \cdot OSC \cdot k_2 \cdot \psi_O} \tag{5.8}$$

With these equations, both concentrations can be calculated from the oxygen occupancy, temperature and volumetric flow. The concentrations are in turn used for the estimation of the reaction rates and, consequently, of ψ_O. The conversion efficiencies of HC, CO and NO_x are further on characterised as static functions of this relative oxygen level variable.

This model may appear to be simpler when compared to other approaches presented in the literature. But, this model is used for the emission factors modelling. Usually, vehicles studied for this purpose are available for a short time and only a limited number of tests are possible. Moreover, the tests are performed on chassis dynamometers and not on engine test benches (which would allow more detailed measurements). Therefore, the goal is not to have a good accuracy on an instantaneous basis, but to have a simple and efficient way of predicting the cumulated emissions over a transient cycle. In fact, the model has only five parameters to be determined (kinetic parameters and OSC) and conversion curves to be estimated. It will be shown that the tuning of these parameters is very simple and can be easily performed. Moreover, the very transparent structure of the model makes extensions or simplifications easy to implement.

5.2.2. Parameter estimation

The present model introduces a set of parameters that has to be estimated with reference to a set of experimental data. For each experiment, modelling provides an estimation for each one of the measured outputs (c_{Oxid}, c_{Red}). The computation, using the model, of each output depends on the values of the model parameters. The tuning of the model requires that the tunable parameters be fitted in order to minimize the error between available measurements and the respective simulations. Hence, the problem of model tuning can be viewed as an optimization problem.

For the oxygen storage submodel, the following parameters have to be identified by tuning:

- Kinetic parameters: this includes the two pre-exponential factors A_i and the activation energies E_i that are incorporated in the reaction rates.
- Oxygen storage capacity: the storage capacity of the catalyst has to be determined simultaneously with the kinetic parameters.

The model was tuned to measurements performed on the chassis dynamometer with the BMW vehicle (see Table 4.1). The already measured driving cycle R3 (see Section 1.3), which covers a large area of different operating points, was used to fit the model parameters.

The performance measure which assesses the goodness-of-fit of the model was chosen to be the sum of squares of the sampled error between measured and computed concentrations of oxidizing and reducing species (c_{Oxid} and c_{Red}) at the catalyst outlet. For the optimization procedure, the nonlinear least-squares error algorithm "lsqnonlin" from the Matlab Optimization Toolbox [55] has been employed.

The results of the tuning for the studied vehicle are presented in the form of simulated vs. measured c_{Oxid} and c_{Red} concentrations at the outlet of the converter. The accuracy of the model in predicting catalyst-out aggregated species is presented in Figure 5.2 for the cycle part from 300s to 400s. The prediction of the model is remarkably good. This successful prediction indicates that the oxygen storage dynamics implemented in the model are capable of modelling the phenomenon with good accuracy.

5.2.3. Static conversion curves

The behaviour of the TWC is characterised by the conversion efficiencies of HC, CO and NO_x. Some of the sixteen transient driving patterns have been employed as experimental data necessary to identify the conversion curves as function of the estimated relative oxygen level. The reason for using more than one transient cycle was to achieve enough points covering all possible ranges of the ROL.

Consider, for example, the instantaneous emission profile during the CADC part 1, which corresponds to an urban driving pattern (Figure 5.3). Obviously,

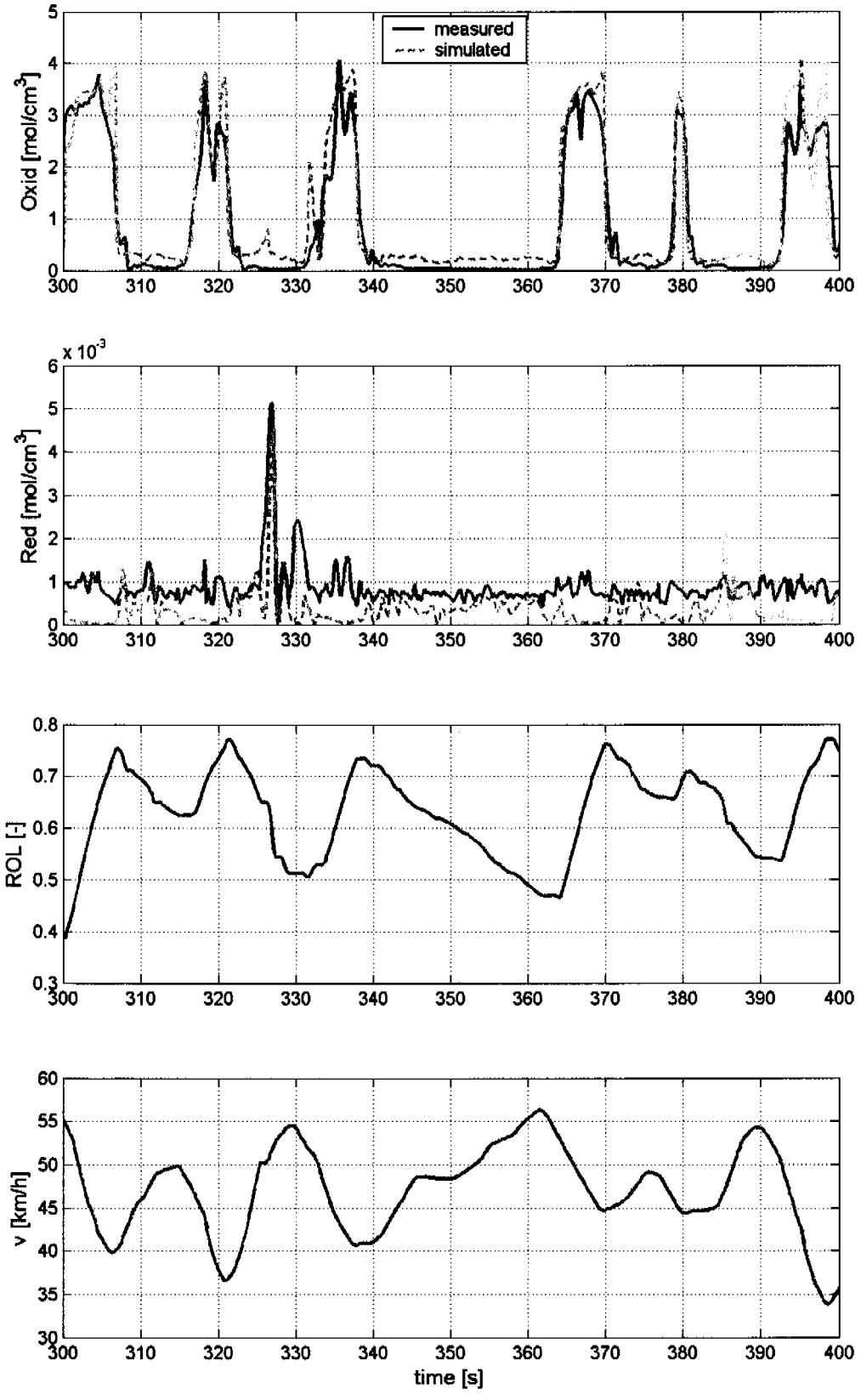

Figure 5.2.: Measured vs. computed concentrations of the oxidising and reducing species.

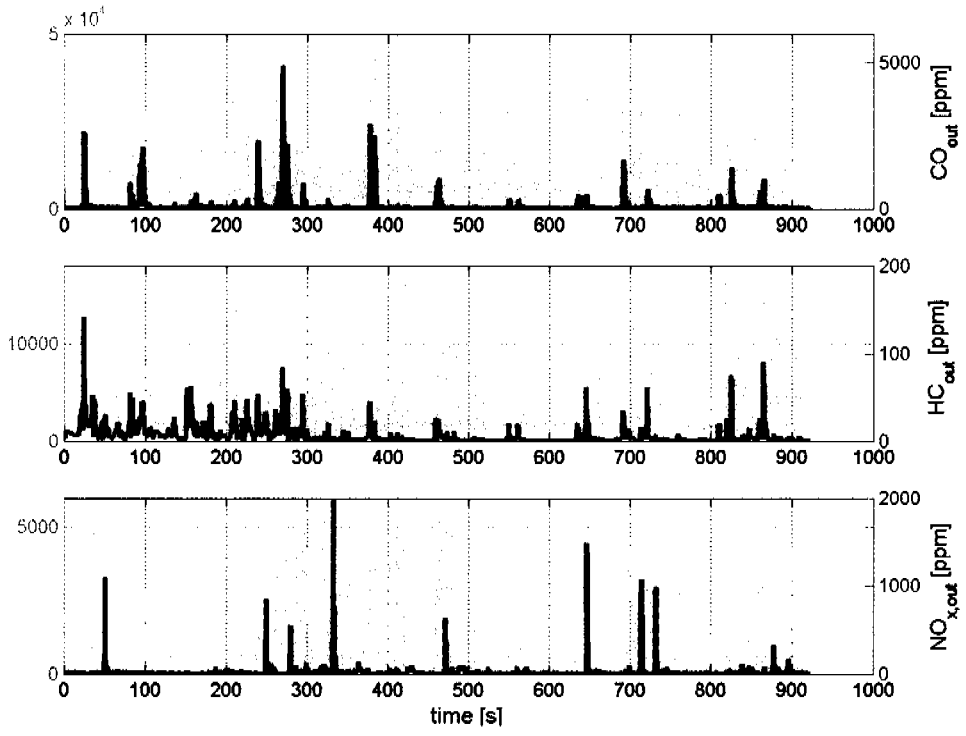

Figure 5.3.: Measured instantaneous NO_x, HC and CO emissions at converter inlet (dashed lines)and outlet (solid lines) over the 900 seconds of the CADC, urban driving pattern.

the specific catalyst attains a significant overall conversion efficiency. The model should be, therefore, capable of matching the catalyst's breakthrough during accelerations, decelerations or fuel cutoff situations.

In order to be consisted with this catalyst's behaviour, first the already identified kinetic parameters and OSC were used to generate the relative oxygen level during the experimental data. Further on, conversion efficiencies of HC, CO and NO_x were determined, but only when the values of the inlet concentrations were above of a certain threshold.

For NO_x, for example, this threshold was set at 500 ppm. If the values of inlet NO_x emissions are below this threshold it makes not a big difference for the cumulated emission value if the conversion efficiency is set at 99% or at 50% range. At points below this threshold, a constant conversion rate is an adequate approximation. For this reason, the emissions below these threshold values were not considered in the identification process of the conversion curves.

Once the events with high inlet concentrations were identified, the conversion efficiencies were determined on an instantaneous basis. However, we have to

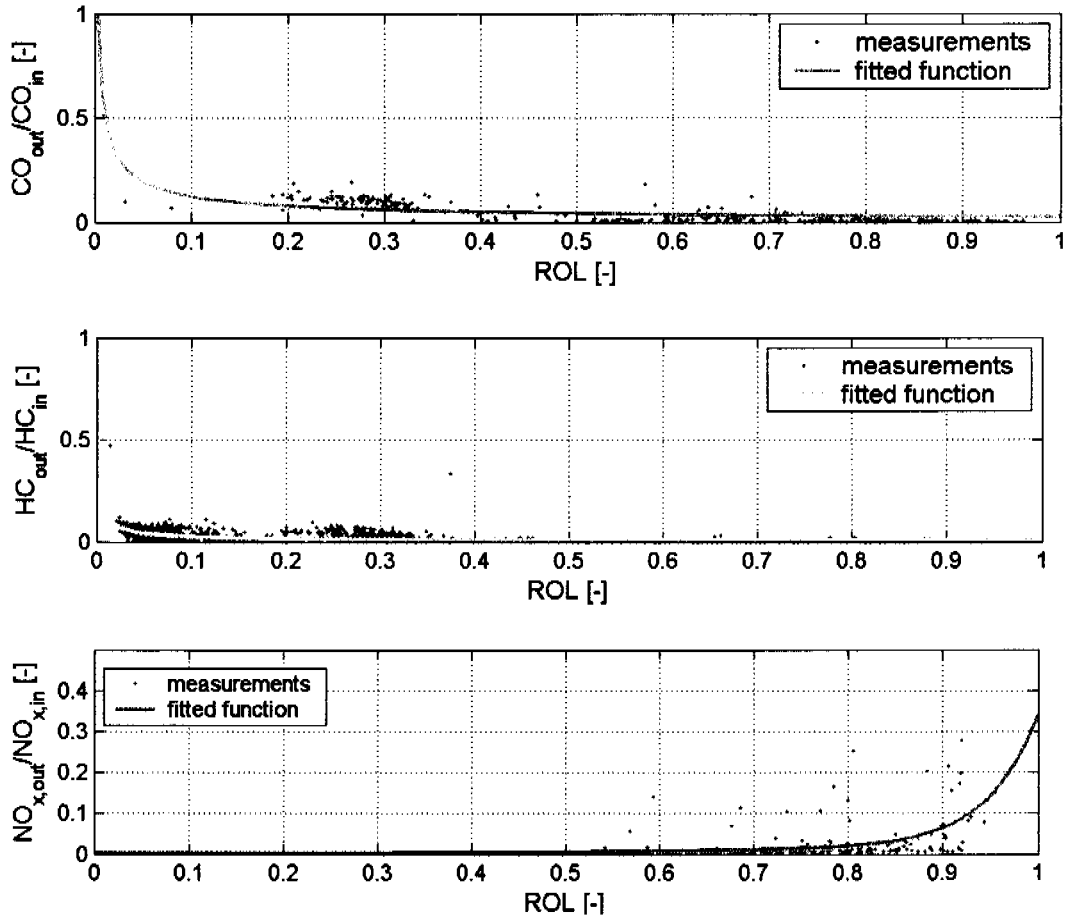

Figure 5.4.: Fitted conversion curves as function of ROL

take into account that both inlet and outlet concentrations are signals reconstructed from the ones recorded at the analyser. But, since this reconstruction has a certain time quality, it is not be advisable to determine the conversions efficiency on a 10 Hz basis, since more errors would be then introduced. For this reason, the signals were averaged over a two seconds window and the conversion rates were determined using these average results.

With this approach, nonlinear static functions were derived by regressing the test data with respect to ROL. Figure 5.4 presents the measured and fitted functions for each of the three pollutants.

A power fit gave the best results for the conversion functions of CO and HC, while for NO_x an exponential fit was chosen. As expected, for HC and CO the catalyst's conversion efficiency is rather high (low outlet-to-inlet ratio) until the oxygen stored in the washcoat is gradually depleted. At low values of ROL, the conversion curves of these pollutants start to rise sharply. For NO_x the opposite

behaviour can be observed, with high conversion efficiency when less oxygen is stored in the catalyst and lower conversion rate when oxygen starts to fill the washcoat.

5.3. Validation

The TWC model's predictive ability was tested for each of the "source" driving cycles. In each case, the following procedure was employed:

- Use already identified kinetic parameters and input variables of the oxygen storage submodel to generate the relative oxygen level over the cycle on an instantaneous basis.
- For each pollutant (CO, HC, NO_x) find the points where inlet concentrations are below the threshold limit. For these points, constant value of 99% conversion efficiency is fixed. Obviously, this procedure has to be applied separately for each emission.
- For the points above the threshold limit, determine the conversion efficiency as function of the corresponding ROL, using the fitted conversion curves. Again, this procedure is considered separately for each pollutant.
- Calculate outlet concentrations from the inlet values and the above determined conversion efficiencies.
- For validation, determine the cumulated emission values over the cycle and compare to the corresponding measured values.

Figure 5.5 presents computed and measured emission factors of the three pollutants over the different driving cycles. Apparently, the model successfully matches the behaviour of the TWC under transient situations. The average of the absolute relative error in the prediction of the emission factors is 14% for CO, 17% for HC and 12% for NO_x. The simulation results correlate to the measured data with a coefficient of determination higher than 0.90 for all the pollutants.

In more detail, the evolution of the cumulated emission values over a urban driving pattern (CADC, part 1) is presented in Figure 5.6. When comparing the computed and measured CO emissions, it can be seen that the prediction of

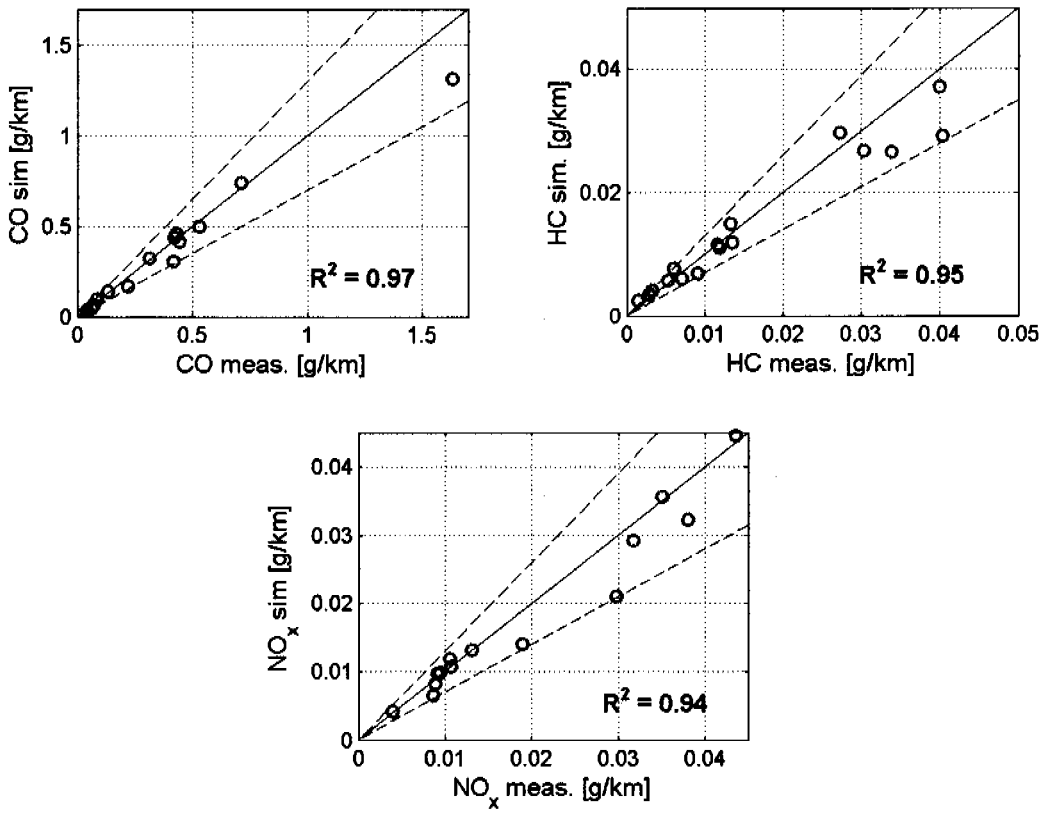

Figure 5.5.: Measured vs. computed catalyst-out emission factors of CO, HC and NO_x using the TWC model

the model is rather good, especially when the order of magnitude of the breakthroughs is considered. Apparently, the model successfully matches the catalyst's behaviour during acceleration. The breakthrough caused by the acceleration at the second 250 is, however, underestimated. This has as consequence the underestimation of the final emission factor value. Thus, there exists room for further improvement of the storage submodel and of the conversion rate function.

The model results for HC are also quite good, again considering the order of magnitude extremely small and rather difficult to match. The emission of the acceleration at second 150 is here underestimated, but this effect is compensated by the overestimation of the breakthrough caused by the acceleration at 450 s. Again, this is the subject for future improvements in the oxygen storage submodel. On a quantitatively basis, the error between computed and measured cumulated values is always below 0.01 g for all cycles. HC breakthrough behavior is predicted with a quite good accuracy, taking into account the complexity of the hydrocarbons composition that is modeled only by one

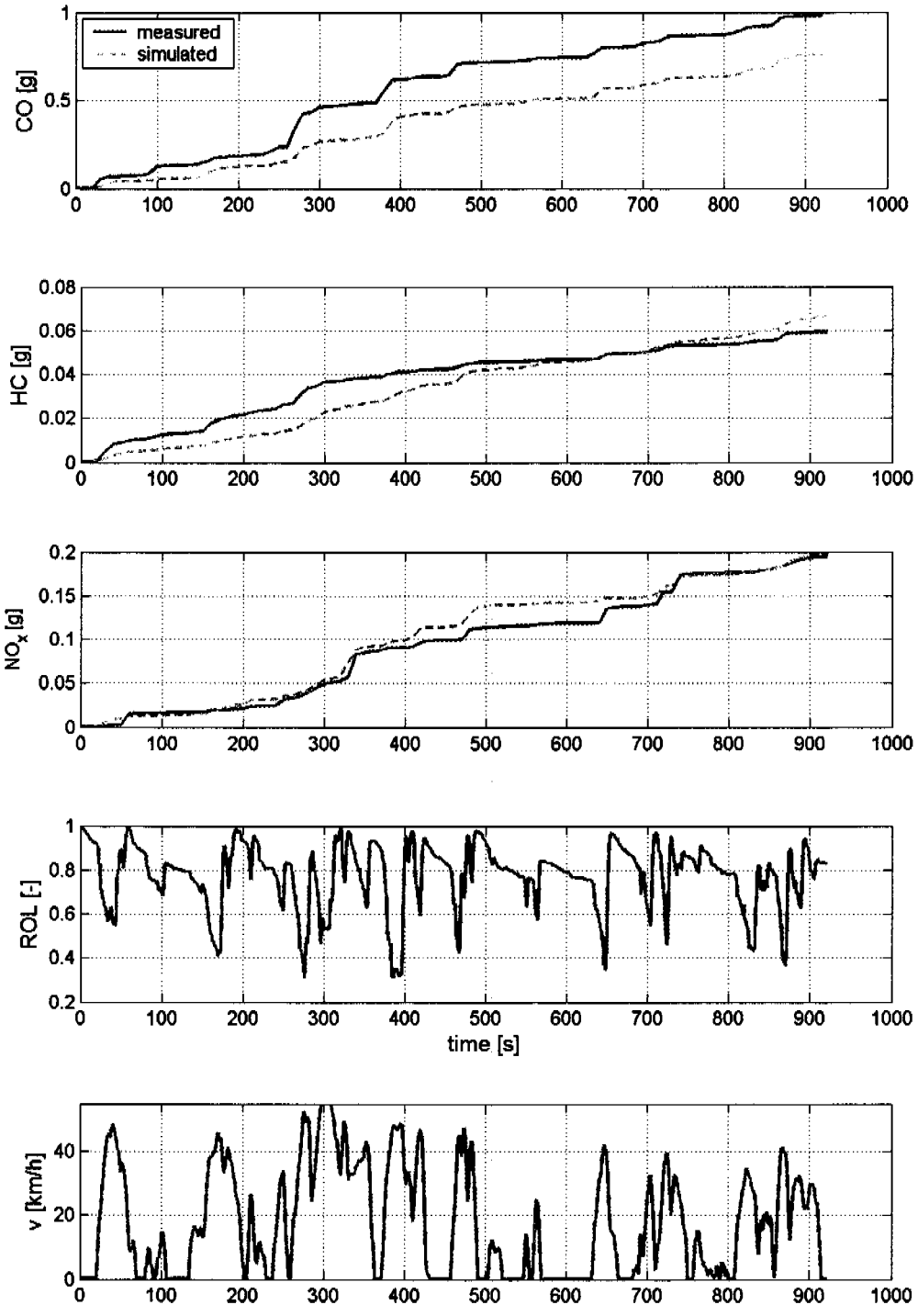

Figure 5.6.: Computed and measured cumulative CO, HC and NO_x emissions at the catalyst-out during CADC, urban part

aggregated component (the *Red* species).

The simulation appears exceptionally good for the computed and measured cumulated NO_x emission values. The model succeeds to match the catalyst's behaviour which causes NO_x breakthroughs during acceleration or fuel cut-off phases. This successful prediction indicates that the oxygen storage reactions that are implemented in the model are capable of modelling the phenomenon with high accuracy.

The above results indicate that the model formulation has the ability to match typical behaviour of a three-way catalytic converter under transient conditions. Additionally, since more than one dynamic driving cycle was used for validation, another important finding is that the model is capable of predicting the catalyst's performance outside the region where it has been tuned.

The influence of the temperature on the conversion curves seemed to be negligible in our case, most likely due to the fact that all cycles under study were warm-cycles. However, in order to extend the model for the cold-start situations, the impact of the temperature onto conversion rate functions should be carefully considered.

5.4. Conclusions

A simplified TWC model has been developed to generate the catalyst-out pollutants. This model includes an oxygen storage submodel based on simplified kinetic reactions mechanism, which has as output the relative oxygen level, and a static submodel for the estimation of pollutants conversion curves as function of ROL. The parameter estimation methodology has been briefly presented and demonstrated in a case study.

To enable an objective assessment of the model accuracy, the methodology has been tested for sixteen transient situations corresponding to different driving patterns. The comparison of measurements and simulation is made in terms of emission factors of CO, HC and NO_x at the converter exit, as well as the computed and measured cumulated CO, HC and NO_x values at the catalyst outlet, the latter being a much more demanding task for a model. The average absolute relative error in the prediction of all pollutants emission factors was found to be no more than 17%. Additionally, the simulated cumulated values follow the same trend taken by the measurements.

The results proved the model capacity of taking into account the changes in the catalyst's behaviour due to transients of the different driving situations. The obtained results can be considered to support a clear demonstration of the attainable accuracy and predictive ability of this TWC model.

Further improvements and developments could be considered for this model. Additionally to ROL, the study of the role of the volumetric flow and/or temperature on conversion curves could give additional benefit in the quality of the results. In this model, simplified assumption considered the TWC as one chamber. A further extension of the present approach could consider the discretisation along the flow axis into a number of cells.

Moreover, this model was used only for warm cycles, but it could be enhanced to generate the cold-start extra emissions by focusing on the effect of temperature variations

More cars equipped with a three-way catalytic converter should be studied for a complete validation.

6. Conclusions and Outlook

During the last decades, the ongoing reduction of emission limits was achieved with complex engine technology, highly efficient exhaust after treatment systems and sophisticated engine control units. This progress has caused an amplification in the difference between emissions in type approval legislative cycles and in real-world driving. Therefore, demand on models able to predict real-world emissions increased, but, due to the more and more complex engine technology, the established models became increasingly inaccurate.

Emissions models are used today to derive emissions inventories at different levels (regional, national, international). Beside that, the need for local data is considerably amplified. Emission estimates for cities, quarters or even small signalised road networks, single streets or tunnels are used as input for traffic control measures, dispersion models and for the design of ventilation systems.

Instantaneous emission models have the advantage of being able to generate the emissions from unmeasured driving patterns using only a small number of measurements. Therefore, research to improve these type of modelling approach is considered.

Modern emissions models are required to simulate fuel consumption and emissions (CO, CO_2, HC, NO_x) for all possible combinations of driving cycles, driving behaviour, vehicle loadings, gradients of the road and thermal conditions with accurate quality. A main question for all approaches is how to reach a good prediction for all the pollutants of modern TWC vehicles under hot running conditions. These emissions are highly influenced by transient excursions of the air-to-fuel ratio to the lean or to the rich side and, consequently, by the resulting efficiency of the catalytic converter.

While most of the emission modellers aim to obtain the best results given a set of available data, our goal was to achieve a desired quality (less than 20% relative error). We started with a simple approach and with a fix set of measurements and we added more complexity and performed additional investigations for the cases where the demanded quality could not be accomplished.

In this thesis, an instantaneous emissions model has been developed, which is based on the simulation of the actual engine conditions using (proportional) engine torque, engine speed and, for modern cars, the derivative of manifold pressure as input variables. Such an approach represents a physically way of describing all different driving situations, in contrast to many statistical approaches. Additionally, various gear-shifts strategies, vehicle loadings, road gradients or combinations of them could be adequately taken into account.

For an accurate instantaneous emissions model, first the frequency of the measurements was considered. Measurements performed with fast sensors showed that most of the emission peaks last less than one second. The frequency content of these signals is 2-4 Hz. Additionally, engine related signals, like manifold pressure, engine speed, engine torque may also change significantly within tenths of a second. Since a significant part of the frequency content of these signals would be lost at the usual sampling rate of 1 Hz, it was decided to collect the data with ten samples per second.

In a next step, the exhaust gas transport dynamics had to be compensated, such that a correct time alignment between emission signals and their generating engine variables was obtained. The modelling of the exhaust gas transport systems was performed using signal processing approaches.

The easiest part of this was the modelling of the raw gas system, i.e. the transport from the raw probe point (at the tailpipe) to the raw analyzer output, since this leads to time-invariant models. Modelling the dynamics in the exhaust system of the car (i.e. catalyst-out until tailpipe) was a more complex step, since the system is time variable, and the most difficult task of all was to model the transport in the dilution system, because it is a combination of the other two problems and, additionally, includes a non-linear static relation.

It has been shown that it is possible to reconstruct the emission signals at the tailpipe location with a time quality of about 2.5 seconds from the dilution measurements out of an overall delay of up to twenty-five seconds. This is a good result in itself. However, the quality is poor compared to the raw system whose inversion has a time quality of about 0.3 seconds out of an physical delay of up to five seconds.

In addition, it is essential for the reconstruction process to know the exhaust volume flow. Thus the original advantage of CVS measurements, of not needing the exhaust volume flow signal, is lost.

Generally, the emission signal at the catalyst-outlet can be reconstructed from

the raw gas measurements with a time quality of about 0.8 seconds.

This allows the emissions data to be correlated to the correct state of the car. Emission models based on mapping the emissions onto engine speed and brake mean effective pressure and using 10 Hz corrected signals give excellent results for exhaust gases (CO, HC, NO_x, CO_2) of the pre Euro-1 gasoline and of diesel vehicles. For three-way catalysts vehicles, the static map gives adequate accuracy for CO_2, but only satisfactory results for all other pollutants. Since most of the emissions of modern catalyst cars are generated during transient situations, the model had to be extended by adding a dynamic variable. The chosen dynamic variable in this case was the derivative of manifold pressure. The engine-out emissions of TWC are very well predicted using the resulting transient 4D maps.

Moreover, the model proved to be able to predict the effects of contributory aspects like changing gear-shift strategies, loads of the car, gradients of the road and combinations of them as it was validated for a number of diesel and modern gasoline vehicles.

Further on, a catalyst model has been developed, which generates the catalyst-out emissions. This model approach considers oxygen release and adsorption phenomena as the main reactions taking place in the catalytic converter. This model is divided into two submodels. The first submodel considers simplified kinetic reactions to generate the relative oxygen level in the catalytic surface. This submodel has a limited number of parameters which could be identified using one of the already tested "source" cycle. Based on the obtained ROL variable, conversion curves for all pollutants (CO, HC, NO_x) are derived as static functions of the relative oxygen level.

This TWC model proved to perform with adequate accuracy over several transient cycles.

The approach presented here offers a variety of further developments. Some of them are listed in the following:

- *Cold start effect*: the present model was concerned only with the prediction of emissions generated during warm cycles. An extended model could consider the effect of temperature to obtain the cold-start extra emissions and possibly to refine the catalytic conversion rate at higher temperatures..

- *Effects of load, gradient and gear-shift strategy*: only a limited sample

of vehicles were tested to check the applicability of the model for forecasting emissions produced by these contributory situations. In order to generate correction factors required by the emission inventories, more vehicles from various categories should be tested.

- *TWC model axial discretization*: the present O_2 storage dynamics submodel considered the TWC as a whole. This model could be discretised along the flow axis into a number of cells. The number of cells remains to be determined. This extension is straightforward.

- *Conversion curves as function of ROL, volumetric flow and temperature*: similar to the approach followed to generate the static conversion functions, the effect of volumetric flow should be analysed in connection with ROL, as it might offer the possibility of improving the overall results.

- *Other pollutants*: The present model was concerned only with the estimation of regulated pollutants. A further development could consider the implementation of a method for the prediction of other pollutants as NO, NH_3, Benzene, Methane, etc.

A. Appendix

A.1. Kinematic characteristics of the real-world driving patterns

Nr.	Driving pattern	Duration [s]	Mean speed [km/h]	Mean acc. $[m/s^2]$	Mean pos. acc. $[m/s^2]$	Idle time [s]	Description
1	CADC, part1	921	17.480	0.000	0.068	28.23 %	urban
2	CADC, part2	862	61.491	0.007	0.052	2.20 %	rural
3	CADC, part3	736	120.338	0.000	0.029	0.00 %	highway
4	AE1R	530	118.300	0.000	0.013	0.00 %	highway, speedy, stable
5	AE2R	530	107.651	-0.003	0.024	0.00 %	highway, speedy, fluctuant
6	A3R	260	100.337	-0.017	0.020	0.00 %	highway, slow, fluctuant
7	A4R	260	89.531	-0.002	0.028	0.00 %	highway, slow, very fluctuant
8	LE1R	260	77.188	0.000	0.021	0.00 %	extra-urban, speedy, stable
9	LE2sR	530	65.593	-0.005	0.031	0.00 %	extra-urban, slow, fluctuant
10	LE2uR	530	52.926	-0.003	0.044	0.00 %	extra-urban, slow, very fluctuant
11	LE3R	260	52.336	0.000	0.027	0.00 %	urban, speedy, fluctuant
12	LE5R	260	31.927	-0.002	0.063	2.69 %	urban, slow, very fluctuant
13	LE6R	530	33.529	-0.003	0.053	4.34 %	urban, stagnant, very fluctuant
14	StGoHW	260	7.084	-0.009	0.018	0.00 %	highway, stop and go
15	StGoUrb	530	4.129	0.000	0.022	24.53 %	urban, stop and go
16	BAB	1000	117.500				highway

Table A.1.: Kinematic characteristic of the "source" real-world driving patterns

A.2. Set-up for the measurements necessary for the transport systems modelling

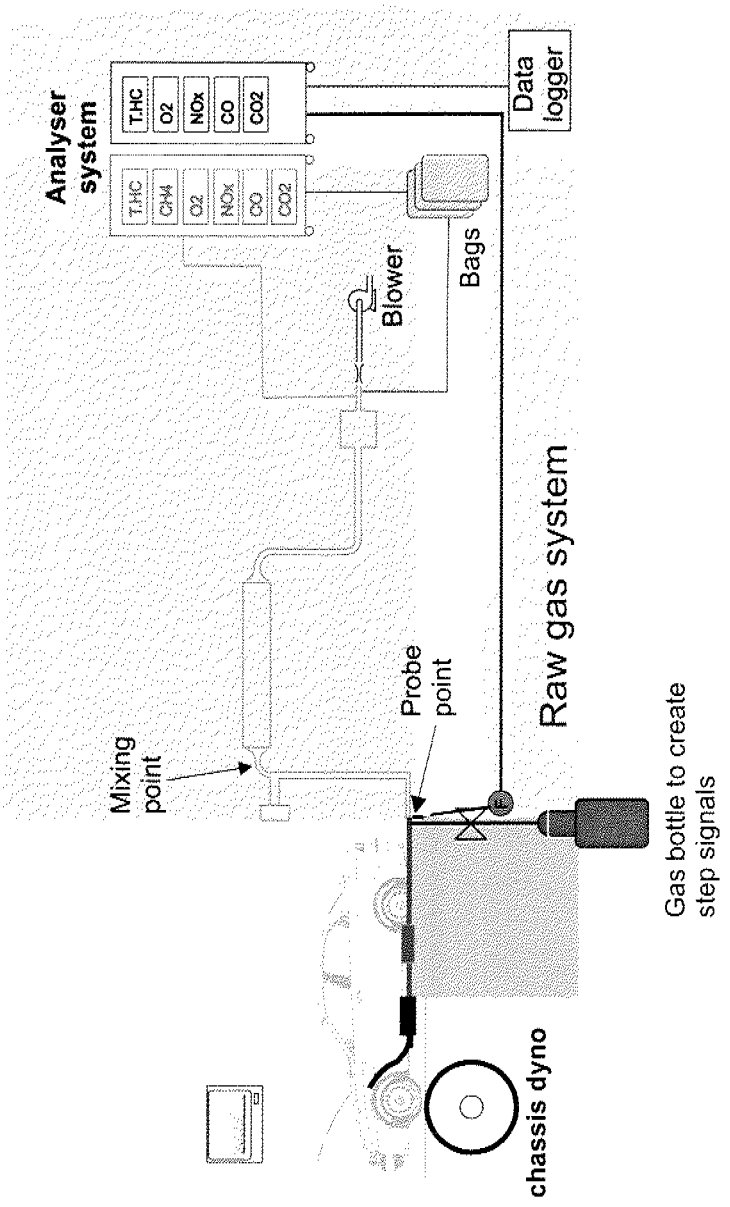

Figure A.1.: Set-up for the measurements necessary for the raw system parameterisation

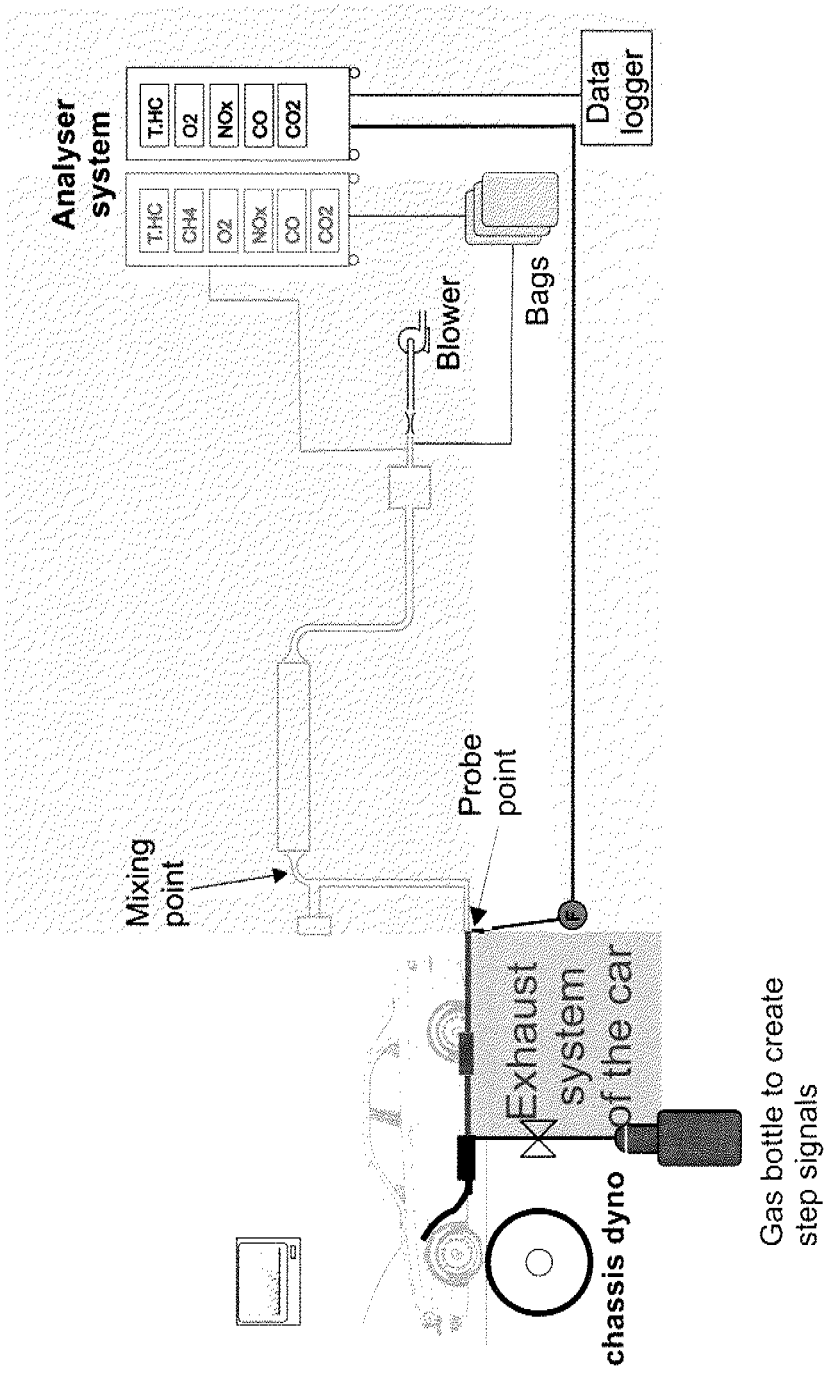

Figure A.2.: Set-up for the measurements necessary for the vehicle exhaust system parameterisation

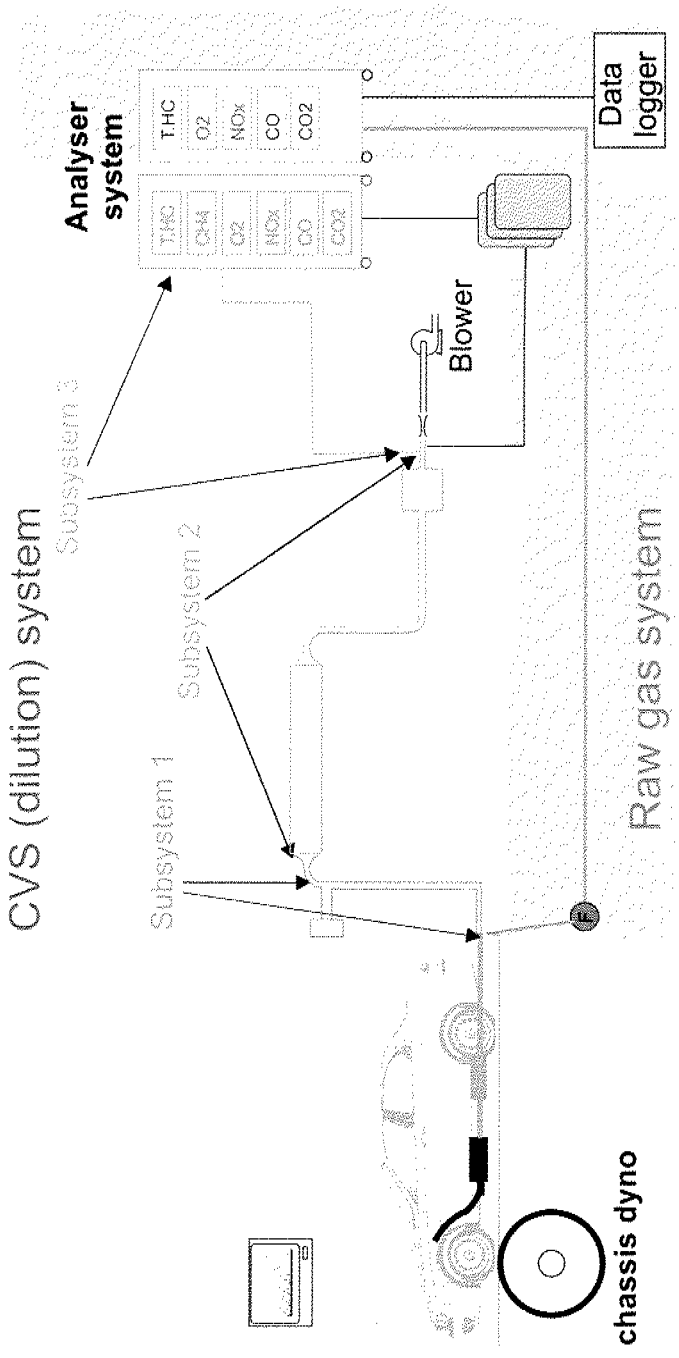

Figure A.3.: CVS subsystems

Bibliography

[1] US Environmental Protection Agency. Assessing the emissions and fuel consumption impacts of intelligent transportation systems. Technical Report 231-R-98-007, U.S. Environmental Protection Agency, Washington D.C., 1998.

[2] K. Ahn, A. Rakha, H.and Trani, and M. Van Aerde. Estimating vehicle fuel consumption and emissions based on instantaneous speed and acceleration levels. *Journal of Transportation Engineering-ASCE*, 128(2):182–190, 2002.

[3] D. Ajtay and M. Weilenmann. Compensation of the exhaust gas transport dynamics for accurate instantaneous emission measurements. *Environmental Science and Technology*, 38(19):5141–5148, 2004.

[4] D. Ajtay and M. Weilenmann. Static and dynamic instantaneous emission modelling. *International Journal of Environment and Pollution*, 22(3):226–239, 2004.

[5] D. Ajtay and M. Weilenmann. Application of vehicle instantaneous emission models at fleet level. In *5th International Conference on Urban Air Quality*, 2005.

[6] D. Ajtay and M. Weilenmann. Towards accurate instantaneous emission models. *Atmospheric Environment*, 39(13):2443–2449, 2005.

[7] D. Ajtay and M. Weilenmann. Validation of instantaneous emission model for different loads, slopes and gear-shift strategies. In *14th International Symposium "Transport and Air Pollution"*, pages 128–134, 2005.

[8] D. Ajtay, M. Weilenmann, T. Auckenthaler, and C. Onder. Modelling catalyst-out nox emissions based on the relative oxygen level in the catalyst. In *13th International Scientific Symposium "Transport and Air Pollution"*, 2004.

[9] M. Andre. The artemis european driving cycles for measuring car pollutant emissions. *Science of the Total Environment*, 73-84:334–335, 2004.

[10] M. Andre, R. Joumard, A.J. Hickman, and D. Hassel. Actual car use and operating conditions as emission parameters - derived urban driving cycles. *Science of the Total Environment*, 147:225–233, 1994.

[11] M. Andre and C. Pronello. Relative influence of acceleration and speed on emissions under actual driving conditions. *International Journal of Vehicle Design*, 18(3-4):340–353, 1997.

[12] P. Andrei. Real-world heavy-duty emissions modeling. Master's thesis, West Virginia University, 2001.

[13] T.S. Auckenthaler, C.H. Onder, H.P. Geering, and J. Frauhammer. Modeling of a three-way catalytic converter with respect to fast transients lambda-sensor relevant exhaust gas components. *Industrial and Engineering Chemistry Research*, 43(16):4780–4788, 2004.

[14] M. Barth, F. An, J. Norbeck, and M. Ross. Modal emissions modeling: A physical approach. *Transportation Research Record*, 1520:81–88, 1996.

[15] M. Barth, T. Younglove, C. Malcolm, and G. Scora. Mobile source emissions new generation model: Using a hybrid database prediction technique. 01-ts-26655-02-dfr, U.S. Environmental Protection Agency, http://www.epa.gov/otaq/models/ngm/cecert.pdf, 2002.

[16] M. Barth, T. Younglove, T. Wenzel, G. Scora, F. An, M. Ross, and J. Norbeck. Analysis of modal emissions from diverse in-use vehicle fleet. *Transportation Research Record*, 1587:73–84, 1997.

[17] H. Bendtsen and L. Reiff. An urban road traffic emissions model. *International Journal of Vehicle Design*, 20(1-4):192–200, 1998.

[18] M. Boaro, F. Giordano, S. Recchia, V. Dal Santo, M. Giona, and A. Trovarelli. On the mechanism of fast oxygen storage and release in ceria-zirconia model catalysts. *Applied Catalysis B - Environmental*, 52:225–237, 2004.

[19] E.P. Brandt, Y. Wang, and J.W. Grizzle. Dynamic modeling of a three-way catalyst for si engine exhaust emission control. *IEEE Transactions on Control Systems Technology*, 8(5):767–776, 2000.

[20] Environmental Protection Agency Air Resources Board California. Methodology for estimating emissions from on-road motor vehicles. volume 1: Introduction and overview. Technical report, California Environmental Protection Agency Air Resources Board, http://www.arb.ca.gov/msei/on-road/mvei7g/mvdocs.htm, 1996.

[21] P. de Haan and M. Keller. Emission factors for passenger cars: application of instantaneous emission modeling. *Atmospheric Environment*, 34(27):4629–4638, 2000.

[22] P. de Haan and M. Keller. Real-world driving cycles for emission measurements: Artemis and swiss cycles. Folgerbeiten zum BUWAL-Bericht SRU Nr. 255 Arbeitsunterlage 25, Swiss Agency for Environment, Forests and Landscape (SAEFL), 2001.

[23] P. de Haan and M. Keller. Modelling fuel consumption and pollutan emissions based on real-world driving patterns: the hbefa approach. *International Journal of Environment and Pollution*, 22(3):240–258, 2004.

[24] P. Degobert. *Automobiles and Pollution*. Society of Automotive Engineers, Inc., 1995.

[25] B. Efron and R.J. Tibshirani. *An introduction to the bootstrap*. Chapman and Hall, New York, 1993.

[26] M. Ekstromm, A. Sjodin, and K. Andreasson. Evaluation of the copert iii emission model with on-road optical remote sensing measurements. *Atmospheric Environment*, 38:6631–6641, 2004.

[27] M. Ergeneman, C. Sorusbay, and A. Goktan. Development of a driving cycle for the prediction of pollutant emissions and fuel consumption. *International Journal of Vehicle Design*, 18(3-4):391–399, 1997.

[28] M. Fisz. *Probability Theory and Mathematical Statistics*. Wiley, 3rd edition, 1963.

[29] D.G. Fox. Uncertainty in air-quality modeling - a summary of the ams workshop on quantifying and communicating model uncertainty, woodshole, mass, september 1982. *Bulletin of the American Meteorological Society*, 65(1):27–36, 1984.

[30] N.L.J. Gense. Driving style, fuel consumption and tailpipe emission. TNO Report oo.0R.VM.021.1/HG, TNO Automotive, Netherlands, 2000.

[31] M. Guenther, M. Vaillancourt, and M. Polster. Advancements in exhaust flow measurement technology. In *SAE Technical Paper*, 2003.

[32] J.Q. Hansen, M. Winther, and S.C. Sorenson. The influence of driving patterns on petrol passenger car emissions. *Science of the Total Environment*, 169(1-3):129–139, 1995.

[33] J. Hao, D. He, Y. Wu, L. Fu, and K. He. A study of the emission and concentration distribution of vehicular pollutants in the urban area of beijing. *Atmospheric Environment*, 34(3):453–465, 2000.

[34] S. Hausberger, J. Rodler, P. Sturm, and M. Rexeis. Emission factors for heavy-duty vehicles and validation by tunnel measurements. *Atmospheric Environment*, 37(37):5237–5245, 2003.

[35] J.G. Hawley, C.D. Bannister, C.J. Brace, A. Cox, D. Ketcher, and R. Stark. Vehicle modal emissions measurement - techniques and issues. *Proceedings of the Institution of Mechanical Engineers Part D-Journal of Automobile Engineering*, 218(D8):859–873, 2004.

[36] M.J. Hazucha, E. Seal, and L.J. Folinsbee. Effects of steady-state and variable ozone concentration profiles on pulmonary function. *American review of respiratory disease*, 146:1487–1493, 1992.

[37] P. Heirigs, S. Delaney, and R. Dulla. Mobile& on-road motor vehicle emissions model, 5 day training course. Technical Report 68-C7-0051, U.S. Environmental Protection Agency, Washington D.C., 2001.

[38] J.B. Heywood. *Internal Combustion Engine Fundamentals*. McGraw-Hill, 1988.

[39] J. Horner. Carbon monoxide: The invisible killer. *Journal of the Royal Society of Health*, 118(3):141–145, 1998.

[40] N.A.H. Janssen, B. Brunekreef, P. van Vliet, F. Aarts, K. Meliefste, H. Harssema, and P. Fischer. The relationship between air pollution from heavy traffic and allergic sensitization, bronchial hyperresponsiveness, and respiratory symptoms in dutch schoolchildren. *Environmental Health Perspectives*, 111(12):1512–1518, 2003.

[41] P. Jost, D. Hassel, and K-S. Sonnborn. Neuartige methode zur ermittlung von emissionsfaktoren für nfz. Tagungsband Abgasemissionen und Immissionen durch den Strassenverkehr 64, Institute of Combustion Engines and Thermodynamics of the Technical University-Graz, 1992.

[42] P. Jost, R. Joumard, and J. Hickman. Influence of instantaneous speed and acceleration on hot passenger car emissions and fuel consumption. In *SAE Paper*, volume 950928, 1995.

[43] R. Joumard, F. Philippe, and R. Vidon. Reliability of the current models of instantaneous pollutant emissions. *Science of the Total Environment*, 235(1-3):133–142, 1999.

[44] M. Keller and P. de Haan. Luftschadstoff-emissionen des strassenverkehrs 1950-2020. Schriftenreihe Umwelt 255, BUWAL, 2000.

[45] M. Keller, P. Koch, J. Heldstab, D. Dähler Staub, and P. de Hann. *Handbook Emission Factors for Road Transport*. UBA Berlin and BUWAL Bern and INFRAS Bern, 1999. CD.

[46] Y. Kishi, S. Katsuk, Y. Yoshikawa, and I. Morita. A method for estimating traffic flow fuel consumption Ű using traffic simulation. *JSAE Review*, 17(3):307–311, 1996.

[47] G. Konstantas and A. Stamatelos. Quality assurance of exhaust emissions test data. *Proceedings of the Institution of Mechanical Engineers Part D-Journal of Automobile Engineering*, 218(D8):901–914, 2004.

[48] H. Kwakernaak and R. Sivan. *Modern Signals and Systems*. Prentice Hall, 1991.

[49] L. Lennart. *System Identification: Theory for the user*. Prentice Hall, 2 edition, 1999.

[50] S.J. Lindley, D.E. Conlan, D.W. Raper, and A.F.R. Watson. Estimation of spatially resolved road transport emissions for air quality management applications in the north west region of england. *Science of the Total Environment*, 235(1-3):119–132, 1999.

[51] D. Mage, G. Ozolins, P. Peterson, A. Webster, R. Orthofer, V. Vandeweerd, and M. Gwynne. Urban air pollution in megacities of the world. *Atmospheric Environment*, 34(5):681–686, 1996.

[52] U. Mathis, M. Mohr, and A.M. Forss. Comprehensive particle characterization of modern gasoline and diesel passenger cars at low ambient temperatures. *Atmospheric Environment*, 39(1):107–117, 2005.

[53] U. Mathis, M. Mohr, R. Kaegi, A. Bertola, and K. Boulouchos. Influence of diesel engine combustion parametes on primary soot particle diameter. *Environmental Science and Technology*, 39(6):1887–1892, 2005.

[54] U. Mathis, M. Mohr, and R. Zenobi. Effect of organic compounds on nanoparticle formation in diluted diesel exhaust. *Atmospheric Chemistry and Physics*, 4:609–620, 2004.

[55] Mathworks. *Optimization Toolbox User's Guide*, 2004.

[56] H. Mayer. Air pollution in cities. *Atmospheric Environment*, 33(24-25):4029–4037, 1999.

[57] H. Müller. Modellierung des abgasstroms. Master's thesis, ETH Zürich, 2001.

[58] E. Nam and M. Ross. A fuel rate based catalyst pass fraction model for predicting tailpipe nox emissions from a composite car. *SAE*, 1999-01-0455, 1999.

[59] L. Ntziachristos, Z. Samaras, S. Eggleston, N. Gorissen, D. Hassel, A.J. Hickman, R. Joumard, R. Rijkeboer, and K.H. Zierock. Copert iii computer programme to calculate emissions from road transport Ű methodology and emission factors. Technical Report 49, European Environment Agency, 2000.

[60] World Health Organisation. Air quality guidelines. Technical report, WHO Regional Office for Europe, 2000.

[61] L. Pelkmans. Decade technical report tr9: Comparative assessment. Technical Report Project NNE5-1999-00270, EU, 2003.

[62] J.P.J. Peyton, J.B. Roberts, J. Pan, and R.A. Jackson. Modeling the transient characteristics of a three-way catalyst. *SAE*, 1999-01-0460, 1999.

[63] G.N. Pontikakis, G.S. Konstantas, and A.M. Stamatelos. Three-way catalytic converter modeling as a modern engineering design tool. *Journal of Engineering for Gas Turbines and Power - Transactions of the ASME*, 126(4):906–923, 2004.

[64] C.A. Pope, M.L. Hansen, R.W. Long, K.R. Nielsen, N.L. Eatough, W.E. Wilson, and D.J. Eatough. Ambient particulate air pollution, heart rate variability, and blood markers of inflammation in a panel of elderly subjects. *Environmental Health Perspectives*, 112(3):339–345, 2004.

[65] Y. Qi, H. Teng, and L. Yu. Microscale emission models incorporating acceleration and deceleration. *Journal of Transportation Engineering-ASCE*, 130(3):348–359, 2004.

[66] H. Rakha, K. Ahn, and A. Trani. Development of vt-micro model for estimating hot stabilized light duty vehicle and truck emissions. *Transportation Research Part D*, 9(1):49–74, 2004.

[67] A.W. Reynolds and B.M. Broderick. Development of an emissions inventory model for mobile sources. *Transportation Research Part D- Transport and Environment*, 5(2):77–101, 2000.

[68] R.A. Rinsky. Benzene and leukaemia: An epidemiologic risk assessment. *Environmental health perspectives*, 82:189–191, 1989.

[69] W.F. Rogge, L.M. Hildemann, M.A. Mazurek, G.R. Cass, and B.R.T. Simoneit. Sources of fine organic aerosol. 2. noncatalyst and catalyst-equipped automobiles and heavy-duty diesel trucks. *Environmental Science and Technology*, 27(4):636–651, 1993.

[70] T. Schweizer, C. Rytz, N. Heeb, and P. Mattrel. Nachführung der emissionsgrundlagen strassenverkehr, teilprojekt emissionsfaktoren, arbeiten 1996. Technical Report 161150, EMPA, 1997.

[71] P.L. Silverston. Automotive exhaust catalysis: Is periodic operation beneficial? *Chemical Engineering Science*, 51(10):2419–2426, 1996.

[72] R. Smit, R. Smokers, and R. Schoen. Versit+ ld: Development of a new emission factor model for passenger cars linking real-world emissions to driving cycle characteristics. In *14th International Symposium "Transport and Air Pollution"*, pages 177–186, 2005.

[73] K.C. Taylor. *Catalysis - Science and Technology*, chapter 2, pages 119–170. Springer, Berlin, 1984.

[74] H.Y. Tong, W.T. Hung, and C.S. Cheung. Development of a driving cycle for hong kong. *Atmospheric Environment*, 33(15):2323–2335, 1999.

[75] D.N. Tsinoglou, G.C. Koltsakis, and Jones J.C.P. Oxygen storage modeling in three-way catalytic converters. *Industrial and Engineering Chemistry Research*, 41:1152–1165, 2002.

[76] Office of Research US Environmental Protection Agency and Development. Air quality criteria for carbon monoxide. Technical Report EPA-600/b-90/045F, Washington DC, US EPA, 1991.

[77] S. Vardoulakis, N. Gonzalez-Flesca, and B.E.A. Fisher. Assessment of traffic-related air pollution in two street canyons in paris: implications for exposure studies. *Atmospheric Environment*, 36(6):1025–1039, 2002.

[78] H.C. Watson, E.E. Milkins, M.O. Preston, C. Chittleborough, and B. Alimoradian. Predicting fuel consumption and emissions- transferring chassis dynamometer results to real driving conditions. In *SAE Technical Paper*, volume 830435, 1983.

[79] M. Weilenmann, C. Bach, and C. Ruedy. Aspects of instantaneous emission measurement. *International Journal of Vehicle Design*, 27:94–104, 2001.

[80] M. Weilenmann, P. Soltic, and D. Ajtay. Describing and compensating gas transport dynamics for accurate instantaneous emission measurement. *Atmospheric Environment*, 37(37):5137–5145, 2003.

[81] B.H. West, R.N. McGill, J.W. Hodgson, S. Sluder, and D.E. Smith. Development of data-based light-duty modal emissions and fuel consumption models. In *SAE Technical Paper*, volume 972910, 1997.

[82] D.C. Wilcox. *Basic Fluid Mechanics*. DCW Industries, 2000.

[83] T. Zachariadis and Z. Samaras. Comparative assessment of european tools to estimate traffic emissions. *International Journal of Vehicle Design*, 18(3-4):312–325, 1997.